12-12-2014

# Freshwater Transitions and the Evolution of Osmoregulation in the Alewife

Jonathan P. Velotta
*University of Connecticut - Storrs*, jonathan.velotta@gmail.com

# Freshwater Transitions and the Evolution of Osmoregulation in the Alewife

Jonathan Paul Velotta

University of Connecticut, 2014

The transition from seawater to freshwater is deeply rooted in the evolutionary history of animals, initiating the radiation and speciation of many taxa. However, crossing the boundary into freshwater from the sea represents a considerable physiological challenge for animals that maintain a near constant internal ion concentration. Because seawater and freshwater differ strongly in solute concentration, the transition into freshwater must involve the evolution of ion and water balance; yet, we have a limited understanding of the physiological modifications that facilitate this transition. Here, I investigate the evolution of the osmoregulatory system upon transition to freshwater using populations of an ancestrally anadromous fish, the Alewife (*Alosa pseudoharengus*), which has become landlocked on multiple, independent occasions. I take an integrative approach, exploring the molecular, physiological, and whole-organism level consequences of the freshwater transition.

Overall, my dissertation demonstrates that the transition to freshwater in the Alewife leads to evolutionary shifts in osmoregulatory capacity, which may be driven by changes in the mechanisms of ion exchange at the gill. In chapter 2, I show that landlocking leads to the partial loss of seawater tolerance and hypoosmoregulatory performance, which may be mediated

through reductions in expression and activity of genes for gill ion secretion. Chapter 3 demonstrates that several independently derived landlocked populations vary in the degree of seawater tolerance loss, and that this variation is negatively correlated with freshwater tolerance. This suggests that trade-offs in osmoregulation follow local adaptation to freshwater. In chapter 4, I use next generation sequencing to show that thousands of genes have differentiated in expression between Alewife life history forms. Comparison of gill transcriptomes of anadromous and landlocked Alewives reveals that changes in the regulation of transcription of genes in gill ion exchange pathways may underlie evolutionary changes in osmoregulation. In chapter 5, I demonstrate that landlocked Alewives are poor swimmers compared to anadromous Alewives, and that differences in swimming ability are not explained by differences in osmoregulatory performance or body shape. These results suggest that reductions in swimming performance among landlocked Alewives may be a function of relaxed selection on migration capacity.

# Freshwater Transitions and the Evolution of Osmoregulation in the Alewife

Jonathan Paul Velotta

B.S., Fairfield University, 2007

A Dissertation

Submitted in Partial Fulfillment of the

Requirements for the Degree of Doctor of Philosophy

at the

University of Connecticut

2014

APPROVAL PAGE

Doctor of Philosophy Dissertation

Freshwater Transitions and the Evolution of Osmoregulation in the Alewife

Presented by

Jonathan Paul Velotta, B.S.

Major Advisor_____
Eric T. Schultz

Associate Advisor _____
Stephen D. McCormick

Associate Advisor _____
Rachel J. O'Neill

Associate Advisor _____
Carl D. Schlichting

Associate Advisor _____
Mark C. Urban

University of Connecticut

2014

**Acknowledgements**

To my parents, Gary and Carmela, for encouraging me to follow my heart.

In memory of Michael F. O'Dea (1962 – 2014).

This work would not have been possible without the tireless support of my advisor, Eric Schultz. I am especially thankful to Stephen McCormick for hosting my research in his lab, and for his continued guidance, as well as to the rest of my committee, Rachel O'Neill, Carl Schlichting, and Mark Urban. Thank you Jessie Rack for your unconditional love and support, and for reminding me that life should be fun. Thank you Brian Walker for infecting me with a passion for physiological ecology. Thank you to my extended family, especially Raphael Santore, for being a guiding force in my life, and to my brother Richard Velotta for reminding me of the importance of family. Special thanks to the Schultz lab, especially Jeffrey Divino, for being an insightful colleague and a good friend. Thank you to all of the undergraduate students that I have had the pleasure of working with in the field and in the lab: Samantha Beynor, Grace Casselberry, Rebecca Colby, Megan Cruz, Anne Ewert, Emily Funk, David Fryxell, and Dante Paolino. Thank you to Andrew Jones for his extensive help in the field. Thank you to all my friends in the EEB department, especially Alejandro Rico-Guevara, William Ryerson, Diego Sustaita, and Timothy Moore for always being insightful and supportive – to many years of collaboration and friendship. Thank you to members of the Rachel O'Neil lab, especially Craig Obergfell for teaching me the skills of a molecular biologist. Thank you to past and present members of the physiology section of the Conte Anadromous Fish Research Center: Arne Christensen, Meghan Nichols, Amy Regish, Andrew Weinstock, and Mike O'Dea (1962 - 2014) – you are missed. And finally, thank you to the readers of this dissertation.

This work was supported by University of Connecticut's Department of Ecology and Evolutionary Biology, Center for Conservation and Biodiversity, and Center for Environmental Science and Engineering, as well as by The Sounds Conservancy of the Quebec-Labrador Foundation, Connecticut Sea Grant, the Lerner-Gray Fund for Marine Research at the American Museum of Natural History, and Sigma-Xi: Grants-in-aid of Research.

## Table of Contents

# Chapter 1

## Introduction

Empirical investigations of contemporary adaptive evolution help to reveal the ecological conditions that influence the course of evolution by natural selection as well as the rate of evolutionary change (Reznick and Ghalambor 2001). Fishes, the oldest and most diverse group of vertebrates on earth, have evolved to tolerate a wide array of environmental conditions, including salinity regimes that differ dramatically in ion concentration for which distinct and opposing mechanisms of physiological regulation are required (Figure 1). Salinity is arguably the single most important physical variable that affects the distribution of fishes in nature (Whitehead 2010), and ecological transitions into novel salinity regimes have clearly involved integrative adaptive evolutionary changes to the physiological systems that determine osmotic tolerance, as well as the molecular genetic machinery that underlies such systems. Transitions from seawater to freshwater have been particularly important in the creation of animal diversity (Lee and Bell 1999) and are deeply rooted in the evolution of fishes, and thus, of the vertebrates in general (Schultz and McCormick 2013). Understanding how modifications of the osmoregulatory system enable invasion of divergent salinity habitats will yield critical insights into the mechanisms by which animals solve complex physiological problems.

Despite its importance to evolutionary history, we have a limited understanding of the evolution of physiological and molecular systems that have allowed fish to invade divergent salinity regimes, though this process is likely to involve modification of the osmoregulatory system (Figure 1). In freshwater, fishes tend to passively gain external water and lose ions across the gills, a challenge that is counteracted by the production of large volumes of highly dilute urine, as well as active uptake of environmental $Na^+$ and $Cl^-$ at gill ionocytes

(hyperosmoregulation). Fishes in seawater face the opposite problem, passively losing water and gaining ions from their environment. To maintain internal ion concentrations below that of their environment (hypoosmoregulation), seawater fish drink large quantities of water, produce isotonic urine, and actively secrete excess internal $Na^+$ and $Cl^-$ at gill ionocytes (Figure 2; Evans et al 2005).

In this dissertation, I explore the evolution of the osmoregulatory system upon transition to freshwater using populations of an ancestrally anadromous fish, the Alewife (*Alosa pseudoharengus*), which has become restricted to freshwater (landlocked) on multiple and independent occasions (Palkovacs et al 2008). I answer the question of whether the transition to an exclusively freshwater environment results in shifts in salinity tolerance limits and osmotic balance in seawater (chapter 2) and/or freshwater, and whether these shifts reflect a trade-off (chapter 3). I then ask what physiological and molecular mechanisms underlie the evolution of osmoregulation via a candidate gene (chapters 2 and 3) and next generation sequencing (RNA-seq; chapter 4) approach. Finally, I ask whether evolutionary changes in osmoregulation alter the ability of fishes to perform critical and dynamic tasks in freshwater and seawater (chapter 5). My research explores the consequences of salinity habitat transitions at several levels of biological organization, examining how molecular, physiological, and whole-organism capabilities evolve. This work is highly integrative, and will greatly advance our understanding of the ways in which fishes can invade novel environments.

Populations of Alewife represent a novel opportunity to study the evolution of osmoregulation. In Connecticut, Alewives exist in two distinct life history forms: an ancestral anadromous form, which migrates to the sea, and a landlocked form, which is restricted to freshwater lakes (Figure 3; Palkovacs et al 2008). Damming of small streams during European

settlement (circa 300-400 years ago) is likely to have trapped juvenile Alewives in their natal lakes, resulting in multiple, independently derived landlocked populations. Patterns of genetic differentiation indicate that landlocked populations were derived independently from a single anadromous ancestor (Palkovacs et al. 2008). This system is ideal to test whether replicate transitions to freshwater result in parallel changes in osmoregulatory function and physiological and molecular regulation, a pattern that would imply natural selection as the cause of change (Endler 1986; Schluter 2000).

The transition to an exclusively freshwater life history is likely to be followed by shifts in salinity tolerance limits and osmoregulatory performance optima. For example, the removal of seawater as a source of selection should lead to the reduction or elimination of seawater osmoregulatory function. Theory predicts that neutral or non-neutral processes should reduce the functioning of a trait when a source of selection on that trait is removed (relaxed selection; Lahti et al 2009). The speed and extent of reduction depend on whether possessing the trait in a new environment is costly or not. Rapid reductions in seawater osmoregulatory function upon adaptation to freshwater are expected if traits for hypoosmoregulation bear a constitutive maintenance cost (e.g., a cost of plasticity; Auld et al 2010) or if there is a trade-off in salinity tolerance, such that maximizing hyperosmoregulation limits the performance of the hypoosmoregulatory system.

Lowered seawater tolerance capabilities have been demonstrated in landlocked populations of salmonid fishes (*Salvelinus alpinus*: Staurnes et al 1992; *Oncorhynchus nerka*: Foote et al 1992) and Threespine Stickleback (*Gasterosteus aculeatus*; McCairns and Bernatchez 2010; DeFaveri and Merila 2014) compared to an anadromous ancestor. Landlocked salmonids also show a reduced ability to regulate $Na^+$ and $Cl^-$ ions in seawater. While these studies are

revealing, they incompletely demonstrate whether adaptation to freshwater limits osmoregulation in the ancestral seawater environment. Salmonid species are not an ideal group since their tolerance of seawater is secondarily derived, and freshwater is the likely ancestral salinity environment (Crespi and Fulton 2004). Threespine Stickleback populations are older (circa 10,000 years in Alaskan populations; Bell and Foster 1994) than Alewife populations, and provide limited insight into whether the osmoregulatory system can evolve rapidly. In this dissertation, I examine the extent to which freshwater adaptation has consequences on seawater osmoregulatory performance. In chapter 2, I investigate differences in seawater osmoregulatory capabilities between one anadromous and one landlocked population, and in chapter 3, I extend this examination to five independently derived landlocked populations. In both chapters, I ask whether there are non-lethal effects on seawater osmoregulatory performance, i.e., whether landlocking limits hypoosmotic balance after several days (chapter 2) or several weeks (chapter 3) in seawater.

Selection on hyperosmoregulatory function should be strong upon transitions to freshwater, since fish must maintain hyperosmotic balance at all life history stages. Several recent studies lend support to this expectation. Freshwater Atlantic killifish (*Fundulus heteroclitus*) have higher survival in response to freshwater (Scott et al 2004) and are better able to regulate $Cl^-$ than individuals from marine/brackish water populations (Scott et al 2004; Whitehead et al 2011, 2012). The freshwater fish *Cyprinodon variegatus hubbsi* is able to regulate plasma $Na^+$ more efficiently than its euryhaline counterpart *C. v. variegatus* (Brix and Grosell 2012). Recent work by Lee et al (2007, 2011) demonstrates that heritable increases in freshwater tolerance and subsequent decreases in seawater tolerance occur rapidly after invasion of freshwater by an ancestrally marine copepod (*Eurytemora affinis*), suggesting a trade-off in

salinity tolerance. In chapter 3, I ask whether landlocked Alewives exhibit improved hyperosmoregulatory function, and whether this improvement is traded-off against hypoosmoregulatory function. If so, this would represent the first instance in fish in which local adaptation to freshwater results in the evolution of salinity tolerance limits in both freshwater and seawater.

The transition to freshwater environments likely involves modification of ion exchange mechanisms at the gills. Several studies have demonstrated evolution of activity and expression of known ion transport pathways (Scott et al 2004; Scott and Schulte 2005; Nilsen et al 2007; see Lee et al 2011 for similar work in copepods) and signatures of selection at osmoregulation loci (Shimada et al 2011; DeFaveri et al 2011; Jones et al 2012; Michalak et al 2014) in freshwater populations. Advances in functional genomic tools have allowed researchers to look broadly at how adaptation to freshwater is mediated by changes in gill transcriptional regulation. Several studies comparing freshwater and brackish water killifish have found divergence in gene expression at loci involved in ion transport, cell-volume regulation, cell stabilization, water transport, and the osmotic stress response (Whitehead et al 2011, 2012; Kozak et al 2013). Constitutive differences in expression of genes with osmoregulatory roles including *AQP3* (a water channel), *claudin-30c* (a regulator of tight-junctions between ionocytes and neighboring cells), and *β-thymosin* (a cytoskeleton organizer) were found between anadromous populations of Alewife and landlocked populations from the Great Lakes and coastal New England (Czesny et al 2012; Michalak et al 2014). A key component missing from this work is a determination of whether functional genomic mechanisms that underlie adaptation to freshwater are conserved across independently evolved populations (i.e., an examination of parallel evolution). In chapters 2 and 3, I examine the evolution of patterns of gene expression in several candidate

osmoregulation loci to determine whether the regulation of ion exchange has evolved among landlocked Alewives. In chapter 4, I take a next generation sequencing approach to study divergence of the gill transcriptome among several independent landlocked Alewife populations in order to reveal the extent to which common or unique mechanisms underlie repeated evolution of osmoregulation. These studies will provide essential insight into the mechanisms that regulate adaptation to salinity.

The active exchange of ions at the gill imposes a significant energetic cost to osmoregulating fish, and can consume anywhere from 10 – 50% of the total energy budget (Bœuf and Payan 2001). Transfer to different salinities consistently affects routine metabolic rate, growth rate, and growth efficiency (Wuenschel et al 2004; Augley et al 2008), and reduces maximal swimming performance (Kolok and Sharkey 1997; Swanson 1998) in several species of fish. In Coho salmon parr (*Oncorhynchus kisutch*), reductions in critical swimming performance after seawater transfer appear to be caused by severe hypoosmotic imbalances (Brauner et al 1992). Impaired osmoregulatory function, therefore, may limit dynamic aspects of whole-organism performance, such as sustained swimming ability. In chapter 5, I ask whether evolutionary changes in osmoregulation have whole-organism performance consequences by measuring sustained swimming performance - an ecologically relevant task for a migratory, schooling species - after freshwater and seawater challenge. The results of this experiment will expand our understanding of the consequences of freshwater transitions by linking evolved changes in regulatory performance (osmoregulation) to dynamic aspects of whole-organism performance (swimming) – a linkage not previously explored.

In summary, through a series of experimental manipulations, I compare anadromous and landlocked Alewives in order to investigate the evolution of osmoregulation upon transition to an

exclusively freshwater life cycle. I explore whether adaptation to freshwater results in shifts in salinity tolerance and osmotic balance capabilities (chapters 2 and 3), what mechanisms of ion exchange have been modified in conjunction with these shifts (chapters 2, 3 and 4), and whether the evolution of osmoregulation has whole-organism performance consequences (chapter 5). This research significantly advances our understanding of the ways in which fishes have solved the complex problem of invading freshwater habitats, an evolutionary transition that has been fundamental to the creation of their own diversity, as well as to the diversity of all land-dwelling vertebrates.

**References**


Augley, J., Huxham, M., Fernandes, T.F., and Lyndon, A.R. (2008). The effect of salinity on growth and weight loss of juvenile plaice (*Pleuronectes platessa,* L): An experimental test. J. Sea. Res. *60*, 292–296.

Auld, J.R., Agrawal, A.A., and Relyea, R.A. (2010). Re-evaluating the costs and limits of adaptive phenotypic plasticity. Proc. R. Soc. B *277*, 503–511.

Barton, M., and Bond, C.E. (2007). Bond's biology of fishes.

Bell, M.A., and Foster, S.A. (1994). The evolutionary biology of the threespine stickleback (Oxford University Press).

Bœuf, G., and Payan, P. (2001). How should salinity influence fish growth? Comp. Biochem. Phys. C *130*, 411–423.

Brauner, C.J., Iwama, G.K., and Randall, D.J. (1994). The effect of short-duration seawater exposure on the swimming performance of wild and hatchery-reared juvenile coho salmon (*Oncorhynchus kisutch*) during smoltification. Can. J. Fish. Aquat. Sci. *51*, 2188–2194.

Brix, K.V., and Grosell, M. (2012). Comparative characterization of $Na^+$ transport in *Cyprinodon variegatus variegatus* and *Cyprinodon variegatus hubbsi*: a model species complex for studying teleost invasion of freshwater. J. Exp. Biol. *215*, 1199–1209.

Czesny, S., Epifanio, J., and Michalak, P. (2012). Genetic divergence between freshwater and marine morphs of alewife (*Alosa pseudoharengus*): A "next-generation" sequencing analysis. PLoS ONE *7*, e31803.

DeFaveri, J., and Merilä, J. (2014). Local adaptation to salinity in the three-spined stickleback? J. Evol. Biol. *27*, 290–302.

DeFaveri, J., Shikano, T., Shimada, Y., Goto, A., and Merilä, J. (2011). Global analysis of genes involved in freshwater adaptation in threespine sticklebacks (*Gasterosteus aculeatus*). Evolution *65*, 1800–1807.

Endler, J.A. (1986). Natural Selection in the Wild (Princeton University Press).

Evans, D.H., Piermarini, P.M., and Choe, K.P. (2005). The multifunctional fish gill: dominant site of gas exchange, osmoregulation, acid-base regulation, and excretion of nitrogenous waste. Physiol. Rev. *85*, 97–177.

Foote, C.J., Wood, C.C., Clarke, W.C., and Blackburn, J. (1992). Circannual cycle of seawater adaptability in *Oncorhynchus nerka*: genetic differences between sympatric sockeye salmon and kokanee. Can. J. Fish. Aquat. Sci. *49*, 99–109.

Jones, F.C., Grabherr, M.G., Chan, Y.F., Russell, P., Mauceli, E., Johnson, J., Swofford, R., Pirun, M., Zody, M.C., White, S., et al. (2012). The genomic basis of adaptive evolution in threespine sticklebacks. Nature *484*, 55–61.

Kolok, A.S., and Sharkey, D. (1997). Effect of freshwater acclimation on the swimming performance and plasma osmolarity of the euryhaline gulf killifish. Trans. Am. Fish. Soc. *126*, 866–870.

Kozak, G.M., Brennan, R.S., Berdan, E.L., Fuller, R.C., and Whitehead, A. (2014). Functional and population genomic divergence within and between two species of killifish adapted to different osmotic niches. Evolution *68*, 63–80.

Lahti, D.C., Johnson, N.A., Ajie, B.C., Otto, S.P., Hendry, A.P., Blumstein, D.T., Coss, R.G., Donohue, K., and Foster, S.A. (2009). Relaxed selection in the wild. Trends Ecol. Evol. *24*, 487–496.

Lee, C.E., Bell, M.A., Lee, C.E., and Bell, M.A. (1999). Causes and consequences of recent freshwater invasions by saltwater animals. Trends Ecol. Evol. *14*, 284–288.

Lee, C.E., Remfert, J.L., and Chang, Y.-M. (2007). Response to selection and evolvability of invasive populations. Genetica *129*, 179–192.

Lee, C.E., Kiergaard, M., Gelembiuk, G.W., Eads, B.D., and Posavi, M. (2011). Pumping ions: rapid parallel evolution of ionic regulation following habitat invasions. Evolution *65*, 2229–2244.

McCairns, R.J.S., and Bernatchez, L. (2010). Adaptive divergence between freshwater and marine sticklebacks: insights into the role of phenotypic plasticity from an integrated analysis of candidate gene expression. Evolution *64*, 1029–1047.

Michalak, K., Czesny, S., Epifanio, J., Snyder, R.J., Schultz, E.T., Velotta, J.P., McCormick, S.D., Brown, B.L., Santopietro, G., and Michalak, P. (2014). Beta-thymosin gene polymorphism associated with freshwater invasiveness of alewife (*Alosa pseudoharengus*). J. Exp. Zool *321*, 233–240.

Nilsen, T.O., Ebbesson, L.O.E., Madsen, S.S., McCormick, S.D., Andersson, E., Björnsson, B.T., Prunet, P., and Stefansson, S.O. (2007). Differential expression of gill $Na^+$,$K^+$-ATPase α - and β-subunits, $Na^+$,$K^+$,$2Cl^-$ cotransporter and CFTR anion channel in juvenile anadromous and landlocked Atlantic salmon *Salmo salar*. J. Exp. Biol. *210*, 2885–2896.

Palkovacs, E.P., Dion, K.B., Post, D.M., and Caccone, A. (2008). Independent evolutionary origins of landlocked alewife populations and rapid parallel evolution of phenotypic traits. Mol. Ecol. *17*, 582–597.

Reznick, D.N., and Ghalambor, C.K. (2001). The population ecology of contemporary adaptations: what empirical studies reveal about the conditions that promote adaptive evolution. Genetica *112-113*, 183–198.

Schluter, D. (2000). The Ecology of Adaptive Radiation (Oxford University Press).

Schultz, E.T., and McCormick, S.D. (2013). Euryhalinity in an evolutionary context. In: McCormick S.D., Farrell A.P., Brauner C.J. (eds) Fish Physiology, vol 32. Academic Press

Scott, G.R., and Schulte, P.M. (2005). Intraspecific variation in gene expression after seawater transfer in gills of the euryhaline killifish *Fundulus heteroclitus*. Comp. Biochem. Phys. A *141*, 176–182.

Scott, G.R., Rogers, J.T., Richards, J.G., Wood, C.M., and Schulte, P.M. (2004). Intraspecific divergence of ionoregulatory physiology in the euryhaline teleost *Fundulus heteroclitus*: possible mechanisms of freshwater adaptation. J. Exp. Biol. *207*, 3399–3410.

Shimada, Y., Shikano, T., and Merilä, J. (2011). A high incidence of selection on physiologically important genes in the three-spined stickleback, *Gasterosteus aculeatus*. Mol. Biol. Evol. *28*, 181–193.

Staurnes, M., Sigholt, T., Lysfjord, G., and Gulseth, O.A. (1992). Difference in the seawater tolerance of anadromous and landlocked populations of arctic char (*Salvelinus alpinus*). Can. J. Fish. Aquat. Sci. *49*, 443–447.

Swanson, C. (1998). Interactive effects of salinity on metabolic rate, activity, growth and osmoregulation in the euryhaline milkfish (*Chanos chanos*). J. Exp. Biol. *201*, 3355–3366.

Whitehead, A. (2010). The evolutionary radiation of diverse osmotolerant physiologies in Killifish (*Fundulus sp*.). Evolution *64*, 2070–2085.

Whitehead, A., Roach, J.L., Zhang, S., and Galvez, F. (2011). Genomic mechanisms of evolved physiological plasticity in killifish distributed along an environmental salinity gradient. PNAS *108*, 6193–6198.

Whitehead, A., Roach, J.L., Zhang, S., and Galvez, F. (2012). Salinity- and population-dependent genome regulatory response during osmotic acclimation in the killifish (*Fundulus heteroclitus*) gill. J. Exp. Biol. *215*, 1293–1305.

Wuenschel, M.J., Jugovich, A.R., and Hare, J.A. (2004). Effect of temperature and salinity on the energetics of juvenile gray snapper (*Lutjanus griseus*): implications for nursery habitat value. J. Exp. Mar. Biol. Ecol. *312*, 333–347.

Zydlewski, J., and McCormick, S.D. (1997). The loss of hyperosmoregulatory ability in migrating juvenile American shad, *Alosa sapidissima*. Can. J. Fish. Aquat. Sci. *54*, 2377–2387.

## Figures

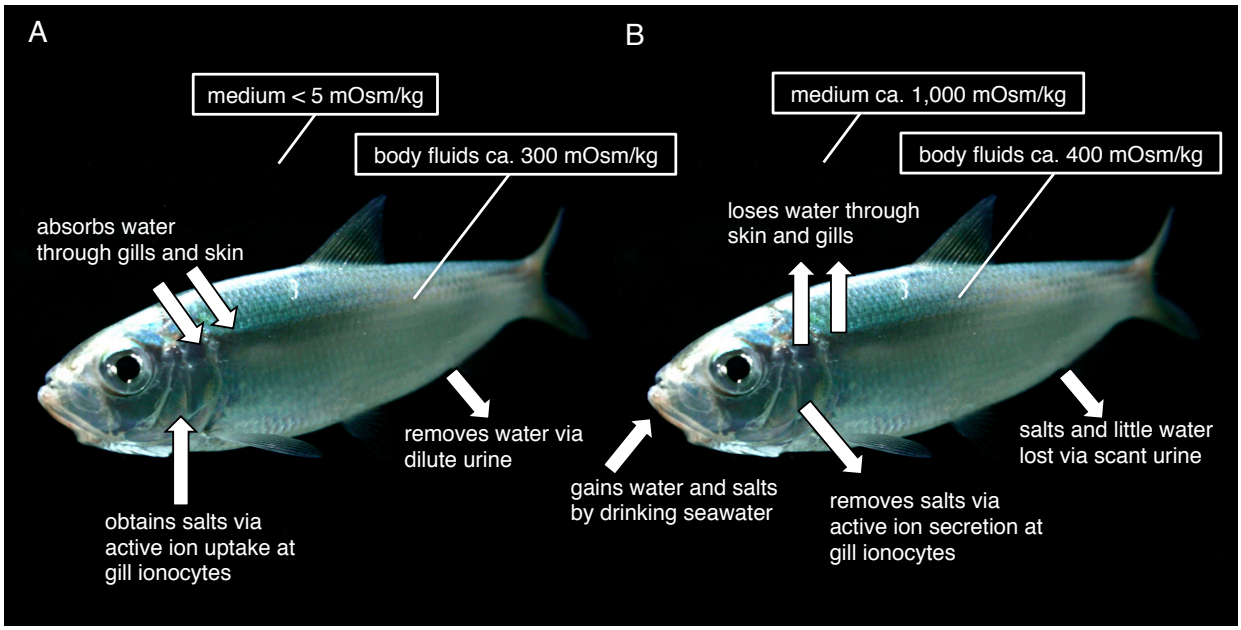


**Figure 1** A: Hyperosmoregulation of a freshwater teleost fish. B: Hypoosmoregulation of a seawater teleost. Figure modified after Barton and Bond 2007. Alewife photograph by Kai Webler.

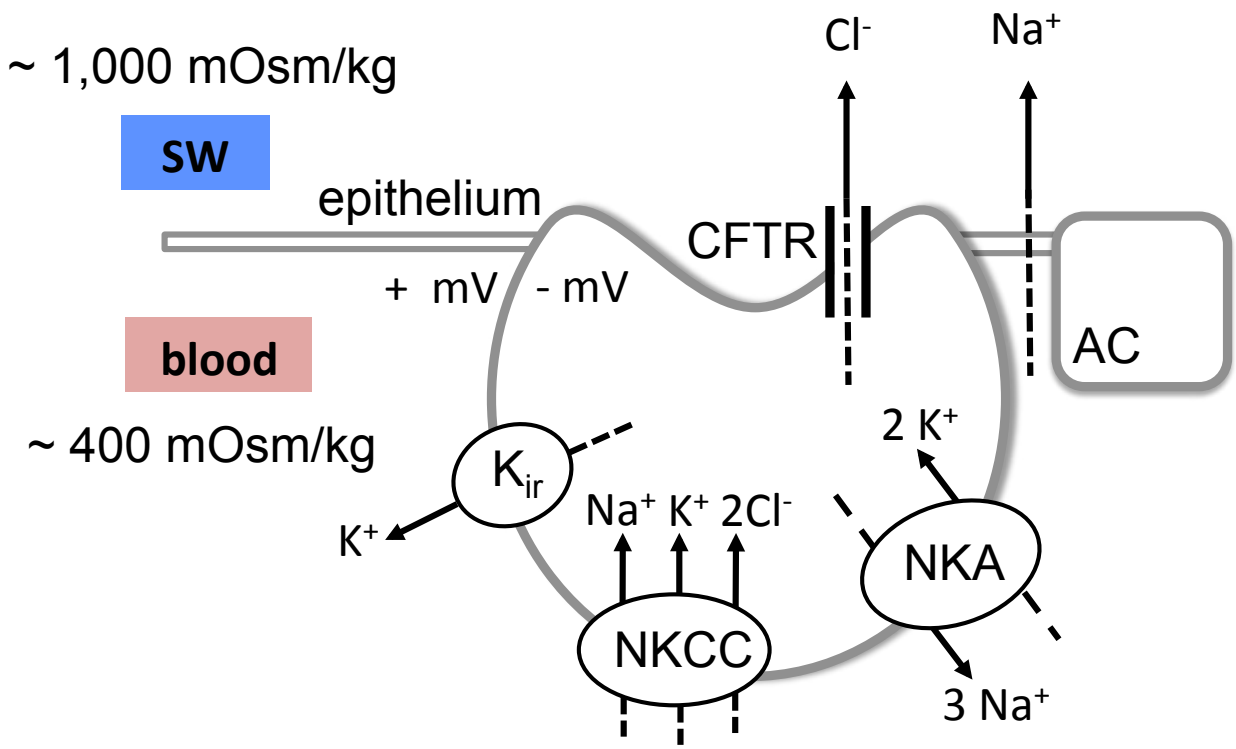


**Figure 2** Model of salt secretion at the teleost gill ionocyte. Plasma $Na^+$, $K^+$, and $Cl^-$ enter the ionocyte through basolateral $Na^+/K^+/2Cl^-$ cotransporter (NKCC). $Na^+$ is recycled back into the plasma via $Na^+/K^+$-ATPase, and $K^+$ is recycled via a $K^+$ channel ($K_{ir}$). $Cl^-$ is removed across the apical membrane through the cystic fibrosis transmembrane conductance regulator homolog (CFTR). The transepithelial electrical potential across the gill epithelium (plasma positive relative to seawater) drives $Na^+$ across leaky tight junctions between ionocytes and neighbor accessory cells (AC).

Anadromous

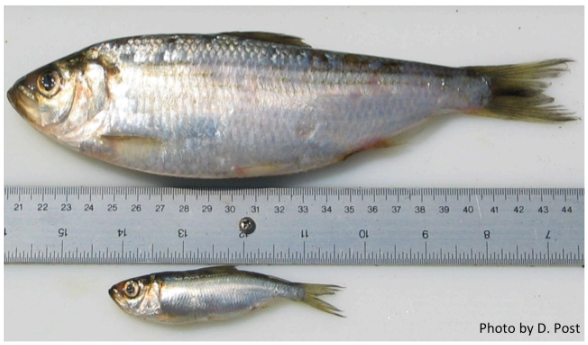


Landlocked

**Figure 3** Comparison of adult anadromous and landlocked Alewives. Landlocked alewives are smaller than anadromous alewives at age, and differ in many morphological and life history traits. Photograph by David Post.

## Chapter 2

### Relaxed selection causes microevolution of seawater osmoregulation and gene expression in landlocked Alewives

Appears as published in: Velotta, J.P., Schultz, E.T., McCormick, S.D., and O'Neill, R.J. 2014. Relaxed selection causes microevolution of seawater osmoregulation and gene expression in landlocked Alewives. Oecologia. 175(4): 1081-1092

### Abstract

Ecological transitions from marine to freshwater environments have been important in the creation of diversity among fishes. Evolutionary changes associated with these transitions likely involve modifications of osmoregulatory function. In particular, relaxed selection on hypo-osmoregulation should strongly affect animals that transition into novel freshwater environments. We used populations of the Alewife (*Alosa pseudoharengus*) to study evolutionary shifts in hypo-osmoregulatory capacity and ion regulation associated with freshwater transitions. Alewives are ancestrally anadromous, but multiple populations in Connecticut have been independently restricted to freshwater lakes; these landlocked populations complete their entire life cycle in freshwater. Juvenile landlocked and anadromous Alewives were exposed to three salinities (1 ppt, 20 ppt and 30 ppt) in small enclosures within the lake. We detected strong differentiation between life history forms: landlocked Alewives exhibited reduced seawater tolerance and hypo-osmoregulatory performance compared to anadromous Alewives. Furthermore, gill $Na^+/K^+$-ATPase activity and transcription of genes for seawater osmoregulation (*NKCC* - $Na^+/K^+/2Cl^-$ cotransporter and *CFTR* - cystic fibrosis transmembrane conductance regulator) exhibited reduced responsiveness to seawater challenge. Our study demonstrates that adaptations of marine-derived species to completely freshwater life cycles involve partial loss of seawater osmoregulatory performance, mediated through changes to ion regulation in the gill.

## Introduction

Among fishes, ecological transitions from marine to freshwater environments have often involved episodes of diversification and adaptive radiation (Schultz and McCormick 2013). Freshwater environments contain a substantial amount of earth's fish diversity (approximately 40%; Nelson 2006) in only a fraction (0.01%) of the available water. The boundary between seawater and freshwater, however, may be a formidable one to cross, since these habitats differ strongly in osmotic pressure and ion concentration (Lee and Bell 1999). Euryhaline species may be uncommonly suited for ecological movement into freshwater due to their ability to tolerate a wide range of salinities (Schultz and McCormick 2013). Adaptive changes that facilitate freshwater transitions have been studied in a number of taxa (e.g., Lee et al. 2011; Whitehead et al. 2011; DeFaveri et al. 2011), but we lack a full understanding of how osmoregulatory mechanisms evolve in response to such movements. Modern ecological transitions in which populations of extant euryhaline species are restricted to freshwater through natural or anthropogenic land-locking events offer an opportunity to study evolutionary changes to osmoregulatory function. Here, we report on micro-evolutionary shifts in osmoregulatory function in an ancestrally anadromous species in which multiple landlocked, entirely freshwater populations exist.

Osmoregulation in teleost fishes involves integrated molecular and biochemical processes that take place within a variety of organs, including the gills (Evans et al. 2005; McCormick and Saunders 1987). These processes differ considerably between salinity environments. In freshwater, fishes passively gain external water and lose ions across all exposed surfaces, especially the gills. Passive ion loss is actively opposed by taking in environmental $Na^+$ and $Cl^-$ at the gills, which maintains internal ion concentrations above that of the environment (hyper-osmoregulation). Fish in seawater passively lose water and gain ions from the environment. To

maintain internal concentrations below ambient, marine fish drink large quantities of seawater and actively secrete the excess $Na^+$ and $Cl^-$ at the gills (hypo-osmoregulation). Several well-studied ion transporters are responsible for ion secretion by gill ionocytes of seawater fishes (Evans et al. 2005): $Na^+/K^+$-ATPase (NKA), $Na^+/K^+/2Cl^-$ cotransporter (NKCC), and cystic fibrosis transmembrane conductance regulator homolog (CFTR).

Transitions from euryhaline to freshwater-restricted life cycles are likely to be followed by strong evolutionary adjustments favoring mechanisms for hyper-osmoregulation. The consequences of such transitions to existing hypo-osmoregulatory mechanisms have not been well characterized for fishes (but see Lee et al. 2003, 2007, 2011 for such work in copepods). Theory predicts that traits with constitutive energetic costs and/or traits subject to neutral evolutionary processes will decay over time following the elimination of a source of selection, a process known as relaxed selection (Lahti et al. 2009). Therefore, when fish become restricted to freshwater, relaxed selection is likely to reduce or eliminate hypo-osmoregulatory function (e.g., in *Salmo salar*; Nilsen et al. 2007). The rate at which trait decay occurs will depend on whether or not the trait bears an energetic cost. Hypo-osmoregulatory mechanisms should decay rapidly upon transition to freshwater if they bear constitutive energetic costs, since traits that reduce fitness should be selected against. If, however, hypo-osmoregulatory mechanisms bear no underlying cost in freshwater, neutral processes alone may still eliminate trait function, albeit more slowly, via genetic drift. Despite its importance to fish diversity and evolution, we do not yet have a full understanding of the details and rapidity of evolutionary changes in osmoregulation after transitions into permanent freshwater habitats, and how function in seawater is affected by such changes.

Research characterizing the evolutionary consequences of freshwater restriction on hypo-osmoregulation has primarily involved comparisons of landlocked and anadromous species in the family Salmonidae, which evolved and diversified in freshwater judging from the life history of basal species (Crespi and Fulton 2004; Stearley 1992; Wilson and Li 1999). For example, reduced seawater tolerance in landlocked populations of anadromous salmonids has been shown for Arctic Char (*Salvelinus alpinus*; Staurnes et al. 1992), Sockeye Salmon (*Oncorhynchus nerka*: Foote et al. 1992) and Atlantic Salmon (*Salmo salar*: Barbour and Garside 1983; Birt and Green 1986; Burton and Idler 1984; Nilsen et al. 2007). These studies indicate that greater seawater sensitivity of landlocked salmonids is also associated with a reduced ability to regulate blood $Na^+$ and $Cl^-$ in seawater (Staurnes et al. 1992; Foote el al. 1992; Nilsen et al. 2007). Research conducted on species with marine ancestry, in which hypo-osmoregulation is a basal condition and for which a freshwater life history is secondarily derived, may shed more light on the evolutionary processes associated with ecological transitions to freshwater.

Studies of freshwater forms of Threespine Stickleback (*Gasterosteus aculeatus*; Bell and Foster 1994) and killifishes of the genus *Fundulus* (Whitehead 2010), both of which are ancestrally marine, has revealed intraspecific changes in osmoregulatory physiology associated with transitions to a completely freshwater life history. In stickleback, survival in seawater is reduced among freshwater or lake populations (DeFaveri and Merila 2013; McCairns and Bernatchez 2010; E. Schultz, unpublished data). Loci under positive selection in the transition from marine to freshwater environments have been identified in stickleback, and include $Na^+/K^+$-ATPase and other genes involved in osmoregulation (DeFaveri et al. 2011; Jones et al. 2012; Shimada et al. 2011). Studies in the killifish *Fundulus heteroclitus* have revealed intraspecific differences in the molecular mechanisms that drive seawater osmoregulation between northern

and southern populations (Scott and Schulte 2005); fish with northern genotypes appear better adapted to freshwater (Able and Palmer 1988; Scott et al. 2004) and occur more frequently in freshwater habitats compared to individuals with southern genotypes (Powers et al. 1986). Changes in the molecular response of northern killifish to seawater are not associated with hypo-osmoregulatory costs; killifish from northern and southern populations maintain plasma $Na^+$ and $Cl^-$ balance after seawater transfer (Scott and Schulte 2005). Few studies have tied evolutionary changes in seawater tolerance and osmoregulatory capacity to associated physiological and molecular mechanisms in a marine-derived species.

Alewife (*Alosa pseudoharengus* [Wilson 1811]) populations in Connecticut provide a distinctive opportunity to study the consequences of freshwater transitions and relaxed selection on seawater osmoregulation. In Alewives, two life history forms exist: an ancestral anadromous form that migrates from seawater to freshwater to spawn, and a landlocked form, in which seawater migration has been eliminated from the life cycle. Population genetic analyses using mitochondrial and microsatellite loci indicate that multiple landlocked Alewife populations in Connecticut are independently derived from a genetically homogeneous anadromous stock (Palkovacs et al. 2008). Divergence estimates using microsatellite loci suggest that landlocked Alewives diverged from the anadromous ancestor no more than 5,000 years ago, and as recently as 300 years ago, depending on the microsatellite mutation rate assumed (Palkovacs et al. 2008). The most likely explanation is that Alewives became restricted to their natal lakes as a result of dam construction during European settlement approximately 300-500 years ago (Palkovacs et al. 2008).

Alewives belong to a predominately marine family of fishes, the Clupeidae, which apparently diversified in seawater (Li and Orti 2007) and in which hypo-osmoregulation is an

ancestral capability. The development of seawater tolerance differs considerably between species in the Salmonidae and Clupeidae, evidence of their distinctive evolutionary histories. Juvenile anadromous salmonids prepare for entry into seawater through a series of preparatory physiological changes that lead to an increase in seawater tolerance just prior to migration, an ontogenetic phase known as smolting (McCormick 2013). Limited data available suggests that clupeids can tolerate seawater well before downstream migration; American Shad (*Alosa sapidissima*) can survive direct transfer to seawater at the larval-juvenile transition when gills develop (Zydlewski and McCormick 1997b), and Alewife tolerance to seawater appears to develop even earlier (Yako 1998). Since hypo-osmoregulation is deeply rooted in Alewife ancestry, the tempo and mode by which they adapt to freshwater restriction may be different than that experienced by ancestrally-freshwater salmonid fishes.

By comparing landlocked and anadromous Alewives, we investigated if relaxed selection on seawater function results in evolutionary changes to seawater tolerance (measured as survival), hypo-osmoregulatory capacity (measured as plasma osmolality after seawater exposure), the expression of two key seawater osmoregulation genes (NKCC and CFTR) and the enzymatic activity of $Na^+/K^+$-ATPase. We exposed wild-caught juvenile Alewives from one anadromous population and two landlocked populations in Connecticut to a series of 60 hour *in situ* salinity challenge experiments, in which fish were transferred directly from their natal lake to 1 ppt (freshwater), 20 ppt (brackish water) and 30 ppt (seawater). We collected juvenile (age 0) Alewives from their natal lakes, since at this life history stage anadromous and landlocked Alewives live in identical salinity environments (approximately 0 ppt) and are naïve to seawater. We hypothesized that land-locking in Alewives would result in significant loss of osmoregulatory function in seawater due to relaxed selection. We predicted that seawater-

challenged landlocked Alewives would experience reductions in tolerance, hypo-osmoregulatory capacity, $Na^+/K^+$-ATPase activity and expression of two seawater genes, *NKCC* and *CFTR,* compared to anadromous Alewives.

## Materials and Methods

### *Animals and experimental procedures*

Anadromous and landlocked young-of-the-year (YOY) Alewives (*Alosa pseudoharengus*) were collected from their natal lakes in coastal Connecticut on six dates in 2009 (Table 1). All animals were handled in accordance with the University of Connecticut's Institutional Animal Care and Use Committee (protocol A09-24). We captured Alewives from three locations: anadromous population from Bride Lake (East Lyme, Connecticut), and landlocked populations from Pattagansett (East Lyme, Connecticut) and Rogers Lakes (Old Lyme, Connecticut, Table 1). The salinity of all three lakes was approximately 0 ppt. Three separate experimental trials were run in separate months (trial 1: September; trial 2: October; trial 3: November; Table 1) towards the end of juvenile anadromous Alewife out-migration (Gahagan et al. 2010). Within each trial, we subjected 10-15 Alewives from one anadromous and one landlocked population to three salinity treatments (1 ppt, 20 ppt, and 30 ppt) for 60 hours (Table 2). We chose this time frame based on the results of salinity challenge experiments in other species (Scott and Schulte 2005; Staurnes et al. 1992; Zydlewski and McCormick 1997a) indicating that most mortality occurred over the first 3 days of exposure, and that perturbations in plasma osmolality were greatest between 1 and 3 days. In addition, a 60-hour time frame allows for measurement of critical changes in transcription (mRNA levels) in response to seawater (Scott and Schulte 2005). Salinity treatment of each population occurred in consecutive weeks,

such that only one population was treated during a given week, followed by the other population the next week (Table 1), allowing for direct comparison of an anadromous and landlocked population at each trial.

Salinity challenges were conducted immediately after capture, when approximately fifteen Alewives were directly transferred to each of the three salinity treatments. Experiments were conducted *in situ* at Bride Lake in 150-liter oval tanks filled with Bride Lake water. Tanks were immersed in the lake to maintain temperature. Landlocked Alewives were transported from their home environment to Bride Lake. To do this, we placed captive Alewives in covered oval tanks (150-liter) filled with lake water and drove them immediately to the Bride Lake site (8 km on average). For consistency, anadromous Alewives were similarly transported after capture, but returned to Bride Lake. Treatment salinities were achieved by dissolving artificial sea salt (Instant Ocean, Spectrum Brands, Madison, WI) in water from Bride Lake. Tanks were aerated with battery-powered units for the duration of the experiment. Experimental tanks were checked for mortalities within the first six to eight hours after the start of salinity treatment, and then approximately every twelve hours thereafter. Any dead fish found were immediately removed and measured for standard length (hereafter, length).

At the end of the 60-hour treatment period, we euthanized remaining fish in 250 mg $l^{-1}$ tricaine methanesulfonate (Argent, Redmond, WA, USA) and measured length. Immediately after euthanasia, blood was drawn from the caudal vessel with 1 ml heparinized hematocrit tubes and centrifuged at 3200g for 5 minutes. Plasma was removed and transferred to 0.5 mL tubes and stored at -80°C. Plasma osmolality (i.e., total plasma ion concentration measured in mosmol/kg) was subsequently measured on a vapor pressure osmometer (Wescor Inc., Logan, Utah) using 8 μL of plasma and following the manufacturer's instructions. For fish in which less than 8 μL of

plasma was collected, samples within a life history form and salinity treatment group were pooled (a total of 27 individuals were pooled). mRNA expression by quantitative real-time polymerase chain reaction (qPCR, n=5 per treatment per life history form) was performed on tissue from four gills arches from each side of the fish, placed directly in liquid nitrogen, and stored at -80°C. The first right gill arch was excised from additional fish (n=8 per treatment per life history form), placed immediately in 100 μl ice-cold SEI buffer (150 mmol $l^{-1}$ sucrose, 10 mmol $l^{-1}$ EDTA, 50 mmol $l^{-1}$ imidazole, pH 7.3) and stored at -80°C for measurement of $Na^+/K^+$-ATPase activity.

*$Na^+/K^+$-ATPase activity and mRNA Expression Assays*

Gill $Na^+/K^+$-ATPase activity (hereafter NKA activity) was determined by the microplate method outlined by McCormick (1993). Following this method, ouabain-sensitive ATPase activity was measured by coupling the production of ADP to NADH using lactic dehydrogenase and pyruvate kinase, in the presence and absence of 0.5 mmol $l^{-1}$ ouabain. Homogenized gill samples were run in duplicate in 96-well microplates at 25°C and read at a wavelength of 340 nm for 10 min on a THERMOmax microplate reader using SOFTmax software (Molecular Devices, Menlo Park, CA, USA). The total protein content of the homogenate was determined using a BCA (bicinchoninic acid) Protein Assay (Pierce, Rockford, IL, USA) in order to normalize NKA activity to the total amount of protein. Activity was calculated as the difference in ATP hydrolysis in the absence and presence of ouabain, expressed as μmol ADP mg $protein^{-1}$ $hour^{-1}$.

Expression of candidate genes was measured by quantitative real-time PCR (qPCR). Total RNA for gene expression analysis was extracted from approximately 30 mg of gill tissue

per sample using the RNeasy Mini Kit (Qiagen, Valencia, CA) following the manufacturer's instructions. Tissue was homogenized using a Kinematica Polytron PT 2100 bench top homogenizer (Kinematica, Inc, Bohemia, NY). We quantified RNA spectrophotometrically, assessed purity (260/280 > 1.8) and checked integrity on a 1% agarose gel. Purified RNA was DNase treated using the TURBO DNA-free kit (Life Technologies, Grand Island, NY) as described by the manufacturer. First strand synthesis of cDNA for use in qPCR was achieved using 500 ng RNA and qScript reverse transcriptase (Quanta Biosciences, Gaithersburg, MD). Quantitative real-time PCR primers for *NKCC*, *CFTR* and elongation factor 1α (*EF1α*, reference gene) were designed using reads generated from gill-specific transcriptome sequence of wild-caught juvenile Alewives (J. Velotta, unpublished). Primer sequences are reported in Table 3.

Target cDNAs were amplified in triplicate by qPCR using a Bio-Rad iCycler (Bio-Rad Laboratories, Hercules, CA) and PerfeCTa SYBR Green Fastmix (Quanta Biosciences). All qPCR reactions were performed using the following cycle conditions: 10 minutes at 95 ºC, 45 cycles of 95 ºC for 20 seconds and 59.5 ºC for 50 seconds. Melt curve analysis was performed following each reaction to confirm that only a single product was produced. We arbitrarily selected a sample of gill tissue from a landlocked Alewife that was not subjected to a salinity challenge experiment to serve as a standard material, referred to as a calibrator sample. Standard curves derived from triplicate dilutions of calibrator samples yielded estimates of amplification efficiency (E), the ability of a primer set to double the target amplicon after each PCR cycle. E values for each primer set were close to the ideal value of 2 (EF1α: 1.94, NKCC: 1.95, CFTR: 1.98). Samples of the calibrator were included on each PCR plate in triplicate. Relative expression was calculated using the $\Delta\Delta C_T$ method (Pfaffl 2001),

$$\Delta\Delta C_T = \frac{E_{tar}^{\Delta C_T tar(calibrator-test)}}{E_{ref}^{\Delta C_T ref(calibrator-test)}} \quad (1)$$

where $E_{tar}$ is the amplification efficiency of the primer for the gene of interest, $E_{ref}$ is the amplification efficiency of the primer for the reference gene, $\Delta C_T$ tar (target) is the difference in cycle threshold value between calibrator and test sample for the gene of interest, and $\Delta C_T$ ref (reference) is the difference in $C_T$ between calibrator and test sample for the reference gene. Note that the purpose of the calibrator $C_T$ value is to account for variance arising from random differences in run conditions from plate to plate. cDNA samples were loaded onto plates in sequential order by time and date of collection. A total of five plates were needed for each gene of interest.

*Statistical analyses*

We used survival analysis to determine differences in survivorship between life history forms (whether anadromous or landlocked) and salinity treatments. Length was included as a continuous covariate since it differed among life history forms and between trials (Table 1). Data were analyzed by fitting a non-parametric survival model (the Cox proportional hazards model) in R version 2.12.1. The Cox method models death rate as a log-linear function of predictors, where regression coefficients give the relative effect of covariates on survivorship (i.e., the proportion of individuals alive at a given time). The model computes a baseline hazard function (i.e., the instantaneous risk of death at baseline levels of covariates) that is modified multiplicatively by the covariates (Venables and Ripley 1999). Trial was used as a stratification variable, which permitted the calculation of separate baseline hazard functions for each case. We computed the hazard ratios (HR) for each parameter of the Cox model using maximum

likelihood estimates in order to compare the hazard rates among treatments and life history forms. For discrete factors in the model (i.e., life history form and salinity) the HR represents the ratio of the hazard rates between a given category and the reference category (selected as anadromous for life history form and 30 ppt for salinity). For continuous covariates (i.e., length), the HR is the ratio of hazard rates for an increase of one unit of the variable.

We used linear mixed effects models to determine differences in mean NKA activity (n = 70 for anadromous; n = 49 for landlocked), log-transformed plasma osmolality (n = 54 for anadromous; n = 36 for landlocked), and log-transformed relative gene expression (n = 27 for anadromous; n = 22 for landlocked). Models included life history form and salinity treatment as fixed effects, with length as a covariate (log-transformed length was used for plasma osmolality and gene expression data). We included two random effects in our model: 1) trial (i.e., September, October or November trial month), and 2) tank (experimental tanks at each level of salinity treatment, life history form and trial were given a unique identifier). This experiment was intended to be a full factorial block design, where trial represents a random blocking variable, and tank represents a plot within a block. As random effects, both trial and tank were expected to influence the variance of the dependent variables; in a mixed effects model these random effects are accounted for in order to properly infer the impact of the fixed effects. We chose this approach over an alternative approach treating trial dates as fixed treatments of interest. Although the latter approach would provide an opportunity to explore seasonal variation in osmoregulatory physiology, more dispersion in sampling dates would be required for an adequate test of seasonal influence. Models were run using the lmer function (*lme4* package) in R version 2.15.2 (R Core Team 2012). Significance testing of linear mixed effects models was conducted using the function pvals.fnc in R (*languageR* package). This function calculates p-

values from a linear mixed model fit with the lmer function by generating confidence intervals from the posterior distribution of 10,000 parameter estimates obtained by Markov chain Monte Carlo simulations (MCMC randomization test). Full models included 3-way interactions of life history form, salinity treatment and length, but were reduced where non-significant interactions ($p > 0.05$) were found. A table summarizing results of final linear mixed effects models (including MCMC upper and lower confidence limits and p-values) is available in supplementary material (Table S1). In models where length was a significant ($p < 0.05$) factor, we estimated least-squares means (LSmeans; Searle et al. 1980) using the PROC GLM procedure in SAS version 9.3. This procedure calculates the mean of each factor at a mean common length. Differences between LSmeans for each factor were determined using a Student's t-test. We analyzed two separate datasets for plasma osmolality values. The first dataset consisted of all samples including those pooled during measurement, but excluding length as a covariate. In the second dataset, we removed pooled samples in order to use length as a covariate in a linear mixed model. Blood samples for plasma osmolality and gill samples for real-time PCR were not obtained during the September trial and as such, analyses for these measures include data from October and November trials only. Eliminating the September trial data from the NKA activity dataset does not affect the findings.

**Results**

The average length of Alewives differed between life history forms and trials (Table 1), which was expected given that landlocked Alewives tend to be smaller overall at age (Scott and Crossman 1973), and that trials were run one month apart. An analysis of variance revealed a significant effect of life history form ($F_{1,228} = 135$; $p < 0.001$) and trial ($F_{2,228} = 483$; $p < 0.001$) on standard length. Survivorship of Alewives differed between salinity treatments and life

history forms (Fig. 1). A Cox proportional hazards model revealed a significant effect of life history form ($z = 2.44$, $p = 0.01$), salinity ($z = 3.85$, $p < 0.001$) and length ($z = -3.83$, $p < 0.001$) on survivorship among all trials. Anadromous Alewives survived nearly all salinity treatments in each trial (the one exception being the 30 ppt treatment during the September trial in which there was 14% mortality). In contrast, 10% to 40% of landlocked Alewives died at each salinity treatment, and mortality rate was higher in seawater than in freshwater (Fig. 1). A Cox proportional hazards model run within landlocked Alewives revealed a significant effect of treatment at 30 ppt ($z = 3.34$, $p < 0.001$) as compared to 1 ppt. The effect of 20 ppt on survival compared to 1 ppt was non-significant ($z = 0.67$, $p = 0.5$). With respect to the main effect of life history form, the hazard ratio for anadromous Alewives was approximately one-fifth that of landlocked Alewives (HR = 0.17). For the main effect of salinity, separate hazard ratios were computed for 1 ppt (HR = 0.15) and 20 ppt (HR = 0.29). These ratios indicate that, compared to 30 ppt, hazard was reduced by 85% and 71% at 1 ppt and 20 ppt, respectively. The estimated hazard ratio for standard length was HR = 0.87, i.e., for every 10 mm increase in length, the risk of death decreased by about 75%.

We detected strong differences in plasma osmolality between life history forms and salinity treatments. Landlocked Alewives had higher plasma osmolality than anadromous Alewives in seawater treatments, and there was a positive effect of salinity on plasma osmolality (Fig. 2). Overall, seawater treatment resulted in higher osmolality among landlocked and anadromous Alewives (MCMC randomization test; $p = 0.002$) in a reduced linear mixed effects model where length was included as a covariate. The strength of the increase in plasma osmolality with salinity differed between landlocked and anadromous Alewives; we found a significant interaction between life history form and salinity treatment (MCMC randomization

test; p = 0.008). The strongest between-life history form difference in plasma osmolality occurred in Alewives treated at 30 ppt; on average, plasma osmolality of landlocked Alewives at 30 ppt was approximately 30 mosmol/kg (8%) higher than anadromous Alewives. A within-treatment linear mixed effects model revealed a significant effect of life history form at 30 ppt (MCMC randomization test; p = 0.05). At 20 ppt, plasma osmolality among landlocked Alewives was 10 mosmol/kg higher (3%) than anadromous Alewives (MCMC randomization test; p = 0.06), and only 2 mosmol/kg (0.6%) higher at 1 ppt (MCMC randomization test; p = 0.70). Analyses that included pooled plasma osmolality samples yielded similar results regarding salinity and life history form effects; we detected a significant life history form by salinity interaction (MCMC randomization test; p = 0.02). The pooled osmolality data are plotted in Figure 2 for completeness.

Gill $Na^+/K^+$-ATPase (NKA) activity increased with salinity treatment for landlocked and anadromous Alewives, but upregulation was weaker among landlocked individuals (Fig. 3). A reduced linear mixed effects model, including two-way interactions among salinity, life history form and length, revealed a significant interaction of life history form and salinity (MCMC randomization test; p = 0.02) as well as an interaction of length with salinity (MCMC randomization test; p = 0.01). We subsequently evaluated life history form differences in NKA activity separately in each of the three salinity treatments by running separate linear mixed effects models. NKA activity was significantly lower in landlocked Alewives compared to anadromous Alewives at 20 ppt (MCMC randomization test; p = 0.04) and 30 ppt (MCMC randomization test; p = 0.002). We found no significant differences in NKA activity between life history forms at 1 ppt (MCMC randomization test; p = 0.30). At 30 ppt, we also detected a significant main effect of length on NKA activity (MCMC randomization test; p = 0.02); NKA

activity is negatively correlated with length ($r = -0.39$; $p = 0.02$). To account for the effect of length, we calculated values for NKA activity at a mean common length (LSmeans) for each level of life history form and salinity treatment (Fig. 3). The LSmeans NKA activity was lower among landlocked Alewives as compared to anadromous Alewives by approximately 20% at 20 ppt (t-test; $p = 0.002$) and 30% at 30 ppt (t-test; $p < 0.0001$). We detected no difference between life history forms at 1 ppt (t-test; $p = 0.30$). These results are consistent with those from the linear mixed effects models.

Landlocked and anadromous Alewives differed in expression of seawater osmoregulation genes *NKCC* and *CFTR* at the gill. Expression of *CFTR* varied with life history form and salinity (Fig. 4). A reduced linear mixed effects model, including only main effects of salinity, life history form and length, revealed that *CFTR* mRNA expression increased significantly with salinity exposure (MCMC randomization test; $p = 0.03$) and that mRNA expression was significantly reduced in landlocked Alewives compared to anadromous Alewives (MCMC randomization test; $p = 0.008$). Although anadromous Alewives had higher *CFTR* expression across all salinity treatments, between-life history form differences in *CFTR* expression were highest at 30 ppt (2-fold difference between life history forms; Fig. 4). Expression of *NKCC* also varied with life history form and salinity (Fig. 5). A linear mixed effects model revealed a significant three-way interaction of life history form, salinity and length (MCMC randomization test; $p = 0.04$). Because this three-way interaction is difficult to interpret, we ran linear mixed effects models separately for each salinity treatment. We found that *NKCC* expression was 4-fold greater among anadromous Alewives at 30 ppt (MCMC randomization test; $p = 0.04$), and over 2-fold greater at 20 ppt (though this effect was non-significant: MCMC randomization test; $p =$

0.11). There were no significant differences in *NKCC* expression between life history forms at 1 ppt (MCMC randomization test; $p = 0.12$).

**Discussion**

Ecological transitions from marine to freshwater environments involve the elimination of seawater as a source of selection (relaxed selection; Lahti et al. 2009). Since relaxed selection is thought to weaken or eliminate trait expression, we predicted that hypo-osmoregulatory function, and the molecular machinery that underlies it, would be reduced in freshwater-restricted, landlocked Alewives, compared to their seawater-migrating anadromous ancestor. We found that permanent freshwater residency in Alewives results in significant reductions in seawater survival and hypo-osmoregulatory capacity, and a weaker response of multiple molecular pathways that drive seawater osmoregulation.

As a model for studying the evolution of osmoregulatory function and associated mechanisms, Alewives are distinct from other species studied previously in several important respects. Alewives are in a predominantly marine family (Nelson 2006). In contrast to freshwater populations of *Fundulus spp.*, landlocked Alewife populations clearly arose as a result of multiple independent isolating events, and there is little or no gene flow of anadromous genotypes into landlocked populations (Palkovacs et al. 2008); this system is therefore ideal for testing parallel evolutionary change. Landlocked populations were founded recently (300-500 year ago; Palkovacs et al. 2008) compared to most landlocked populations of Threespine Stickleback (circa 10,000 years ago; Bell and Foster 1994), allowing us to test whether the osmoregulatory system can evolve on shorter time scales than has been previously established. Comparison of Alewives to sticklebacks, killifishes, and salmonids, provide an opportunity to examine whether freshwater restriction results in convergent changes to osmoregulatory

function. Given their ancestry and unique life history, landlocked Alewives are ideal for examining the outcome of relaxed selection on hypo-osmoregulation.

Juvenile anadromous Alewives were more tolerant of all salinities than landlocked Alewife juveniles, and in particular, there was a pronounced difference in survivorship between life history forms challenged at 30 ppt seawater (Fig. 1). Survival of anadromous Alewives at all salinity treatments was high (no more than 14% mortality at 30 ppt, and no deaths at 1 ppt or 20 ppt). The broad tolerance of anadromous Alewives was expected given their life history. Survival differences between life history forms were the least pronounced in 1 ppt freshwater (an 11% difference on average), slightly greater in 20 ppt seawater (a 17% difference on average), and dramatically different in 30 ppt seawater (a 40% difference on average; Fig. 1). We did not expect to find life history form differences in tolerance at 1 ppt since both landlocked and anadromous individuals inhabit freshwater as juveniles. Lowered survival in 1 ppt among landlocked Alewives may be caused by a higher sensitivity to the stress of handling (J. Velotta, personal observation), rather than a true reduction in tolerance of 1 ppt. Regardless, the strong effect of 30 ppt treatment on landlocked Alewife survival, as well as prominent life history form differences at this salinity, indicate that landlocked Alewives have a reduced ability to tolerate seawater compare to anadromous Alewives. This evolutionary shift may be caused in part by changes to the physiological and molecular mechanisms that regulate ion secretion in seawater.

Reduced seawater survival in landlocked Alewives is consistent with findings in landlocked life history forms of salmonids (e.g., Arctic Char: Staurnes et al. 1992) and of species with marine ancestry (e.g., Threespine Stickleback: McCairns and Bernatchez 2010; killifish: Scott and Schulte 2005). Interspecific differences in seawater tolerance have also been observed, particularly among closely related species of killifishes. In the genus *Lucania*, the stenohaline

freshwater species *L. goodei* survives considerably less well in seawater than its euryhaline congener *L. parva* (Fuller 2008). Whitehead (2010) examined 23 species of *Fundulus* and demonstrated that each of five independent transitions into freshwater has resulted in a significant loss of salinity tolerance. Taken together, evolution of reduced seawater tolerance accompanying adaptation to an entirely freshwater environment appears to be common among highly divergent groups of fishes, both intra- and inter-specifically, and may therefore represent a ubiquitous evolutionary consequence of ecological transitions to freshwater.

There are several physiological explanations for the observed differences in hypo-osmoregulatory capacity between landlocked and anadromous Alewives. One possibility is that landlocked Alewives experience reductions in osmosensing, a process involving the detection of osmotic changes, which activates ion transport processes that restore homeostasis (Evans 2010). Another possible (though not mutually exclusive) explanation is that land-locking has resulted in reduced ion secretory capacity or control over ion permeability. Reductions in ion secretory capacity are likely to be the result of changes in the function of ion transporters in gill ionocytes, which are equipped with a suite of well-characterized ion transport proteins (Evans et al. 2005). We chose to analyze life history form differences in several ion transporters involved in seawater osmoregulation as a way of assessing changes in the mechanisms that promote ion secretion at the gills. Although we did not attempt to assess differences in osmosensing between life history forms, future work should be aimed at establishing whether landlocked Alewives show reduced osmosensing capabilities in seawater.

We found that $Na^+/K^+$-ATPase activity increased with seawater exposure among anadromous Alewives (Fig. 3). This result corresponds with previous studies of anadromous Alewives that demonstrated that NKA activity increased by 75% after long-term seawater

acclimation (Christensen et al. 2012; McCormick et al. 1997). Upregulation of NKA activity in seawater has also been reported in American Shad (a congener of the alewife; Zydlewski and McCormick 1997b). In our study, upregulation of NKA activity with salinity was dramatically reduced in landlocked Alewives (Fig. 3), which may, at least in part, account for their reduced hypo-osmoregulatory capacity. Such reductions in upregulation of NKA activity among freshwater-adapted populations is consistent with that found in the copepod *Eurytemora affinis* by Lee et al. (2011), and the killifish by Scott and Schulte (2005).

We found a negative correlation between gill NKA activity and fish length, which was unexpected. Ion flux rates may be greater for smaller fish and it is possible that higher gill NKA activity is due to higher demand for active ion uptake in smaller individuals. Alternatively, there may be size-dependent developmental differences in gill NKA activity related to the acquisition of salinity tolerance and subsequent migration. However, since migrating anadromous individuals are generally larger than non-migrants (Gahagan et al. 2010), we would have expected a positive (rather than negative) relationship with size and NKA activity, which is upregulated prior to seawater migration in other alosines (Zydlewski and McCormick 1997a). Regardless, when we calculate NKA activity at a mean common length (LSmeans), we find consistent patterns as with linear mixed effects models, indicating that differences in fish length is not the likely driver of reduced NKA activity among landlocked Alewives.

Among anadromous and landlocked Alewives, seawater exposure resulted in upregulation of *NKCC* and *CFTR* mRNA (Figs. 4 and 5), which is consistent with these transporters' roles in ion secretion (Evans et al., 2005). *NKCC* and *CFTR* expression among landlocked Alewives, however, showed a weaker response to seawater relative to expression by anadromous Alewives (Figs. 4 and 5). Land-locking, therefore, appears to have resulted in

reduced responsiveness of hypo-osmoregulatory pathways to seawater, which is consistent with findings in freshwater adapted populations of the killifish *Fundulus heteroclitus* (Scott and Schulte 2005). Recent work has identified interspecific changes in seawater function that mirror the intraspecific changes found here. *NKA* and *NKCC* mRNA is expressed at lower levels in the stenohaline freshwater *L. goodei* compared to its euryhaline congener, *L. parva,* when fish are transferred to seawater (Berdan and Fuller 2012). Currently, we have no evidence to suggest that landlocked and anadromous life history forms differ constitutively in hypo-osmoregulatory function. Our results strongly suggest that the physiological plasticity associated with the response to seawater challenge (i.e., the upregulation of NKA activity, *NKCC* and *CFTR* expression in seawater) has been reduced in landlocked forms. Constitutive expression differences between landlocked an anadromous forms of fish have been explored previously (in Atlantic salmon; Nilsen et al 2007), and future studies will address this issue in Alewives.

A weaker response of the physiological pathways involved in hypo-osmoregulation among landlocked Alewives likely accounts for reduced ion secretory capabilities in seawater, and may have contributed to their higher mortality relative to anadromous counterparts. NKA, NKCC and CFTR allow for the secretion of excess $Na^+$ and $Cl^-$ out of gill ionocytes in hypo-osmoregulating fishes. $Na^+/K^+$-ATPase is the primary driving force for ion secretion at the gill; it establishes a strong electrochemical gradient by maintaining low intracellular $Na^+$ levels and keeping ionocytes negatively charged. NKCC co-transports $Na^+$, $K^+$ and $Cl^-$ into the cell, and $Cl^-$ is then secreted through CFTR, an apical ion channel. $Na^+$ ions are subsequently secreted paracellularly through shallow tight junctions between ionocytes and accessory cells (Evans et al. 2005; Hwang and Lee 2007; Marshall and Grosell 2006). Lowered activity of NKA and expression of *NKCC* and *CFTR* in landlocked Alewives likely reduces $Na^+$ and $Cl^-$ secretion at

gill ionocytes, which may account for the observed reductions in hypo-osmoregulatory capacity. In particular, NKCC and CFTR are the primary ion transporters by which $Cl^-$ is secreted at the gill, and the same upstream transcription factors and/or hormones may control their expression.

Evolutionary changes in seawater survival, hypo-osmoregulatory capacity and the expression and activity of pathways involved in ion secretion among landlocked Alewives may be the result of relaxed selection, since the presumed source of selection for hypo-osmoregulatory function (i.e., seawater) has been eliminated from their life cycle. Traits that regulate hypo-osmoregulatory function may bear constitutive maintenance costs even in freshwater environments where they are not being expressed. Trait loss is predicted to occur rapidly where constitutive costs are high since they would reduce fitness (Lahti et al. 2009). Trait decay would proceed more slowly (or not at all) when positively correlated with other functional traits or if there were no energetic costs to maintaining hypo-osmoregulatory function in the freshwater environment. Given that the time since divergence from the anadromous ancestor is short (circa 300-500 years), and that we have demonstrated significant differences in survival and osmoregulatory function in seawater, it is likely that hypo-osmoregulatory function bears a high maintenance cost in Alewives, and that natural selection is acting to reduce or eliminate it in landlocked forms. Rapid evolutionary reductions in seawater survival and NKA activity have been observed previously in the euryhaline copepod *Eurytemora affinis* following invasion into freshwater (Lee et al. 2011; Lee et al. 2007; Lee et al. 2003). To our knowledge, the decay of hypo-osmoregulatory function in landlocked Alewives presented here is the most rapid of such declines in a marine derived fish documented to date (e.g., several hundred years compared to approximately 10,000 years in threespine stickleback; Bell and Foster 1994). Convergent patterns of reduced hypo-osmoregulatory function and changes to salt-secreting pathways among

freshwater forms of salmonids (e.g., Nilsen et al 2007), killifish (e.g., Scott and Schulte 2005), Threespine Stickleback (e.g., McCairns and Bernatchez 2010), and now Alewives, suggests that such changes represent important adaptations to ecological movement into freshwater and are ubiquitous consequences of relaxed selection on seawater function.

The tempo and mode of evolutionary change in hypo-osmoregulation may differ among independently derived landlocked Alewife populations, particularly if they differ in time since divergence from the anadromous ancestor. The possibility of among-landlocked population differences is interesting and will be the subject of future experimentation, but could not be adequately addressed with the current study design. It is also possible that the life history form divergence in hypo-osmoregulatory function we observe is the result of environmental effects on osmoregulatory phenotypes acting on the young Alewives or through maternal effects. One way to eliminate such effects is to breed and rear animals from different life history forms in a common laboratory environment (a common-environment experiment sensu Conover and Schultz 1995). Since the lakes in this study do not differ in salinity regime, and since no individuals from either life history form experienced seawater prior to testing, environmental effects that would have caused divergence in salinity tolerance or osmoregulatory capacity are likely to be minimal or non-existent.

An alternative, but not mutually exclusive, explanation is that reductions in seawater function among landlocked Alewives may be caused by selection favoring enhanced freshwater performance. Selection for improved ion uptake in freshwater may increase fitness in landlocked forms, especially by enhancing survival in winter months. In anadromous Alewives, cold freshwater induces mortality and reduces plasma and muscle sodium levels relative to fish at warmer temperatures (McCormick et al. 1997; Stanley and Colby 1971). Some freshwater

populations of euryhaline species have higher survival in freshwater (Lee et al. 2007; Lee et al. 2003) and better regulation of plasma ions (Whitehead et al. 2011) during freshwater challenge relative to seawater or brackish populations of the same species. These studies have also identified several ion transporters under selection in freshwater (e.g., V-type H+-ATPase: Lee et al. 2011). Freshwater challenges in killifish indicate that enhanced freshwater tolerance among freshwater-associated populations corresponds with improved plasma $Cl^-$ regulation (Scott et al. 2004; Whitehead et al. 2012). If there is a physiological tradeoff associated with osmoregulatory function in different salinity environments, enhanced osmoregulatory function in freshwater could lead to reduced function in seawater. In particular, selection for improved plasma $Cl^-$ regulation in freshwater may trade-off against $Cl^-$ secretion in seawater, which may explain the strong reductions in transcription of *NKCC* and *CFTR* (the main $Cl^-$ transporters in seawater ionocytes of the gill). It will be of value to determine ion uptake capacity in landlocked and anadromous Alewives in order to elucidate the effects of evolutionary changes in freshwater capacity as a result of land-locking.

In summary, ecological transitions into freshwater have led to substantial reductions in seawater tolerance and hypo-osmoregulatory capacity in landlocked Alewives, which are likely driven by changes in the molecular machinery that regulate ion secretion, namely the reduced response of NKA, CFTR and NKCC to seawater. Because fish in landlocked lakes no longer need to function in seawater, we interpret these changes as the result of relaxed selection on hypo-osmoregulatory function. The present study represents a novel combination of findings and a greater integration of the molecular, physiological and whole-organism level responses to seawater than has been conducted previously. This work also confirms that Connecticut Alewives can serve as a model system to explore the evolution of osmoregulatory function after

adaptation to a fully freshwater life cycle. Although our targeted approach has identified specific ion transporters that may be subject to evolutionary change associated with freshwater transitions, more research is needed on other important osmoregulatory effectors in seawater (e.g., aquaporins) and freshwater (e.g., $Na^+/H^+$ exchanger, $Na^+/Cl^-$ cotransporter, V-type $H^+$-ATPase) in order to provide insight into the suite of evolutionary changes associated with movement in freshwater.

**Acknowledgements**

We thank Dr. David M. Post, Andrew Jones, and Megan Cruz for their help collecting juvenile Alewives. We thank Dr. Arne K. Christensen for assisting in gill tissue sample collection, and Michael O'Dea for assisting in sample collection and for running $Na^+/K^+$-ATPase activity assays. We also thank Emily Funk for assisting with real-time quantitative PCR assays. Many thanks to Carl Schlichting, Mark Urban, Brian G. Walker, Alejandro Rico-Guevara, Jeffrey Divino, and two anonymous reviewers for providing helpful comments on the manuscript. This study was funded by Connecticut Sea Grant, the University of Connecticut Center for Environmental Science and Engineering, the American Museum of Natural History Lerner Gray Fund, the University of Connecticut Department of Ecology and Evolutionary Biology, and Sigma Xi Grants-in-Aid of Research. The authors declare no conflicts of interest.

**References**

Able KW, Palmer AR (1988) Salinity effects on fertilization success and larval mortality of *Fundulus heteroclitus*. Copeia:345-350

Bell MA, Foster SA (1994) The evolutionary biology of the threespine stickleback. Oxford University Press, Oxford

Berdan EL, Fuller RC (2012) Interspecific divergence of ionoregulatory physiology in killifish: insight into adaptation and speciation. J Zool 287:283-291

Christensen AS, Hiroi J, Schultz ET, McCormick SD (2012) Branchial ionocyte organization and ion-transport protein expression in juvenile alewives acclimated to freshwater or seawater. J Exp Biol 215:642-652

Conover DO, Schultz ET (1995) Phenotypic similarity and the evolutionary significance of countergradient variation. Trends Ecol Evol 10:248-252

Crespi BJ, Fulton MJ (2004) Molecular systematics of Salmonidae: combined nuclear data yields a robust phylogeny. Mol Phylogenet Evol 31:658-679

DeFaveri J, Merila J (2013) Local adaptation to salinity in the three-spined stickleback? J Evol Biol

DeFaveri J, Shikano T, Shimada Y, Goto A, Merila J (2011) Global analysis of genes involved in freshwater adaptation in threespine sticklebacks (*Gasterosteus aculeatus*). Evolution 65:1800-1807

Evans DH, Piermarini PM, Choe KP (2005) The multifunctional fish gill: dominant site of gas exchange, osmoregulation, acid-base regulation, and excretion of nitrogenous waste. Physiol Rev 85:97-177

Evans TG (2010) Co-ordination of osmotic stress responses through osmosensing and signal transduction events in fishes. J Fish Biol 76:1903-1925

Foote CJ, Wood CC, Clarke WC, Blackburn J (1992) Circannual cycle of seawater adaptability in *Oncorhynchus nerka*: Genetic differences between sympatric sockeye salmon and kokanee. Can J Fish Aquat Sci 49:99-109

Fuller RC (2008) A test for a trade-off in salinity tolerance in early life-history stages in *Lucania goodei* and *L. parva*. Copeia 2008:154-157

Gahagan BI, Gherard KE, Schultz ET (2010) Environmental and endogenous factors influencing emigration in juvenile anadromous alewives. Trans Am Fish Soc 139:1069-1082

Hwang P-P, Lee T-H (2007) New insights into fish ion regulation and mitochondrion-rich cells. Comp. Biochem. Phys., A 148:479-497

Jones FC et al. (2012) A genome-wide SNP genotyping array reveals patterns of glodbal and repeated species-pair divergence in sticklabacks. Curr. Biol. 22:83-90

Lahti DC et al. (2009) Relaxed selection in the wild. Trends Ecol Evol 24:487-496

Lee CE, Bell MA (1999) Causes and consequences of recent freshwater invasions by saltwater animals. Trends Ecol Evol 14:284-288

Lee CE, Kiergaard M, Gelembiuk GW, Eads BD, Posavi M (2011) Pumping ions: rapid parallel evolution of ion regulation following habitat invasions. Evolution 65:2229-2244

Lee CE, Remfert JL, Chang Y-M (2007) Response to selection and evolvability of invasive populations. Genetica 129:179-192

Lee CE, Remfert JL, Gelembiuk GW (2003) Evolution of physiological tolerance and performance during freshwater invasions. Integr Comp Biol 43:439-449

Li C, Orti G (2007) Molecular phylogeny of Clupeiformes (Actinopterygii) inferred from nuclear and mitochrondrial DNA sequences. Mol Phylogenet Evol 44:386-398

Marshall WS, Grosell M (2006) Ion transport, osmoregulation, and acid-base balance. In: Evans DH, Claiborne JB (eds) The Physiology of Fishes, 3rd edn. CRC Taylor and Francis, Boca Raton, FL, pp 177-230

McCairns RJS, Bernatchez L (2010) Adaptive divergence between freshwater and marine sticklebacks: insights into the role of phenotypic plasticity from and integrated analysis of candidate gene expression. Evolution 64:1029-1047

McCormick SD (1993) Methods of nonlethal gill biopsy and measurement of Na+, K+-ATPase activity Can J Fish Aquat Sci 50:656-658

McCormick SD (2013) Smolt Physiology and Endocrinology. In: McCormick SD, Farrell AP, Brauner CJ (eds) Fish Physiology, vol 32. Academic Press

McCormick SD, Saunders RL (1987) Preparatory physiological adaptations for marine life of salmonids: osmoregulation, growth, and metabolism. In: Dadswell MJ, Klauda RJ, Moffitt CM, Saunders RL, Rulifson RA, Cooper JE (eds) Common Strategies of Anadromous and Catadromous Fishes. American Fisheries Society, Bethesda, MD, pp 223-229

McCormick SD, Shrimpton JM, Zydlewski JD (1997) Temperature effects on osmoregulatory physiology of juvenile anadromous fish. In: Wood CM, McDonald DG (eds) Global Warming: Implications for Freshwater and Marine Fish. Society of Experimental Biology Seminar Series 61

Nelson JS (2006) Fishes of the World. John Wiley & Sons, New York

Palkovacs EP, Dion KB, Post DM, Caccone A (2008) Independent evolutionary origins of landlocked alewife populations and rapid parallel evolution of phenotypic traits. Mol Ecol 17:582-597

Pfaffl MW (2001) A new mathematical model for relative quantification in real-time RT-PCR. Nucleic Acids Res 29:e45

Powers DA et al. (1986) Genetic variation in *Fundulus heteroclitus*: geographic distribution. Am. Zool. 26:131-144

Schultz ET, McCormick SD (2013) Euryhalinity in an evolutionary context. In: McCormick SD, Farrell AP, Brauner CJ (eds) Fish Physiology, vol 32. Academic Press

Scott GR, Rogers JT, Richards JG, Wood CM, Schulte PM (2004) Intraspecific divergence of ionregulatory physiology in the euryhaline teleost *Fundulus heterclitus*: possible mechanisms of freshwater adaptation. J Exp Biol 207:3399-3410

Scott GR, Schulte PM (2005) Intraspecific variation in gene expression after seawater transfer in gills of euryhaline killifish *Funulus heterclitus*. Comp Biochem Phys A 141:176-182

Scott WB, Crossman EJ (1973) Freshwater Fishes of Canada

Searle SR, Speed FM, Milliken GA (1980) Marginal means in the linear model: an alternative to least squares means. Amer Statistician 34:216-221

Shimada Y, Shikano T, Merila J (2011) A high incidence of selection on physiolically important genes in the threespine stickleback, *Gasterosteus aculeatus*. Mol Biol Evol 28:181-193

Stanley JG, Colby PJ (1971) Effects of temperature on electrolyte balance and osmoregulation in the alewife (*Alosa pseudoharengus*) in fresh and sea water. Trans Am Fish Soc 100:624-638

Staurnes M, Sigholt T, Lysfjord G, Gulseth O (1992) Difference in the seawater tolerance of anadromous and landlocked populations of Arctic char (*Salvelinus alpinus*). Can J Fish Aquat Sci 49:443-447

Stearley RF (1992) Historical ecology of Salmoninae, with special reference to Oncorhynchus. In: Mayden RL (ed) Systematics, historical ecology, and North American Freshwater Fishes. Standford Press, Stanford

Venables WN, Ripley BD (1999) Modern applied statistics with s-plus. Springer-Verlag, New York, New York

Whitehead A (2010) The evolutionary radiation of diverse osmotolerant physiologies in killifish (*Fundulus sp.*). Evolution 64:2070-2085

Whitehead A, Roach JL, Zhang S, Galvez F (2011) Genomic mechanisms of evolved physiological plasticity in killifish distributed along an environmental salinity gradient. PNAS 108:6193-6198

Whitehead A, Roach JL, Zhang S, Galvez F (2012) Salinity- and population-dependent genome regulatory response during osmotic acclimation in the killifish (*Fundulus heteroclitus*) gill. J Exp Biol 215:1293-1305

Wilson MVH, Li GQ (1999) Osteology and systematic position of the Eocene salmonid *Eosalmo driftwoodensis* Wilson from western North America. Zool J Linn Soc 125:279-311

Yako LA (1998) Community interactions influencing juvenile anadromous herring in freshwater : migration cues and predation. In: Wildlife and Fisheries Biology, vol. M.S. University of Massachusetts, Amherst, p 124

Zydlewski J, McCormick SD (1997a) The loss of hyperosmoregulatory ability in migrating juvenile shad, *Alosa sapidissima*. Can J Fish Aquat Sci 54:2377-2387

Zydlewski J, McCormick SD (1997b) The ontogeny of salinity tolerance in the American shad, *Alosa sapidissima*. Can J Fish Aquat Sci 54:182-189

**Tables**

**Table 1** Details of salinity challenge experiments. Trials consisted of one comparison between landlocked and anadromous Alewives, each consisting of 60-hour salinity challenges at 1 ppt, 20 ppt and 30 ppt. Lakes are located in East Lyme, Connecticut (Bride Lake and Pattagansett Lake) and Old Lyme, Connecticut (Rogers Lake). Mean standard length ± standard error of the mean of fish from each salinity challenge is also reported

| Trial | Life History Form | Location | Date (2009) | Length (mm) |
|---|---|---|---|---|
| Sep | Landlocked | Rogers Lake | 09-Sep – 11-Sep | 48.5 ± 0.9 |
| Sep | Anadromous | Bride Lake | 15-Sep – 18-Sep | 56.8 ± 0.8 |
| Oct | Landlocked | Pattagansett Lake | 29-Sep – 02-Oct | 61.6 ± 0.7 |
| Oct | Anadromous | Bride Lake | 06-Oct – 09-Oct | 70.2 ± 0.5 |
| Nov | Landlocked | Pattagansett Lake | 17-Nov – 20-Nov | 78.2 ± 0.6 |
| Nov | Anadromous | Bride Lake | 10-Nov – 12-Nov | 73.2 ± 0.6 |

**Table 2** The number of Alewives stocked from each population (A: Anadromous; L: Landlocked) in each salinity treatment (1 ppt, 20 ppt, 30 ppt) during each trial (Sep: September; Oct: October; Nov: November).

| | 1 ppt | | 20 ppt | | 30 ppt | |
|---|---|---|---|---|---|---|
| **Trial** | **A** | **L** | **A** | **L** | **A** | **L** |
| Sep | 15 | 12 | 15 | 11 | 14 | 12 |
| Oct | 10 | 14 | 15 | 14 | 13 | 15 |
| Nov | 14 | 11 | 12 | 11 | 13 | 11 |

**Table 3** Primer sequences (F: forward; R: reverse) for each candidate gene (*CFTR* and *NKCC*) and a reference gene (EF1α). Product size indicates the size of the pcr amplicon expressed in number of base pairs (bp). Primers were designed from Alewife gill transcriptome sequence (J. Velotta, unpublished).

| Gene | Primer sequence | Product size (bp) |
|---|---|---|
| *CFTR* | F: TTCCCTGACAAGCTGGACT<br>R: GTGCAGGTGGAGAAGGAGTC | 197 |
| *EF1α* | F: GCTGGAAAATCGAGCGTAAG<br>R: CACGGGTACGGTTCCAATAC | 155 |
| *NKCC* | F: ACCACCATTACTGGCGTCTC<br>R: TACATGGCTACTGCCACAGC | 158 |

**Figures**

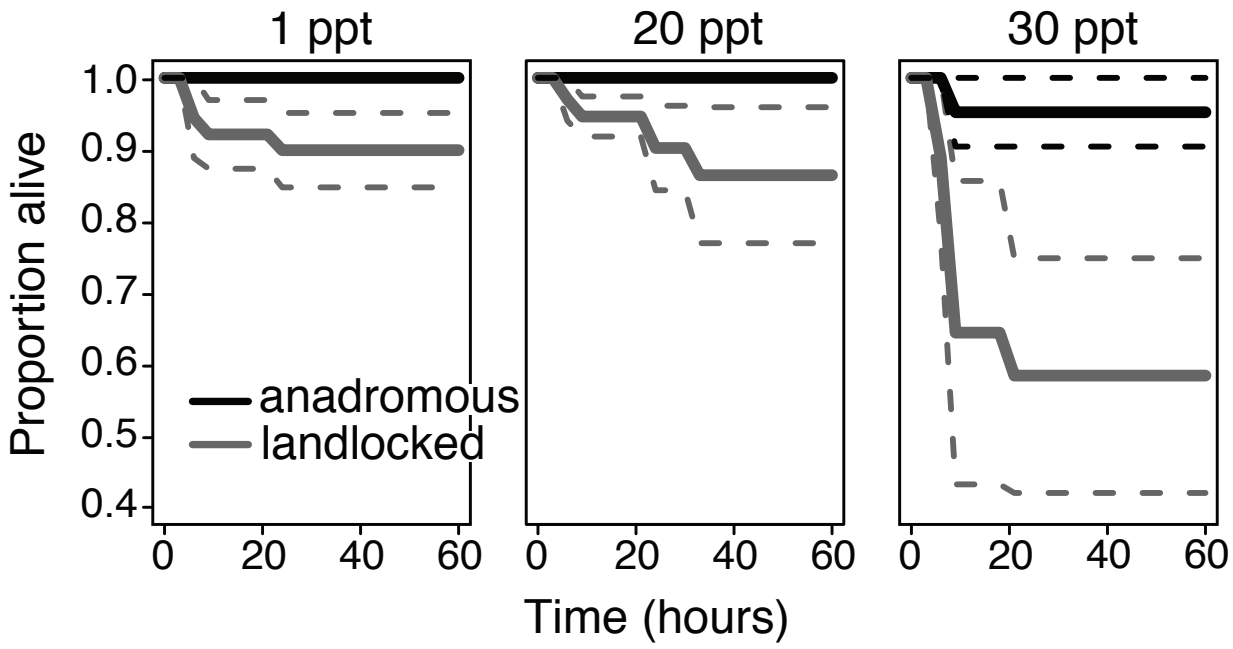


**Figure 1** Survival of Alewives for each of three salinity treatments: 1 ppt, 20 ppt, 30 ppt. Solid lines represent the mean proportion of anadromous (black lines) and landlocked (gray lines) Alewives alive over time. Treatments were checked every 12 hours for mortality. Dotted lines are mean proportion alive ± standard error of the mean. There is a significant main effect of population ($p = 0.01$)

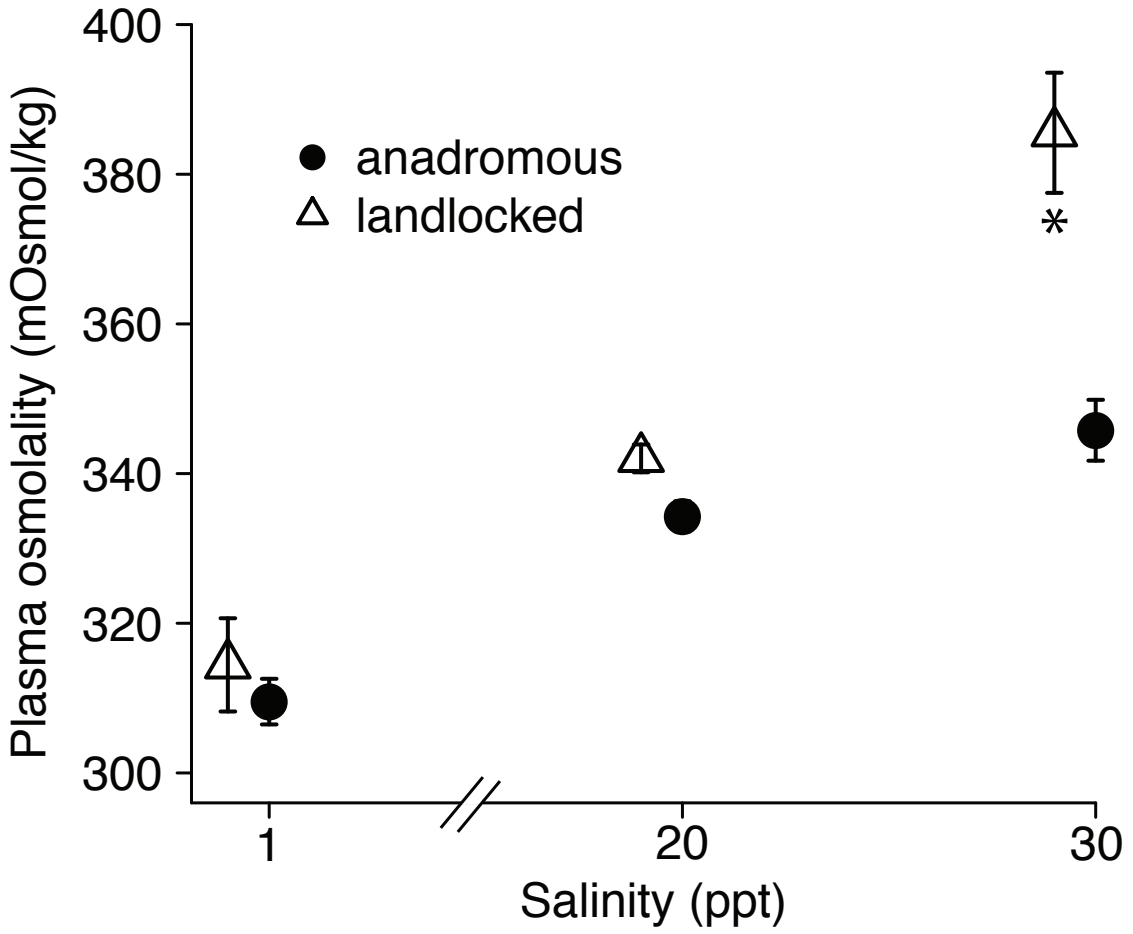


**Figure 2** Plasma osmolality of anadromous Alewives (black circles) at 1 ppt (n = 15), 20 ppt (n = 25), and 30 ppt (n = 23); and landlocked Alewives (open triangles) at 1 ppt (n = 16), 20 ppt (n = 18), and 30 ppt (n = 12). Values are mean plasma osmolality (mOsmol/kg) ± standard error of the mean. * p = 0.05 for population effect at 30 ppt. Values represent plasma osmolality from pooled-sample dataset. Values were offset by 0.5 ppt for landlocked Alewives to eliminate overlap of data points

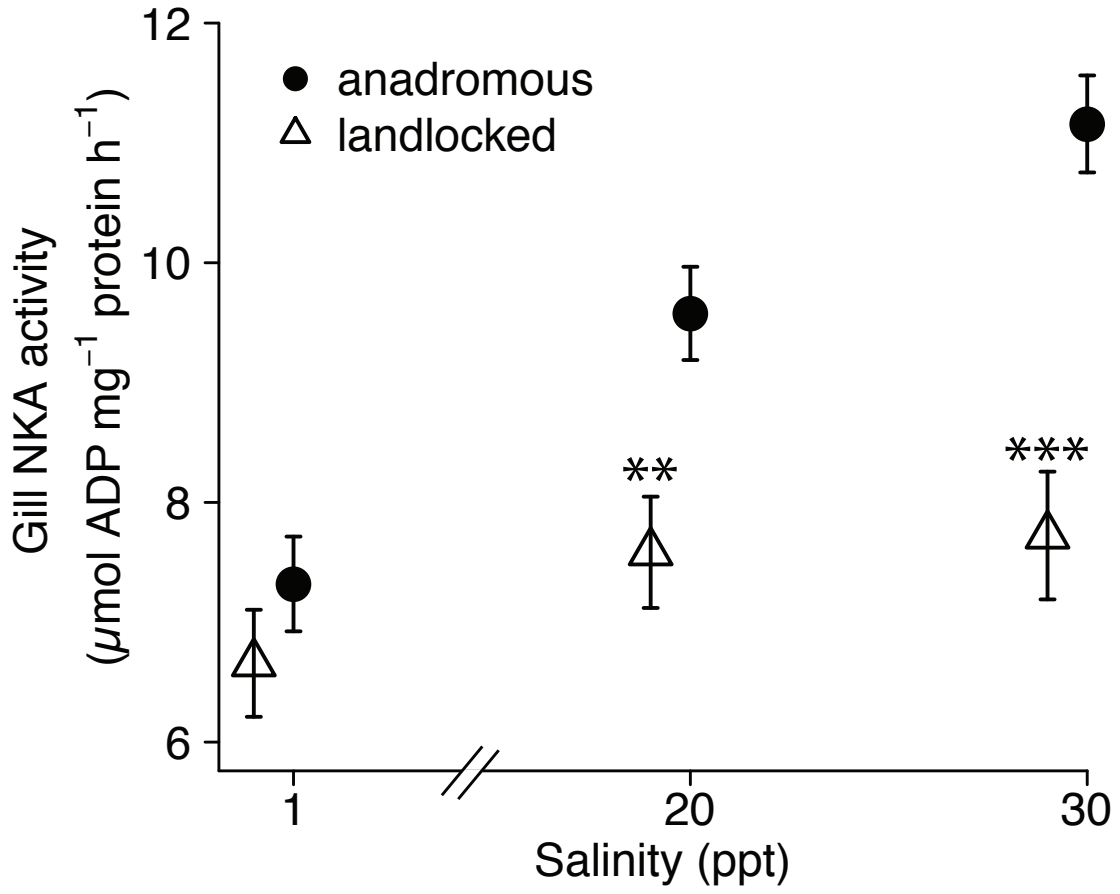


**Figure 3** Gill $Na^+/K^+$-ATPase activity of anadromous Alewives (black circles) at 1 ppt (n = 23), 20 ppt (n = 24), and 30 ppt (n = 23); and landlocked Alewives (open triangles) at 1 ppt (n = 19), 20 ppt (n = 17), and 30 ppt (n = 13). Values are LSmeans of NKA activity (μmol ADP · mg protein $^{-1}$ · hour $^{-1}$) ± standard error of the mean. ** p = 0.002, *** p < 0.0001 for population effect at 20 ppt and 30 ppt, respectively. Values were offset by 0.5 ppt for landlocked Alewives to eliminate overlap of data points

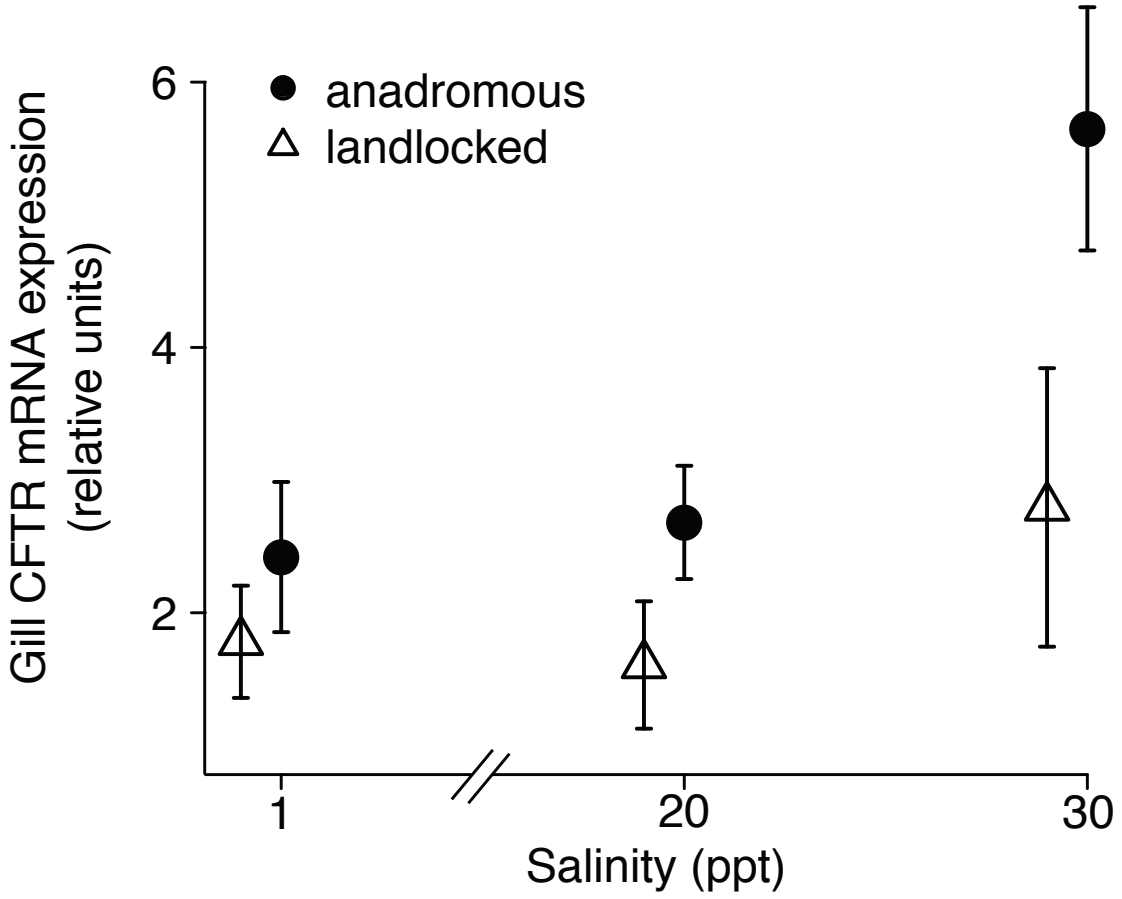


**Figure 4** Relative gill mRNA expression of *CFTR* of anadromous Alewives (black circles) at 1 ppt (n = 8), 20 ppt (n = 9), and 30 ppt (n = 10); and landlocked Alewives (open triangles) at 1 ppt (n = 9), 20 ppt (n = 8), and 30 ppt (n = 5). Values are mean relative units (expression value relative to *EF1*$\alpha$) ± standard error of the mean. There is a significant main effect of population ($p = 0.008$). Values were offset by 0.5 ppt for landlocked Alewives to eliminate overlap of data points

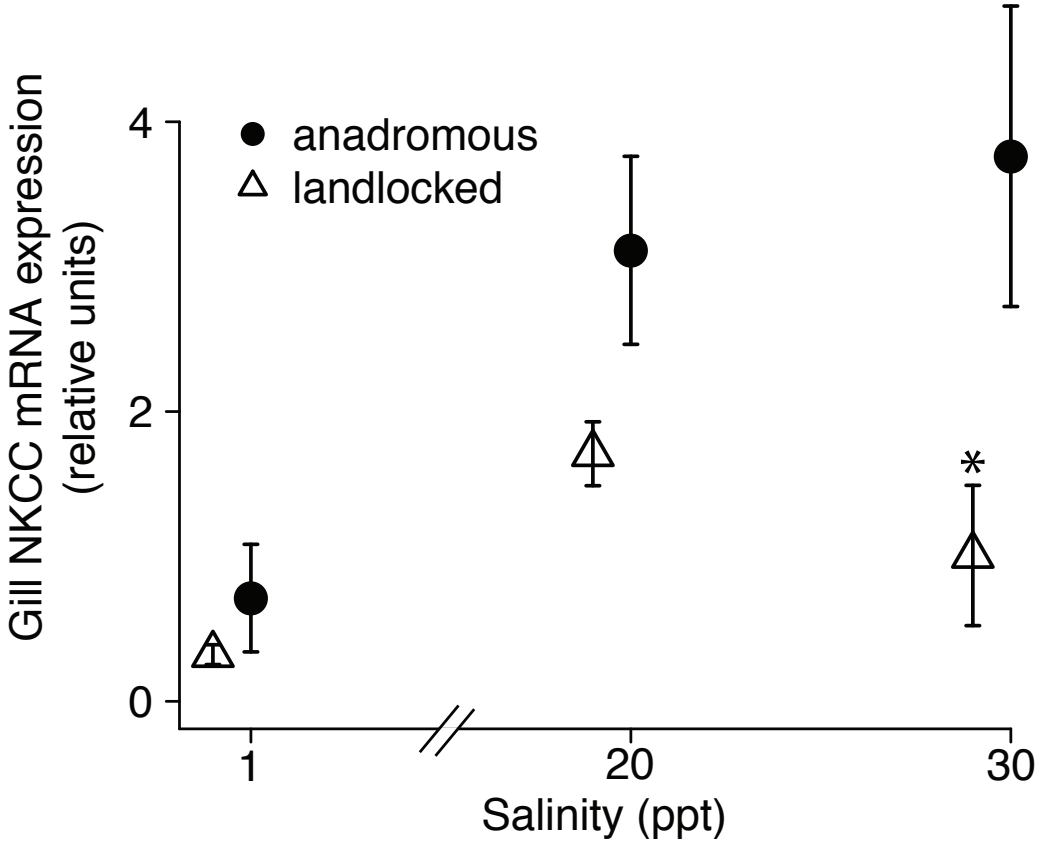


**Figure 5** Relative gill mRNA expression of *NKCC* of anadromous Alewives (black circles) at 1 ppt (n = 7), 20 ppt (n = 9), and 30 ppt (n = 10); and landlocked Alewives (open triangles) at 1 ppt (n = 9), 20 ppt (n = 8), and 30 ppt (n = 5). Values are mean relative units (expression value relative to *EF1*$\alpha$) ± standard error of the mean. * p = 0.04 for population effect at 30 ppt. Values were offset by 0.5 ppt for landlocked Alewives to eliminate overlap of data points

**Supplementary Table S1** Summary of final (reduced) linear mixed effects models. Bold P-values indicate statistical significance at the $p < 0.05$ level.

| Response | Fixed effect | Estimate | MCMC lower 95th | MCMC upper 95th | P-value | Random effect | Variance | Standard deviation |
|---|---|---|---|---|---|---|---|---|
| *log(plasma osmolality)* | life history form | -0.008 | -0.028 | 0.011 | 0.407 | tank | 4.30E-05 | 0.007 |
| | salinity | 0.033 | 0.015 | 0.050 | **0.002** | trial | 1.00E-04 | 0.010 |
| | salinity*life history form | 0.037 | 0.013 | 0.063 | **0.008** | | | |
| | log(standard length) | 0.010 | -0.128 | 0.143 | 0.921 | | | |
| *log(plasma osmolality) at 0 ppt* | life history form | -0.003 | -0.023 | 0.018 | 0.716 | tank | 0.00E+00 | < 0.001 |
| | standard length | 0.010 | -0.256 | 0.241 | 0.984 | trial | 0.00E+00 | < 0.001 |
| *log(plasma osmolality) at 20 ppt* | life history form | 0.015 | 0.001 | 0.027 | 0.058 | tank | 4.60E-06 | 0.002 |
| | standard length | 0.106 | -0.056 | 0.221 | 0.249 | trial | 4.90E-06 | 0.002 |
| *log(plasma osmolality) at 30 ppt* | life history form | 0.028 | 0.002 | 0.056 | **0.049** | tank | 3.80E-17 | 6.20E-09 |
| | standard length | 0.011 | -0.252 | 0.300 | 0.807 | trial | 3.40E-04 | 0.018 |

Table S1 continued

| | | | | | | | | |
|---|---|---|---|---|---|---|---|---|
| *log(plasma osmolality) - pooled data* | life history form | 0.014 | -0.037 | 0.062 | 0.571 | tank | 4.60E-04 | 0.022 |
| | salinity | 0.111 | 0.060 | 0.156 | **0.004** | trial | 1.20E-04 | 0.011 |
| | salinity*life history form | 0.086 | 0.017 | 0.158 | **0.023** | | | |
| *NKA activity* | life history form | -1.080 | -5.336 | 5.366 | 0.981 | tank | 1.549 | 1.245 |
| | salinity | 10.875 | 5.725 | 19.724 | **0.001** | trial | 0.595 | 0.771 |
| | salinity*life history form | -2.915 | -5.506 | 0.572 | **0.024** | | | |
| | standard length | -0.040 | -0.094 | 0.066 | 0.728 | | | |
| | standard length*salinity | -0.108 | -0.235 | -0.035 | **0.011** | | | |
| | standard length*life history form | 0.001 | -0.089 | 0.068 | 0.767 | | | |
| *NKA activity at 0 ppt* | life history form | -1.131 | -3.209 | 1.117 | 0.297 | tank | 2.847 | 1.687 |
| | standard length | -0.062 | -0.125 | 0.029 | 0.242 | trial | 1.449 | 1.204 |
| *NKA activity at 20 ppt* | life history form | -1.990 | -3.795 | -0.151 | **0.042** | tank | 0.928 | 0.964 |
| | standard length | 0.018 | -0.085 | 0.139 | 0.693 | trial | 0.658 | 0.811 |
| *NKA activity at 30 ppt* | life history form | -3.469 | -5.452 | -1.834 | **0.002** | tank | 0.110 | 0.332 |
| | standard length | -0.136 | -0.222 | -0.036 | **0.016** | trial | < 0.001 | < 0.001 |

Table S1 continued

| | | | | | | | | |
|---|---|---|---|---|---|---|---|---|
| *log(CFTR expression)* | life history form | -0.369 | -0.622 | -0.097 | **0.008** | tank | 0.037 | 0.192 |
| | salinity | 0.323 | 0.036 | 0.602 | **0.027** | trial | 0.017 | 0.129 |
| | log(standard length) | -4.022 | -8.110 | 0.265 | 0.056 | | | |
| *log(NKCC expression)* | life history form | -20.031 | -38.480 | -1.634 | **0.033** | tank | 4.93E-14 | < 0.001 |
| | salinity | -19.918 | -37.892 | -3.219 | **0.024** | trial | 0.026 | 0.160 |
| | log(standard length) | -9.013 | -17.928 | -0.765 | **0.030** | | | |
| | log(standard length)*salinity*life history form | -14.805 | -27.582 | -1.120 | **0.038** | | | |
| *log(NKCC expression) at 0 ppt* | life history form | -0.641 | -1.296 | 0.193 | 0.118 | tank | 0.061 | 0.248 |
| | log(standard length) | -7.891 | -20.922 | 7.172 | 0.439 | trial | 0.159 | 0.398 |
| *log(NKCC expression) at 20 ppt* | life history form | -0.398 | -0.743 | 0.099 | 0.113 | tank | 0.0421 | 0.205 |
| | log(standard length) | -2.274 | -6.279 | 4.999 | 0.917 | trial | 0.051 | 0.226 |
| *log(NKCC expression) at 30 ppt* | life history form | -0.561 | -1.035 | -0.085 | **0.035** | tank | 1.549 | 1.245 |
| | log(standard length) | 2.537 | -4.204 | 7.246 | 0.297 | trial | 0.595 | 0.771 |

## Chapter 3

## Local adaptation to freshwater is associated with trade-offs in osmoregulation and parallel changes in gene expression in landlocked Alewives


### Abstract

Since freshwater and seawater require opposing osmoregulatory machinery, local adaptation to one salinity may be expected to reduce performance in the other. Yet the extent to which adaptation to salinity leads to a trade-off in osmoregulation is not well understood. I used populations of the Alewife (*Alosa pseudoharengus*) to examine this question. Alewives are ancestrally anadromous, and multiple populations have been independently restricted to freshwater (landlocked). I conducted a series of salinity challenge experiments, whereby juvenile Alewives from one anadromous and several landlocked populations were exposed to freshwater and seawater in the field and in the laboratory. Independently derived landlocked populations varied in the degree of seawater tolerance loss in response to field salinity challenge. In the laboratory, landlocked Alewives exhibited improved freshwater tolerance, which was correlated with reductions in seawater tolerance and hypoosmotic balance, suggesting that trade-offs in osmoregulation are associated with local adaptation to freshwater. I detected differentiation between Alewife life history forms in the expression of an ion uptake gene (*NHE3*), and in gill $Na^+/K^+$-ATPase activity. Trade-offs in osmoregulation may be mediated by the enhanced responsiveness of an ion uptake pathway, as well as the diminished responsiveness of a salt-secreting pathway.


### Introduction

Spatial variation in the strength of natural selection can lead to adaptation of populations to their local environment. Local adaptation to one environment may reduce an organism's

fitness in alternative environments, indicating a trade-off. Trade-offs in fitness are believed to be a primary way by which genetic variation is maintained, leading to functional specialization (Futuyma and Moreno 1988), phenotypic diversification (Schluter 2000), and ecological speciation (Rundle and Nosil 2005). However, a recent analysis indicates that trade-offs associated with local adaptation may be weak (Hereford 2009). The strength of a trade-off appears to be greatest when heterogeneity between local and foreign environments is large (assuming this translates into heterogeneous selection pressures; Hereford 2009). For aquatic animals, freshwater and seawater represent contrasting environments with opposing physiological demands; the concentration of salts in freshwater and seawater differ by several orders of magnitude, requiring the uptake of ions in freshwater (hyperosmoregulation) and their secretion in seawater (hypoosmoregulation; Evans et al 2005). Examining populations that have adapted to novel salinity regimes may yield insights into the processes of local adaptation and associated fitness trade-offs in nature.

Salinity is one of the most important environmental variables affecting the diversification and distribution of aquatic animals (Lee and Bell 1999), including fishes (Schultz and McCormick 2013). The broad salinity tolerance limits of many marine fish were first observed by Darwin (1876), and were recently quantified (Whitehead 2010; Schultz and McCormick 2013). Species that specialize on freshwater, however, often have more narrow tolerance limits, and are unable to acclimate to high salinities (e.g., Whitehead 2010). Thus, on a macroevolutionary scale, evidence of trade-offs in salinity tolerance is weak. Yet because differences between salinity regimes require opposing physiological machinery, local adaptation to a particular osmotic niche may require shifts in both lower and upper salinity tolerance limits, i.e., a trade-off. This expectation is supported by recent research: colonization of freshwater by

euryhaline fishes is accompanied by improvements in freshwater osmoregulatory performance and ion uptake capacity (Scott et al 2004; Whitehead et al 2011, 2012), a reduction of seawater tolerance and ion secretion capacity (Fuller 2009; McCairns and Bernatchez 2010; DeFaveri and Merilä 2014; Velotta et al 2014), or both (Lee et al 2007, 2011).

I explored whether the transition to exclusively freshwater habitats results in local adaptation, and whether this adaptation is associated with a trade-off in salinity tolerance and osmoregulatory function. Populations of Alewife (*Alosa pseudoharengus*) provide a unique opportunity to test this hypothesis. Alewives, which inhabit the coastal waters of eastern North America, are ancestrally anadromous and make annual spawning migrations to coastal streams and ponds (Scott and Crossman 1973; Fay et al 1983). In Connecticut, multiple populations of Alewives have been independently, and recently (300-400 years), restricted to freshwater (landlocked) most likely as the result of dam construction during American colonial-period development (Palkovacs et al 2008). Landlocked populations are ideal for this test: population genetic analyses using mitochondrial and microsatellite loci indicate that multiple landlocked populations in Connecticut are independently derived from an anadromous ancestor (Palkovacs et al 2008). Furthermore, Alewives belong to a predominantly marine family, the Clupeidae, in which seawater is likely to be the ancestral environment (Li and Orti 2009) and hypoosmoregulation an ancestral capability.

Landlocked Alewife populations differ from their anadromous ancestor in their degree of genetic divergence, indicating that they may have been established at different times (Palkovacs et al 2008), and therefore may differ in the degree of adaptation to freshwater. Variation in salinity tolerance among landlocked populations will allow us to test whether freshwater and seawater tolerances are negatively correlated among multiple populations (a trade-off). In

addition, I exploit this system to explore the molecular basis of local adaptation, which remains poorly understood (Savolainen et al 2013). Several candidate genes are likely to evolve in response to local adaptation to a novel salinity. The use of multiple, independently derived populations allow us to test for parallel evolution in the responses of these candidate loci. Since local adaptation can conceivably result from stochastic evolutionary forces (e.g., genetic drift), parallel adaptation of independent populations lends support to the argument that natural selection is the driver of change (Kawecki and Ebert 2004).

Adaptation to novel salinity environments involves changes in the mechanisms of ion exchange at the gills, and several studies have shown evolution of activity and expression of known ion transport pathways (Scott et al 2004; Scott and Schulte 2005; Nilsen et al 2007; Lee et al 2011, Whitehead et al 2011, 2012; Czesny et al 2012; Velotta et al 2014) and signatures of selection on osmoregulation loci (Shimada et al 2011; DeFaveri et al 2011; Jones et al 2012; Michalak et al 2014). For fishes, ion exchange at the gill is accomplished by the coordination of ion transport proteins. In both freshwater and seawater, basolaterally located $Na^+$/ $K^+$-ATPase (NKA) generates an electrochemical gradient that drives all ion exchange (Evans et al 2005). Several models for $Na^+$ uptake in freshwater exist: 1) apical transport via $Na^+/H^+$ exchanger member 3 (NHE3; Wantanabe et al 2008; Inokuchi et al 2008); 2) passive transport through a putative epithelial channel, electrically coupled to a V-type proton ATPase (VATP; Evans et al 2005), and 3) electroneutral import via an apical $Na^+/Cl^-$ cotransporter (NCC). Alewives appear to lack apical NCC (Hiroi and McCormick 2012), so it was not considered in this study. In seawater, $Na^+/K^+/2Cl^-$ co-transporter (NKCC) transports $Na^+$, $K^+$ and $Cl^-$ into ionocytes down an electrochemical gradient generated by NKA. $Cl^-$ is secreted through CFTR (cystic fibrosis transmembrane conductance regulator), an apical ion channel, and $Na^+$ ions are secreted

paracellularly through leaky tight junctions between ionocytes and accessory cells (Evans et al 2005; Hwang and Lee 2007). I investigated two candidate pathways for hyperosmoregulation (expression of NHE3 and VATP), and two for hypoosmoregulation (NKA activity and expression of NKCC).

I compared Alewives from an anadromous population to independently derived landlocked populations in two experiments: 1) an acute (24 hour) field seawater challenge, followed by 2) a two-week freshwater and seawater challenge on laboratory-acclimated fish. The field seawater challenge experiment was designed to determine whether landlocked populations differ in their degree of seawater tolerance and enabled us to test whether seawater tolerance covaries with genetic divergence from the anadromous ancestor. These results informed selection of two landlocked populations that contrasted in their degree of osmoregulatory divergence, allowing us to test the prediction that inter-population differences in seawater tolerance are inversely correlated with freshwater tolerance (i.e., a trade-off). I measured survival and plasma osmolality (total solute concentration; an indicator of osmoregulatory performance) after exposure to freshwater and seawater. I then determined whether gill NKA activity, and expression of genes for freshwater ion uptake (*NHE3*, *VATP*) and seawater ion secretion (*NKCC*) evolve along with osmoregulatory performance, and whether these changes occur in parallel. I predicted that landlocked Alewives would exhibit higher expression of genes for ion uptake (*NHE3* and *VATP*), and reduced activity and expression of genes for ion secretion (NKA activity and *NKCC* expression).

## Methods and Materials

*Acute seawater challenge*

Young-of-the-year (YOY) Alewives from one anadromous and five landlocked sites were captured by purse seine from their natal lakes in Connecticut in August through September 2011 (Figure 1, Table 1). I transported Alewives from each site to the University of Connecticut in 19-liter buckets with aeration. A small amount of salt (1 ppt; lake water mixed with artificial sea salt; Instant Ocean, Spectrum Brands, Madison, WI) was added to transport tanks, since it reduces stress and mortality associated with handling (Stanley and Colby 1971; Johnson and Metcalf 1982; Nikinmaa et al 1983; Carneiro and Urbinati 2001). Fish from each site were transported and treated on separate days (see Table S1). I held fish in outdoor enclosures overnight at 1 ppt in 150-liter oval tanks with aeration, and removed any mortalities resulting from transport stress. Approximately 25 Alewives per population were then immediately transferred to replicate tanks containing 1 ppt freshwater (control treatment) or full-strength seawater (35 ppt) for 24 hours. Salinities were achieved by mixing artificial sea salt with conditioned, de-chlorinated tap water. I checked each tank for mortality hourly for the first 12 hours, and then again after 24 hours.

*Laboratory-acclimation salinity challenge*

Anadromous and landlocked YOY Alewives from A-Bride, L-Pattagansett, and L-Rogers were captured by purse seine from their natal lakes in coastal Connecticut in October 2011. Captured Alewives were immediately transported to the Conte Anadromous Fish Research Center in Turners Falls, Massachusetts in aerated 190-liter cylindrical containers at 1 ppt. Once in the laboratory, Alewives were held at 1 ppt for 1 day, after which salinity was decreased to 0.5

ppt (final rearing salinity). I segregated Alewives by site and held them in separate 1,200-liter re-circulating oval tanks fitted with charcoal filtration systems for one month prior to experimentation. Fish were maintained between 14.5°C – 16°C with an ambient photoperiod, and fed to satiation once daily with Biotrout fish food (Bio-Oregon, Westbrook, ME).

I subjected laboratory-acclimated anadromous and landlocked Alewives to four salinity treatments for two weeks (15 days). Low-ion freshwater (salinity = 0 ppt; mean conductivity = 19.9 ± 6.8 μS) and 30 ppt seawater treatments were conducted from 16 November – 1 December 2011 (Trial 0/30). I then subjected Alewives to two additional seawater treatments (full-strength seawater: 35 ppt; and a hyper-saline treatment: 40 ppt) from 20 December 2011 - 3 January 2012 (Trial 35/40). Space constraints in the laboratory required that I conduct trials at different times. In each treatment, approximately 25-35 Alewives from each site were immediately transferred from 0.5 ppt rearing tanks to replicate 250-liter re-circulating oval tanks with charcoal filtration. Low-ion freshwater was prepared by running filtered, de-chlorinated tap water through a resin-filled cartridge (Culligan International Company, Rosemont, IL, USA). Seawater treatments were prepared by dissolving artificial sea salt (Crystal Sea Marine Mix, Marine Enterprises International, Baltimore, MD, USA) in filtered, de-chlorinated tap water. Experimental tanks were checked for mortalities daily, and any dead fish were immediately removed and measured for length.

Blood and gill tissue were sampled before transfer to salinity treatments (pre-transfer) and at several time points post-exposure. For trial 0/30, I sampled Alewives at days 1, 2, 5, and 14, and for trial 35/40 at days 2 and 14. I chose this sampling design to correspond to times at which I expected to observe survival differences, perturbations in osmotic balance, and responses of ion transporters to salinity. At each sampling, I euthanized fish in 250 mg $l^{-1}$ tricaine

methanesulfonate (MS-222; Argent, Redmond, WA, USA) and measured their fork length ($L_f$), total length ($L_t$) and mass. I then severed the caudal peduncle and collected blood from each fish in a heparinized micro-hematocrit tube. Following centrifugation at 3200g for 5 min, plasma was removed and transferred to 0.5 mL tubes and stored at -80°C. Plasma osmolality, the concentration of plasma solutes, was subsequently measured on a vapor pressure osmometer (Wescor Inc., Logan, Utah, USA) using 8 μL of plasma following the manufacturer's instructions. The left gill arches were removed, trimmed from the bone and placed in 1 mL of RNAlater solution (Ambion, Life Technologies, Grand Island, NY, USA) which was incubated at 4°C overnight and then stored at -20°C. I then excised and trimmed the first right gill arch from each fish, and placed samples in 100 μL of ice-cold SEI buffer (150 mmol $l^{-1}$ sucrose, 10 mmol $l^{-1}$ EDTA, 50 mmol $l^{-1}$ imidazole, pH 7.3) and stored at -80°C for measurement of $Na^+$/ $K^+$-ATPase activity.

*Gill $Na^+$/ $K^+$-ATPase activity and quantitative real-time PCR assays*

Gill $Na^+$/ $K^+$-ATPase activity was determined by the microplate method following McCormick (1993). In this method, ouabain-sensitive ATPase activity was measured by the production of ADP to NADH using lactic dehydrogenase and pyruvate kinase in the presence and absence of 0.5 $mmol^{-1}$ ouabain. Gill tissue samples were homogenized and run in duplicate in 96-well microplates at 25°C. Samples were read at a wavelength of 340 nm for 10 min on a THERMOmax microplate reader using SOFTmax software (Molecular Devices, Menlo Park, CA, USA). Total protein content of the homogenate was determined using a BCA (bicinchoninic acid) Protein Assay (Pierce, Rockford, IL, USA), which served to normalize NKA activity to the

amount of protein in the gill sample. I calculated NKA activity as the difference in ATP hydrolysis in the absence and presence of ouabain, expressed as μmol ADP mg protein$^{-1}$ hour $^{-1}$.

Gene expression was measured using quantitative real-time PCR (qPCR). For this assay, I analyzed gill tissue from trial 0/30 on days 0, 1, 2, and 14. Total RNA was extracted from approximately 30 mg of homogenized gill tissue using the RNeasy Mini Kit (Qiagen, Valencia, CA, USA) following the manufacturer's instructions. I quantified RNA spectrophotometrically and assessed the purity (260/280 > 1.8) of each sample. Purified RNA was treated with DNase to eliminate contaminating DNA using the TURBO DNA-free kit (Life Technologies, Grand Island, NY, USA). I verified the integrity of a subset (15%) of purified, DNase-treated RNA samples on an Agilent 2100 Bioanalyzer using the RNA 6000 Nano Kit (Agilent Technologies, Inc., Santa Clara, CA, USA) following the manufacturer's instructions. First strand synthesis of cDNA was achieved using the High-Capacity cDNA Reverse Transcription Kit with RNase Inhibitor (Life Technologies, Grand Island, NY, USA) using 500 ng RNA as a template. qPCR primers (Table 2) for candidate genes *NKCC*, *VATP, NHE,* and a reference gene (*elongation factor 1α* (*EF1α*)) were designed using sequences generated from a gill transcriptome of wild-caught juvenile Alewives (unpublished data).

Target cDNA was amplified in triplicate by qPCR on a Bio-Rad iCycler (Bio-Rad Laboratories, Hercules, CA, USA) and Bio-Rad's iTaq Universal SYBR Green Supermix. Reaction conditions for qPCR were as follows: 10 minutes at 95°C, 45 cycles of 95°C for 20 seconds and 60°C for 50 seconds. Melt curve analysis was performed following each reaction to ensure that a single qPCR product was produced. I combined gill RNA from acclimated, pre-transfer samples from A-Bride, L-Pattagansett, and L-Rogers to serve as standard material, referred to as the calibrator sample. Standard curves derived from triplicate dilutions of the

calibrator yielded an estimate of amplification efficiency (E-value) for each set of primers; E-values for each primer set were determined by averaging results from three separate standard curve runs, and were near the ideal value of 2.0 (EF1α: 1.93; NKCC: 2.08; VATP: 1.97; NHE: 1.93). Samples from the calibrator were included on each qPCR plate in triplicate in order to account for variance arising from random differences in run conditions from plate to plate. cDNA samples were randomized before loading onto each qPCR plate, and a total of 42 plates were run. Relative expression was calculated as $\Delta\Delta C_T$ (Pfaffl 2001),

$$\Delta\Delta C_T = \frac{E_{tar}^{\Delta C_T tar(calibrator-test)}}{E_{ref}^{\Delta C_T ref(calibrator-test)}} \quad (1)$$

where: $E_{tar}$ is the amplification efficiency of the primer for the gene of interest, $E_{ref}$ is the amplification efficiency of the primer for the reference gene (i.e., *EF1α*), $\Delta C_T$ tar (target) is the difference in cycle threshold value between calibrator and test sample for the gene of interest, and $\Delta C_T$ ref (reference) is the difference in $C_T$ between calibrator and test sample for the reference gene.

*Statistical analyses*

Survival after acute and laboratory-acclimation salinity exposures was analyzed using a generalized linear mixed effects model (GLMM; *lmer* function in the *lme4* package in R version 3.1.0) fitting survival as a binary response variable. For acute salinity challenge, I treated tank and trial date as random effects, and site (A-Bride, L-Amos, L-Long, L-Pattagansett, L-Quonnipaug, L-Rogers) and salinity (1 ppt, 35 ppt) as fixed effects. I used the proportion of individuals alive or dead at the end of the 24-hr acute seawater challenge as the response variable. As such, I was unable to incorporate length as a covariate in this model. In laboratory-

acclimation exposures, GLMMs included site (A-Bride, L-Pattagansett, or L-Rogers) and salinity (0 ppt, 30 ppt, 35 ppt, and 40 ppt treatments) as fixed effects, and tank and trial (trial 0/30 and 35/40) as random effects. In GLMMs for laboratory-acclimation trials, length was included as a covariate. I also used survival analysis (Cox proportional hazards model; *coxph* function in the *survival* package in R version 3.1.0) to determine differences in survivorship between sites and salinity treatments in the laboratory-acclimation experiment. The Cox method models death rate as a log-linear function of predictors, where regression coefficients give the relative effect of covariates on survivorship. The model computes a baseline hazard function that is modified multiplicatively by the covariates (Venables and Ripley 1999).

To determine whether variation in seawater survival among landlocked populations is related to the degree of genetic differentiation from the anadromous ancestor, I correlated seawater survival (from the acute salinity challenge) with pairwise $F_{ST}$ using Spearman's rank correlation in R version 3.1.0 (*cor.test* function). To determine seawater survival probability, I divided average seawater survival by average freshwater survival for each site; in this way, variation in freshwater survival is an indication of variation in transport and handling-related stress. Pairwise $F_{ST}$ between each landlocked site and A-Bride were obtained from Palkovacs et al. (2008), who used one mitochondrial locus (control region; CR1) and six microsatellite loci. Seawater survival was correlated with $F_{ST}$ values from mitochondrial and microsatellite loci separately.

Linear mixed effects models were used to assess differences in mean plasma osmolality (n = 12 per site per salinity per time point), NKA activity (n=12 per site per salinity per time point), and candidate gene expression (n=8 per site per salinity per time point). Response variables were log transformed to meet assumptions of normality. Model generation was

implemented using the *lmer* function in R (*lme4* package; R version 3.1.0). Full models included site (A-Bride, L-Pattagansett or L-Rogers), salinity (0 ppt, 30 ppt, 35 ppt and 40 ppt), and time (pre-transfer and all sampling time-points) as fixed effects, with length ($L_t$) used as a covariate. I included tank as a random effect. P-values were calculated with the *summary* function in the *LmerTest* package (R version 3.1.0) using restricted maximum likelihood and Satterthwaite estimation for denominator degrees of freedom. I used a model reduction approach, whereby full models were reduced where non-significant interaction terms were detected ($P < 0.05$).

**Results**

*Survival*

Response to 24-hr acute seawater challenge differed between landlocked and anadromous Alewives (Figure 2). Survival at 1 ppt was high in Alewives from all populations, ranging from 89%-100%. Seawater survival was considerably lower among landlocked populations, which varied from 4 – 45% survival compared to nearly 70% for A-Bride. I detected a significant population x salinity interaction for all landlocked sites compared to A-Bride, with the exception of L-Long (results of GLMM presented in Table 3). I found that seawater survival among landlocked Alewife populations is negatively correlated with genetic distance ($F_{ST}$ based on CR1 mitochondrial locus) from A-Bride (Figure 3). A negative correlation between seawater survival and microsatellite-based $F_{ST}$ returned a similar result, though it was not significant ($\rho = -0.60$; $P = 0.067$). I chose L-Pattagansett and L-Rogers for laboratory-acclimation challenges, since these populations differ in both genetic differentiation and seawater tolerance.

Survivorship in freshwater and seawater differed considerably between anadromous and both landlocked populations of Alewife in laboratory-acclimation challenges (Figure 4). I

detected a significant site x salinity interaction between A-Bride and L-Rogers at 35 ppt and 40 ppt compared to 0 ppt (Table 4). The GLMM yielded no statistically significant differences between A-Bride and L-Pattagansett ($P > 0.05$). I also detected a significant effect of length on survival, in which smaller fish were more likely to die (Table 4). In low-ion freshwater, survival was lower for anadromous Alewives (66%) than landlocked Alewives from L-Rogers (99%; significant effect of site in a Cox proportional hazards model, $z = -2.39$, $P = 0.016$). The difference in low-ion freshwater survival between L-Pattagansett and A-Bride (66% vs. 56%, respectively) was not statistically significant ($z = 1.53$, $P = 0.13$). I detected negligible mortality in landlocked and anadromous Alewives at 30 ppt ($P > 0.05$). Differences in survivorship between life history forms were detected for full-strength seawater (35 ppt) and hyper-saline (40 ppt) treatments. Survival of anadromous Alewives in 35 ppt seawater (96%) was higher than Alewives from L-Pattagansett (92%; $z = 2.91$, $P = 0.004$), and L-Rogers (72%; $z = 4.17$, $P < 0.0001$). At 40 ppt, no fish from L-Rogers survived ($z = 8.65$; $P < 0.0001$ for site effect), and survival of L-Pattagansett Alewives was lower than for A-Bride (46% vs. 82%, respectively; $z = 4.17$, $P < 0.0001$). I also detected a significant positive relationship between fish length and survivorship among Alewives treated with low-ion freshwater ($z = -1.97$, $P = 0.049$), 35 ppt ($z = -4.07$, $P < 0.0001$), and 40 ppt seawater ($z = -2.54$, $P = 0.011$).

*Plasma osmolality*

Low-ion freshwater and seawater treatments altered plasma osmolality for anadromous and landlocked Alewives over the two-week time course in laboratory-acclimation challenges (Figure 5), with landlocked Alewives exhibiting higher osmolality in response to seawater. A full model with site, salinity, and time included as fixed effects revealed a significant three-way interaction ($P < 0.001$), so linear mixed effects models were run for each salinity treatment

separately (results presented in Table S2). Low-ion freshwater treatment resulted in the continual decline of plasma osmolality among all populations (significant main effect of day; Table S2), and between-population differences in plasma osmolality were not detected ($P > 0.05$). At 30 ppt, plasma osmolality increased strongly for Alewives from L-Pattagansett and L-Rogers, particularly on day 1, while fish from A-Bride maintained steadier levels (Figure 5). I also detected a significant positive effect of length on plasma osmolality at 30 ppt. Full-strength seawater and hyper-saline treatments resulted in dramatically higher plasma osmolality for landlocked Alewives. I detected a significant interaction of site and day for L-Pattagansett at 35 ppt and 40 ppt, and for L-Rogers at 35 ppt compared to A-Bride. By day 15, the model revealed no statistically significant interactions or main effects (Table S2).

*Gill $Na^+/K^+$-ATPase activity*

Gill NKA activity increased over time in response to all salinities, and this increase was strongest after seawater challenge (Figure 6). The increase in gill NKA activity in response to salinity was more pronounced for anadromous Alewives, which had higher pre- and post-transfer levels (Figure 6). I analyzed each salinity treatment using separate linear mixed effects models (Table S2), since the full model revealed a significant three-way interaction ($P < 0.05$). In low-ion freshwater, gill NKA activity increased by day 15 and was significantly higher among A-Bride Alewives than Alewives from either landlocked population. At 30 ppt, gill NKA also increased post-exposure and was lower for L-Pattagansett Alewives. No statistical differences in gill NKA activity were found between A-Bride and L-Rogers ($P > 0.05$) at 30 ppt. Transfer to full-strength seawater and hyper-saline treatment resulted in upregulation of gill NKA activity that was more pronounced in anadromous Alewives than in landlocked Alewives (Figure 6). I detected a statistically significant interaction of site and day for L-Rogers compared to A-Bride

at 35 ppt, and for L-Pattagansett compared to A-Bride at 40 ppt. NKA was generally lower for landlocked Alewives, and a significant main effect of site was detected for L-Pattagansett and L-Rogers at 35 ppt, and L-Pattagansett at 40 ppt.

*Gene expression*

Gene expression was modified by salinity exposure, but there were few overall differences between anadromous and landlocked Alewives (Figure 7). Expression of *NHE3* in response to low-ion freshwater increased by day 15 compared to pre-transfer levels, and was not significantly different between life history forms ($P > 0.05$; Table S2; Figure 7A). At 30 ppt seawater, expression of *NHE3* was higher overall for landlocked alewives from L-Pattagansett and L-Rogers compared to A-Bride, and was significantly upregulated at day 2 compared to pre-transfer across all sites (Table S2). Expression of *VATP* was not affected by salinity treatment ($P > 0.05$; Figure 7B), but did differ between anadromous and landlocked Alewives in seawater (Table S2). *NKCC* mRNA expression was downregulated in response to freshwater and upregulated in response to seawater (Figure 7C). In low-ion freshwater, *NKCC* transcription was lower than pre-transfer levels at day 1 and day 2 among all populations. In seawater, *NKCC* expression was significantly upregulated at day 1 and day 2, but returned to pre-transfer levels by day 15 among all populations (Table S2). Pre-transfer *NKCC* expression was highest in fish from L-Pattagansett, which exhibited higher expression overall compared to A-Bride in seawater. Seawater *NKCC* expression was comparable for A-Bride and L-Rogers Alewives ($P > 0.05$).

**Discussion**

I have provided the first evidence of local adaptation to salinity in any species of fish that conforms to the 'local versus foreign' criterion set forth by Kawecki and Ebert (2004), in which

local individuals have higher fitness than foreign individuals in their local habitat across all environments. Satisfying the local vs. foreign criterion is the strongest evidence of local adaptation since it suggests a direct trade-off via divergent selection acting on genetic differences in relative fitness in either habitat (Kawecki and Ebert 2004). I demonstrated that landlocked populations of Alewife are locally adapted to freshwater and that this adaptation is associated with a trade-off in tolerance between freshwater and seawater. This finding is novel for teleost fishes, and is consistent with previous studies on copepods (Lee et al 2007). My results are consistent with the expectation that trade-offs associated with local adaptation are likely in cases where selective differences between derived and ancestral habitats are large (Hereford 2009). Furthermore, I have identified several molecular mechanisms that may underlie local adaptation to salinity: gill NKA activity, a major component of ion exchange, is lower among landlocked Alewives; and transcription of *NHE3*, a $Na^+$ channel, is consistently higher among landlocked Alewives.

*Local adaptation to salinity and associated trade-offs*

Acute seawater challenges revealed that several landlocked Alewife populations have reduced seawater tolerance compared to an anadromous population (Figure 2), consistent with our previous findings (Velotta et al 2014). I also found that differences in seawater tolerance among landlocked populations are correlated with genetic distance ($F_{ST}$) from the anadromous population (Figure 3). To the extent that $F_{ST}$ measures neutral genetic differentiation, greater sensitivity to seawater appears to evolve the longer populations have been landlocked. Differences among landlocked populations in seawater tolerance may also be due to differences in effective population size ($N_e$), though I currently do not have estimates of $N_e$ for these populations.

L-Pattagansett and L-Rogers were chosen to represent the range of responses to seawater for laboratory-acclimation challenges, allowing a test of the prediction that the loss of seawater tolerance is associated with a proportional gain in freshwater tolerance (a trade-off). I predicted that since L-Rogers is the least seawater tolerant and most genetically differentiated from A-Bride, it would exhibit the greatest tolerance of freshwater, while L-Pattagansett - intermediate in genetic differentiation and seawater tolerance - would exhibit an intermediate tolerance of freshwater.

This prediction was borne out in my results: landlocked Alewives are locally adapted to freshwater; increases in tolerance of low-ion freshwater have traded-off against tolerance of seawater. First, I found a significant site x population interaction for survival between A-Bride and L-Rogers Alewives (Table 3), which is diagnostic of local adaptation. Second, my prediction that the degree of seawater sensitivity would be inversely proportional to the degree of freshwater tolerance was supported: the more seawater-sensitive population (L-Rogers) had greater tolerance of freshwater, while tolerance of seawater and freshwater was intermediate in L-Pattagansett (Figure 4). This provides strong evidence that trade-offs in osmotic tolerances reflect local adaptation in Alewives.

Osmotic balance in response to seawater is reduced among independently derived landlocked populations, providing evidence that adaptation to freshwater results in lowered osmoregulatory performance. When challenged at all levels of seawater, landlocked Alewives lost osmotic balance more severely and for significantly longer than anadromous Alewives. By contrast, anadromous Alewives maintained a near-constant plasma osmolality, indicating a high degree of physiological plasticity (Figure 5). After two weeks at 35 ppt, anadromous Alewife plasma osmolality (average = 345 mOsm/kg) was comparable to that of congeneric seawater-

acclimated American Shad (*Alosa sapidissima*) (335 ± 4 mOsm/kg; Zydlewski and McCormick 1997). Although osmolality in seawater declined by day 15, it was higher among landlocked Alewives from L-Pattagansett (~355 mOsm/kg) and L-Rogers (~ 370 mOsm/kg) than anadromous Alewife and American Shad acclimation values (see above), suggesting that surviving landlocked Alewives may not be fully acclimated to seawater.

Alewives from both anadromous and landlocked populations lost plasma osmolality in low-ion freshwater over the time course of the experiment, and I detected no population level divergence in freshwater osmotic balance (Figure 5). These results did not fit my predictions; I expected landlocked Alewives to maintain osmotic balance in low-ion freshwater to a greater degree than anadromous Alewives. Freshwater populations of Atlantic killifish (*Fundulus heteroclitus*) maintain osmotic balance after seawater-to-freshwater transfer better than seawater-derived populations, which exhibit excursions after transfer (Whitehead et al 2011, 2012; Scott et al 2004). Alewives appear not to have acclimated to low-ion freshwater even after two weeks of exposure; plasma osmolality was on average 291 mOsmol/kg for surviving Alewives, which is lower than the value for American Shad in freshwater (318 ± 4.8 mOsmol/kg; Zydlewski and McCormick 1997) and lower than the average value for all diadromous fishes in freshwater for which data is available (311 ± 6.5 mOsmol/kg; Nordlie 2009). In addition, plasma osmolality in freshwater declined steadily, showing no signs of returning to pre-transfer levels (approximately 338 mmol/kg; Figure 5). The salinity of the low-ion freshwater treatment (0 ppt and approximately 20 μS) was lower than the salinity of natal lakes (0 – 0.1 ppt and approximately 50 -100 μS), which may have contributed to the low post-exposure osmolality levels. The steady decline in osmolality in freshwater may have also contributed to mortality for A-Bride and L-Pattagansett Alewives. The high survival of L-Rogers in low-ion freshwater (Figure 4), despite

the decline of plasma osmolality, indicates that this population is robust to changes in osmolality, and that the tolerance of low plasma ion levels may be an adaptive response to an exclusively freshwater life history.

*Molecular mechanisms of local adaptation*

Several candidate molecular pathways showed variation, suggesting that they may underlie local adaptation to salinity. Gill NKA activity is reduced in independently derived populations of landlocked Alewives in response to freshwater and seawater compared to the anadromous population (Figure 6). Reductions in gill NKA activity in response to seawater likely contribute to reduced seawater tolerance and hypoosmoregulatory performance among landlocked Alewives, since NKA is the primary driver of ion secretion at the gill (Evans et al 2005). The parallel nature of this change suggests that lowered gill NKA activity is adaptive among landlocked populations. The ability to upregulate NKA in response to seawater may be costly among landlocked Alewives if, for example, there is a constitutive cost of its regulation (e.g., Auld et al 2010). Upregulation of gill NKA activity in seawater is therefore likely to be selected against after introduction to freshwater, where seawater has been removed as selection pressure. Lowered gill NKA activity in seawater among landlocked Alewives is consistent with our previous findings *in situ* (Velotta et al 2014). Here, I show that the patterns of differentiation of seawater NKA activity are the same when animals are acclimated to a common laboratory environment, and that this pattern is similar for two independently derived populations.

In freshwater, lowered gill NKA activity in landlocked Alewives may be an adaptive response to living in low productivity environments, as suggested by Aykanat et al (2011) for Steelhead trout. Since powering NKA is energetically expensive (Tseng and Hwang 2008), and since freshwater tends to be less productive than seawater, selection may favor individuals with

reduced activity. Growth rates are lower for landlocked Alewives than for anadromous Alewives both in the wild (Scott and Crossman 1973) and in the laboratory (J. Velotta, unpublished data), providing additional support that lowered energy expenditure may be an adaptive response to freshwater.

My results are consistent with studies from other species: freshwater populations of copepods have reduced NKA activity at any salinity compared to their seawater ancestor (Lee et al 2011), and landlocked Atlantic salmon cannot upregulate gill NKA activity to the same degree anadromous salmon can (Nilsen et al 2007). Thus, multiple freshwater forms of several unrelated taxa have converged on lower gill NKA activity relative to the seawater ancestor, providing robust support that changes in NKA activity underlie adaptation to freshwater. Additional evidence is provided by population genetic studies showing that NKA is under selection in freshwater populations of Threespine Stickleback (Hohenlohe et al 2010; Shimada et al 2011; DeFaveri et al 2011; Jones et al 2012), and that NKA mRNA expression in response to salinity is lowered among landlocked populations of Steelhead trout (Aykanat et al 2011).

Among anadromous Alewives, expression of *NHE3* was upregulated in response to freshwater and downregulated in response to seawater (Figure 5A), consistent with its putative role in gill $Na^+$ uptake (Figure 7A; Scott et al 2005; Hiroi et al 2008; Wanatabe et al 2008; Inokuchi et al 2008). This result differs from a previous study of Alewife by Christensen et al (2012), who demonstrated that immunohistochemical expression of NHE3 is similar in the freshwater and seawater gill. For landlocked Alewives, expression of *NHE3* was upregulated in freshwater and in seawater, where it remained high throughout the experiment. My results therefore suggest that landlocked Alewives do not downregulate *NHE3* transcription in response to seawater. The parallel evolution of high *NHE3* expression across salinity environments is

consistent with the expectation that landlocked Alewives increase the regulation of transporters involved in ion uptake as an adaptive response to a fully freshwater life history. To my knowledge, this is the first documentation of population-level divergence of *NHE3* in any fish species.

Transcription of *VATP* was not increased by freshwater exposure in landlocked or anadromous Alewives (Figure 7B), which may indicate that it plays a minimal role in ion uptake in the Alewife gill. This was an unexpected finding since electrogenic apical *VATP* has been suggested to drive passive $Na^+$ uptake in the fish gill (Katoh et al. 2003; Evans et al. 2005). I did, however, observe a variable pattern of *VATP* transcription in response to seawater between Alewife life history forms (Figure 7B); transcription of *VATP* was not responsive to seawater for anadromous Alewives, but was for L-Rogers Alewives. L-Pattagansett Alewives had greater pre-transfer expression than any other population, and expression remained high throughout the time course. My results differ from those of Lee et al. (2011), who showed that freshwater-adapted copepods have evolved elevated VATP activity and transcription in response to freshwater. This may reflect taxon-specific differences in the role of VATP in acclimation to freshwater on physiological time scales, and/or in adaptation to freshwater on an evolutionary scale.

In a previous study, Alewives from A-Bride showed stronger upregulation of *NKCC* in response to 30 ppt seawater than Alewives from L-Pattagansett (Velotta et al. 2014). In this study, transcription of *NKCC* in response to freshwater and seawater varied between anadromous and landlocked Alewives, but the results did not conform to my predictions. I expected expression of *NKCC* in response to seawater to be higher for anadromous Alewives, reflecting its role in gill $Cl^-$ secretion. However, although *NKCC* appears to be upregulated after seawater exposure, its transcription was highest among L-Pattagansett fish. High expression of *NKCC*

among L-Pattagansett fish may be a compensatory response to seawater challenge; greater osmotic imbalance at 30 ppt may lead to the recruitment of more NKCC transcripts. However, these results may also reflect differences in experimental design in which acclimation to a common laboratory environment influences the transcriptional response to salinity differently than when animals are not acclimated.

*Conclusions*

By comparing anadromous Alewives to independently derived landlocked populations, I demonstrated that tolerance of low-ion freshwater is correlated with reduced hypoosmoregulatory ability, suggesting that trade-offs in salinity tolerance and osmoregulatory function are associated with local adaptation to freshwater, the first of such evidence in any species of fish. Natural selection for enhanced hyperosmoregulation may directly result in reduced hypoosmoregulatory function if, for example, these processes are governed by an antagonistic pleiotropy, such that alleles that maximize freshwater performance are detrimental to seawater performance. I cannot, however, rule out the possibility that changes in osmoregulatory performance have evolved via genetic drift. For example, relaxed selection on hypoosmoregulatory function in landlocked Alewives – which do not experience seawater - could result in the deterioration of seawater tolerance via accumulation of deleterious mutations to genes that regulate ion secretion (Lahti et al. 2009). However, that osmoregulatory divergence has occurred relatively recently (likely 300-400 years; Palkovacs et al 2008), that these changes are reciprocal nature (high freshwater tolerance is opposed by low seawater tolerance), and that they occur in parallel, suggest that natural selection is likely operating on osmoregulatory function in landlocked Alewives.

I acknowledge the possibility that environmental or maternal effects may influence life history form divergence. However, to minimize environmental influences, I acclimated Alewives to a common salinity in the laboratory, which acts to limit physiological differences due to differences in the animal's native environment (Whitehead and Crawford 2006; Whitehead et al 2011, 2012). Furthermore, the lakes used in this study differ little in salinity regime (Table 1), which is the environmental variable that should influence osmoregulation the most. Therefore, environmental effects that may have caused the population-level differences I observed in this study may be minimal or non-existent.

My results add to the growing body of literature suggesting that changes in $Na^+/ K^+$-ATPase – one of the most important enzymes involved in ion regulation - may underlie adaptation to freshwater (e.g., Nilsen et al 2007; Lee et al. 2011; McCairns and Bernatchez 2010; DeFaveri et al 2011; Jones et al 2012). Furthermore, I provide the first account of evolutionary shifts in the transcriptional response of *NHE3* to salinity. Future work should be aimed at clarifying the role of gene expression in adaptation to freshwater, including the role of genome-wide transcriptional changes, which will uncover novel pathways involved in adaptation to salinity.

**References**

Auld, J.R., Agrawal, A.A., and Relyea, R.A. (2010). Re-evaluating the costs and limits of adaptive phenotypic plasticity. Proc. R. Soc. B *277*, 503–511.

Aykanat, T., Thrower, F.P., and Heath, D.D. (2011). Rapid evolution of osmoregulatory function by modification of gene transcription in steelhead trout. Genetica *139*, 233–242.

Carneiro, P.C.F., and Urbinati, E.C. (2001). Salt as a stress response mitigator of matrinxã, *Brycon cephalus* (Günther), during transport. Aquac. Res. *32*, 297–304.

Christensen, A.K., Hiroi, J., Schultz, E.T., and McCormick, S.D. (2012). Branchial ionocyte organization and ion-transport protein expression in juvenile alewives acclimated to freshwater or seawater. J. Exp. Biol. *215*, 642–652.

Crespi, B.J., and Fulton, M.J. (2004). Molecular systematics of Salmonidae: combined nuclear data yields a robust phylogeny. Mol. Phylogenet. Evol. *31*, 658–679.

Czesny, S., Epifanio, J., and Michalak, P. (2012). Genetic divergence between freshwater and marine morphs of alewife (*Alosa pseudoharengus*): A "next-generation" sequencing analysis. PLoS ONE *7*, e31803.

Darwin, C.R. (1876). The origin of species by means of natural selection, or the preservation of favoured races in the struggle for life. (London: John Murray).

DeFaveri, J., and Merilä, J. (2014). Local adaptation to salinity in the three-spined stickleback? J. Evol. Biol. *27*, 290–302.

DeFaveri, J., Shikano, T., Shimada, Y., Goto, A., and Merilä, J. (2011). Global analysis of genes involved in freshwater adaptation in threespine sticklebacks (*Gasterosteus aculeatus*). Evolution *65*, 1800–1807.

Evans, D.H., Piermarini, P.M., and Choe, K.P. (2005). The multifunctional fish gill: dominant site of gas exchange, osmoregulation, acid-base regulation, and excretion of nitrogenous waste. Physiol. Rev. *85*, 97–177.

Fay, C.W., Neves, R.J., and Pardue, G.B. (1982). Species profiles: life histories and environmental requirements of coastal fishes and invertebrates (Mid-Atlantic). Alewife/Blueback Herring. Biological Report - United States Fish and Wildlife Service *82*.

Fuller, R.C. (2009). A test for a trade-off in salinity tolerance in early life-history stages in *Lucania goodei* and *L. parva*. Copeia *2008*, 154–157.

Futuyma, D.J., and Moreno, G. (1988). The evolution of ecological specialization. Ann. Rev. Ecol. Syst. *19*, 207–233.

Hereford, J. (2009). A quantitative survey of local adaptation and fitness trade-offs. Am. Nat. *173*, 579–588.

Hiroi, J., and McCormick, S.D. (2012). New insights into gill ionocyte and ion transporter function in euryhaline and diadromous fish. Resp. Physiol. Neurobi. *184*, 257–268.

Hiroi, J., Yasumasu, S., McCormick, S.D., Hwang, P.-P., and Kaneko, T. (2008). Evidence for an apical Na–Cl cotransporter involved in ion uptake in a teleost fish. J. Exp. Biol. *211*, 2584–2599.

Hohenlohe, P.A., Bassham, S., Etter, P.D., Stiffler, N., Johnson, E.A., and Cresko, W.A. (2010). Population genomics of parallel adaptation in threespine stickleback using sequenced RAD tags. PLoS Genet. *6*, e1000862.

Hwang, P.-P., and Lee, T.-H. (2007). New insights into fish ion regulation and mitochondrion-rich cells. Comp. Biochem. Phys. A *148*, 479–497.

Inokuchi, M., Hiroi, J., Watanabe, S., Hwang, P.-P., and Kaneko, T. (2009). Morphological and functional classification of ion-absorbing mitochondria-rich cells in the gills of Mozambique tilapia. J. Exp. Biol *212*, 1003–1010.

Johnson, D.L., and Metcalf, M.T. (1982). Causes and controls of freshwater drum mortality during transportation. Trans. Am. Fish. Soc. *111*, 58–62.

Jones, F.C., Grabherr, M.G., Chan, Y.F., Russell, P., Mauceli, E., Johnson, J., Swofford, R., Pirun, M., Zody, M.C., White, S., et al. (2012). The genomic basis of adaptive evolution in threespine sticklebacks. Nature *484*, 55–61.

Katoh, F., Hyodo, S., and Kaneko, T. (2003). Vacuolar-type proton pump in the basolateral plasma membrane energizes ion uptake in branchial mitochondria-rich cells of killifish *Fundulus heteroclitus*, adapted to a low ion environment. J. Exp. Biol. *206*, 793–803.

Kawecki, T.J., and Ebert, D. (2004). Conceptual issues in local adaptation. Ecol. Lett. *7*, 1225–1241.

Lahti, D.C., Johnson, N.A., Ajie, B.C., Otto, S.P., Hendry, A.P., Blumstein, D.T., Coss, R.G., Donohue, K., and Foster, S.A. (2009). Relaxed selection in the wild. Trends Ecol. Evol. *24*, 487–496.

Lee, C.E., Bell, M.A., Lee, C.E., and Bell, M.A. (1999). Causes and consequences of recent freshwater invasions by saltwater animals. Trends Ecol. Evol. *14*, 284–288.

Lee, C.E., Remfert, J.L., and Chang, Y.-M. (2007). Response to selection and evolvability of invasive populations. Genetica *129*, 179–192.

Lee, C.E., Kiergaard, M., Gelembiuk, G.W., Eads, B.D., and Posavi, M. (2011). Pumping ions: rapid parallel evolution of ionic regulation following habitat invasions. Evolution *65*, 2229–2244.

Li, C., and Ortí, G. (2007). Molecular phylogeny of Clupeiformes (Actinopterygii) inferred from nuclear and mitochondrial DNA sequences. Mol. Phylogenet. Evol. *44*, 386–398.

McCairns, R.J.S., and Bernatchez, L. (2010). Adaptive divergence between freshwater and marine sticklebacks: insights into the role of phenotypic plasticity from an integrated analysis of candidate gene expression. Evolution *64*, 1029–1047.

Michalak, K., Czesny, S., Epifanio, J., Snyder, R.J., Schultz, E.T., Velotta, J.P., McCormick, S.D., Brown, B.L., Santopietro, G., and Michalak, P. (2014). Beta-thymosin gene

polymorphism associated with freshwater invasiveness of alewife (*Alosa pseudoharengus*). J. Exp. Zool *321*, 233–240.

Nikinmaa, M., Soivio, A., Nakari, T., and Lindgren, S. (1983). Hauling stress in brown trout (*Salmo trutta*): Physiological responses to transport in fresh water or salt water, and recovery in natural brackish water. Aquaculture *34*, 93–99.

Nilsen, T.O., Ebbesson, L.O.E., Madsen, S.S., McCormick, S.D., Andersson, E., Björnsson, B.T., Prunet, P., and Stefansson, S.O. (2007). Differential expression of gill $Na^+$,$K^+$-ATPase α - and β-subunits, $Na^+$,$K^+$,$2Cl^-$ cotransporter and CFTR anion channel in juvenile anadromous and landlocked Atlantic salmon *Salmo salar*. J. Exp. Biol. *210*, 2885–2896.

Nordlie, F.G. (2009). Environmental influences on regulation of blood plasma/serum components in teleost fishes: a review. Rev. Fish. Biol. Fisheries *19*, 481–564.

Palkovacs, E.P., Dion, K.B., Post, D.M., and Caccone, A. (2008). Independent evolutionary origins of landlocked alewife populations and rapid parallel evolution of phenotypic traits. Mol. Ecol. *17*, 582–597.

Pfaffl, M.W. (2001). A new mathematical model for relative quantification in real-time RT–PCR. Nucl. Acids Res. *29*, e45–e45.

Rundle, H.D., and Nosil, P. (2005). Ecological speciation. Ecol. Lett. *8*, 336–352.

Savolainen, O., Lascoux, M., and Merilä, J. (2013). Ecological genomics of local adaptation. Nat. Rev. Genet. *14*, 807–820.

Schluter, D. (2000). The Ecology of Adaptive Radiation (Oxford University Press).

Schultz, E.T., and McCormick, S.D. (2013). Euryhalinity in an evolutionary context. In: McCormick SD, Farrell AP, Brauner CJ (eds) Fish Physiology, vol 32. Academic Press

Scott, G.R., and Schulte, P.M. (2005). Intraspecific variation in gene expression after seawater transfer in gills of the euryhaline killifish *Fundulus heteroclitus*. Comp. Biochem. Phys. A *141*, 176–182.

Scott, W., and Crossman, E. (1973). Freshwater fishes of Canada. Fisheries Research Board of Canada Bulletin *184*.

Scott, G.R., Rogers, J.T., Richards, J.G., Wood, C.M., and Schulte, P.M. (2004). Intraspecific divergence of ionoregulatory physiology in the euryhaline teleost *Fundulus heteroclitus*: possible mechanisms of freshwater adaptation. J. Exp. Biol. *207*, 3399–3410.

Shimada, Y., Shikano, T., and Merilä, J. (2011). A high incidence of selection on physiologically important genes in the three-spined stickleback, *Gasterosteus aculeatus*. Mol. Biol. Evol. *28*, 181–193.

Stanley, J.G., and Colby, P.J. (1971). Effects of temperature on electrolyte balance and osmoregulation in the alewife (*Alosa pseudoharengus*) in fresh and sea water. Trans. Am. Fish. Soc. *100*, 624–638.

Tseng, Y.-C., and Hwang, P.-P. (2008). Some insights into energy metabolism for osmoregulation in fish. Comp. Biochem. Phys. C *148*, 419–429.

Velotta, J.P., McCormick, S.D., O'Neill, R.J., and Schultz, E.T. (2014). Relaxed selection causes microevolution of seawater osmoregulation and gene expression in landlocked Alewives. Oecologia *175*, 1081–1092.

Venables, W.N., and Ripley, B.D. (2002). Modern Applied Statistics with S (Springer Science & Business Media).

Watanabe, S., Niida, M., Maruyama, T., and Kaneko, T. (2008). $Na^+/H^+$ exchanger isoform 3 expressed in apical membrane of gill mitochondrion-rich cells in Mozambique tilapia *Oreochromis mossambicus*. Fisheries Sci. *74*, 813–821.

Whitehead, A. (2010). The evolutionary radiation of diverse osmotolerant physiologies in Killifish (*Fundulus sp*.). Evolution *64*, 2070–2085.

Whitehead, A., and Crawford, D.L. (2006). Neutral and adaptive variation in gene expression. PNAS *103*, 5425–5430.

Whitehead, A., Roach, J.L., Zhang, S., and Galvez, F. (2011). Genomic mechanisms of evolved physiological plasticity in killifish distributed along an environmental salinity gradient. PNAS *108*, 6193–6198.

Whitehead, A., Roach, J.L., Zhang, S., and Galvez, F. (2012). Salinity- and population-dependent genome regulatory response during osmotic acclimation in the killifish (*Fundulus heteroclitus*) gill. J. Exp. Biol. *215*, 1293–1305.

Zydlewski, J., and McCormick, S.D. (1997). The loss of hyperosmoregulatory ability in migrating juvenile American shad, *Alosa sapidissima.* Can. J. Fish. Aquat. Sci. *54*, 2377–2387.

**Tables**

**Table 1** Study site details. A map of study site locations is presented in Figure 1.

| Site | Location (CT) | Coordinates | Life history form | Abbreviation | Salinity (ppt) | Conductivity (µS) |
|---|---|---|---|---|---|---|
| Bride Lake | East Lyme | 41.33, -72.24 | Anadromous | A-Bride | 0.1 | 112.0 |
| Amos Lake | Preston | 41.52, -71.98 | Landlocked | L-Amos | 0.1 | 96.9 |
| Long Pond | North Stonington | 41.45, -71.95 | Landlocked | L-Long | 0.0 | 70.2 |
| Quonnipaug Lake | Guilford | 41.39, -72.70 | Landlocked | L-Quonnipaug | 0.1 | 163.3 |
| Pattagansett Lake | East Lyme | 43.37, -72.23 | Landlocked | L-Pattagansett | 0.1 | 77.2 |
| Rogers Lake | Old Lyme | 41.37, -72.30 | Landlocked | L-Rogers | 0.0 | 44.7 |

**Table 2** Primer sequences (F: forward; R: reverse) for candidate osmoregulation genes (*NHE3*, *NKCC, VATP*) and a reference gene (*EF1α*). Product size indicates the size of the PCR amplicon in base pairs (bp). Primers were designed from Alewife gill transcriptome sequence (J. Velotta, unpublished).

| Gene | Primer Sequence | Product size (bp) |
|---|---|---|
| *NHE3* | F: GCACCACGCTCATAGTCATC<br>R: GTTCCGCTCTCTTCACCTTC | 93 |
| *NKCC* | F: AGGCAAGTCAGCAGTTCCAG<br>R: AGCAGGTATGGGATGAGCAG | 100 |
| *VATP* | F: GCGTGTGGAGGGAAGAAA<br>R: GGGATTGGATGGGTGATGT | 81 |
| *EF1α* | F: AGGCTGACTGTGCTGTGTTG<br>R: ACGGGTCTGTCCGTTCTTG | 80 |

**Table 3** Results of generalized linear mixed effects models testing for variation in survival probability for acute challenge experiment. A-Bride and 1 ppt were used as references for significance testing for site and salinity effect, respectively.

| **Fixed Effect** | **Estimate** | **z-value** |
|---|---|---|
| **Site** | | |
| L-Amos | 0.08 | 0.09 |
| L-Long | 0.08 | 0.11 |
| L-Pattagansett | 0.41 | 0.55 |
| L-Quonnipaug | - 0.93 | - 1.31 |
| L-Rogers | - 0.04 | - 0.06 |
| **Salinity** | | |
| 35 ppt | - 1.79 | - 3.47 *** |
| **Site x Salinity** | | |
| L-Amos x 35 ppt | - 2.53 | - 2.39 * |
| L-Long x 35 ppt | - 0.87 | - 1.02 |
| L-Pattagansett x 35 ppt | - 1.75 | - 2.05 * |
| L-Quonnipaug x 35 ppt | - 2.00 | - 2.05 * |
| L-Rogers x 35 ppt | - 3.10 | - 3.41 *** |

* $P < 0.05$, ** $P < 0.01$, *** $P < 0.001$

**Table 4** Results of generalized linear mixed effects models testing for variation in survival probability for laboratory-acclimation salinity challenge experiment. A-Bride and 0 ppt were used as references for significance testing for site and salinity effect, respectively.

| Fixed Effect | Estimate | z-value |
|---|---|---|
| **Site** | | |
| L-Pattagansett | 2.53 | 3.79 *** |
| L-Rogers | -2.35 | - 2.11 * |
| **Salinity** | | |
| 30 ppt | - 3.14 | - 2.85 *** |
| 35 ppt | - 1.67 | --1.93 * |
| 40 ppt | 0.06 | 0.11 |
| **Site x Salinity** | | |
| L-Pattagansett x 30 ppt | 0.56 | 0.40 |
| L-Pattagansett x 35 ppt | 0.72 | 0.63 |
| L-Pattagansett x 40 ppt | 1.29 | 1.65 |
| L-Rogers x 30 ppt | 3.27 | 1.77 |
| L-Rogers x 35 ppt | 5.89 | 4.08 *** |
| L-Rogers x 40 ppt | 5.70 | 5.17 *** |
| **Covariate** | | |
| Length | -1.39 | -6.05 *** |

* $P < 0.05$, ** $P < 0.01$, *** $P < 0.001$

**Figures**

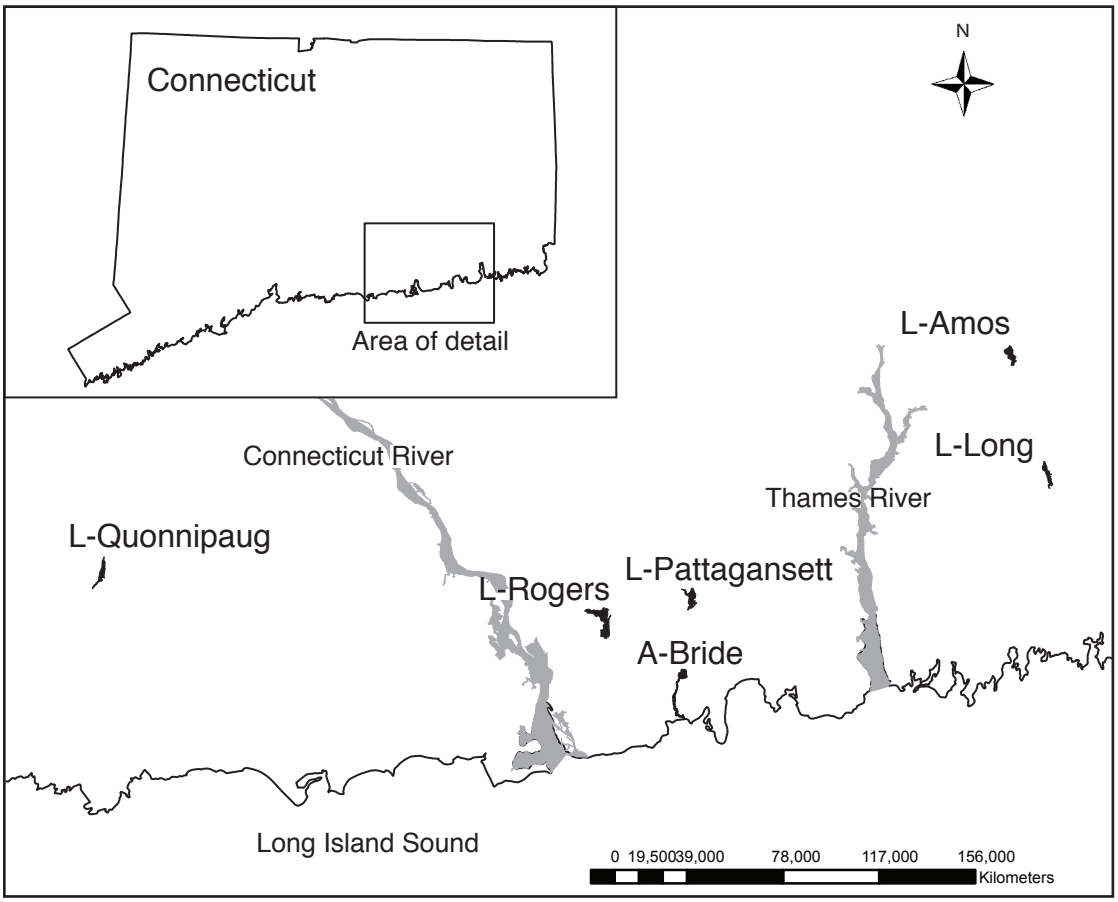


**Figure 1** Map of study sites in Connecticut, USA. Study site details are listed in Table 1. The L prefix denotes landlocked sites, and the A denotes the anadromous site.

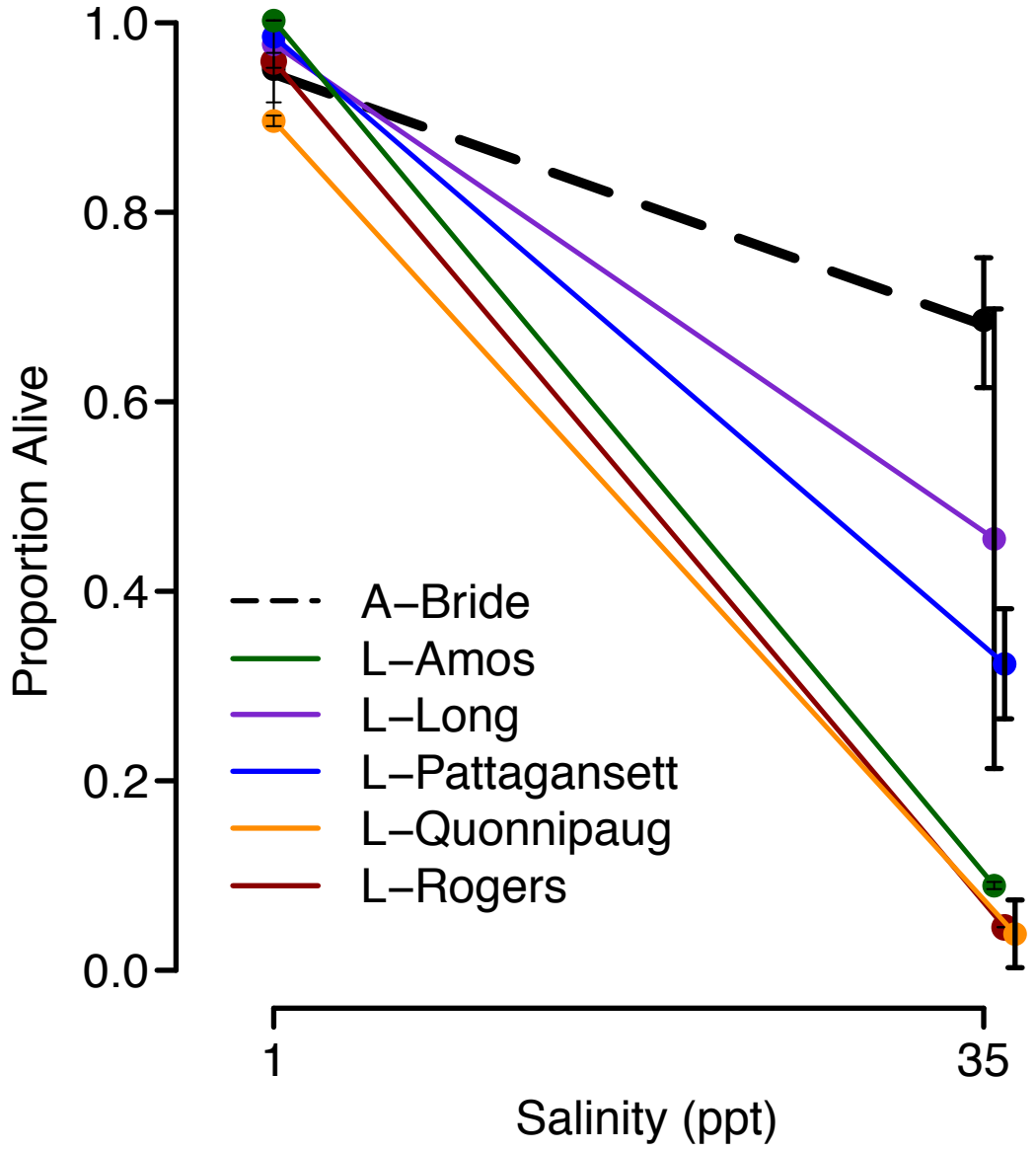


**Figure 2** Survival of anadromous (dashed line) and landlocked (solid lines) Alewives after 24-hour acute challenge at 1 ppt and 35 ppt. The L prefix denotes landlocked, the A denotes anadromous. Each point is the mean value ± standard error of the mean. See Table 3 for results of generalized linear mixed effects models.

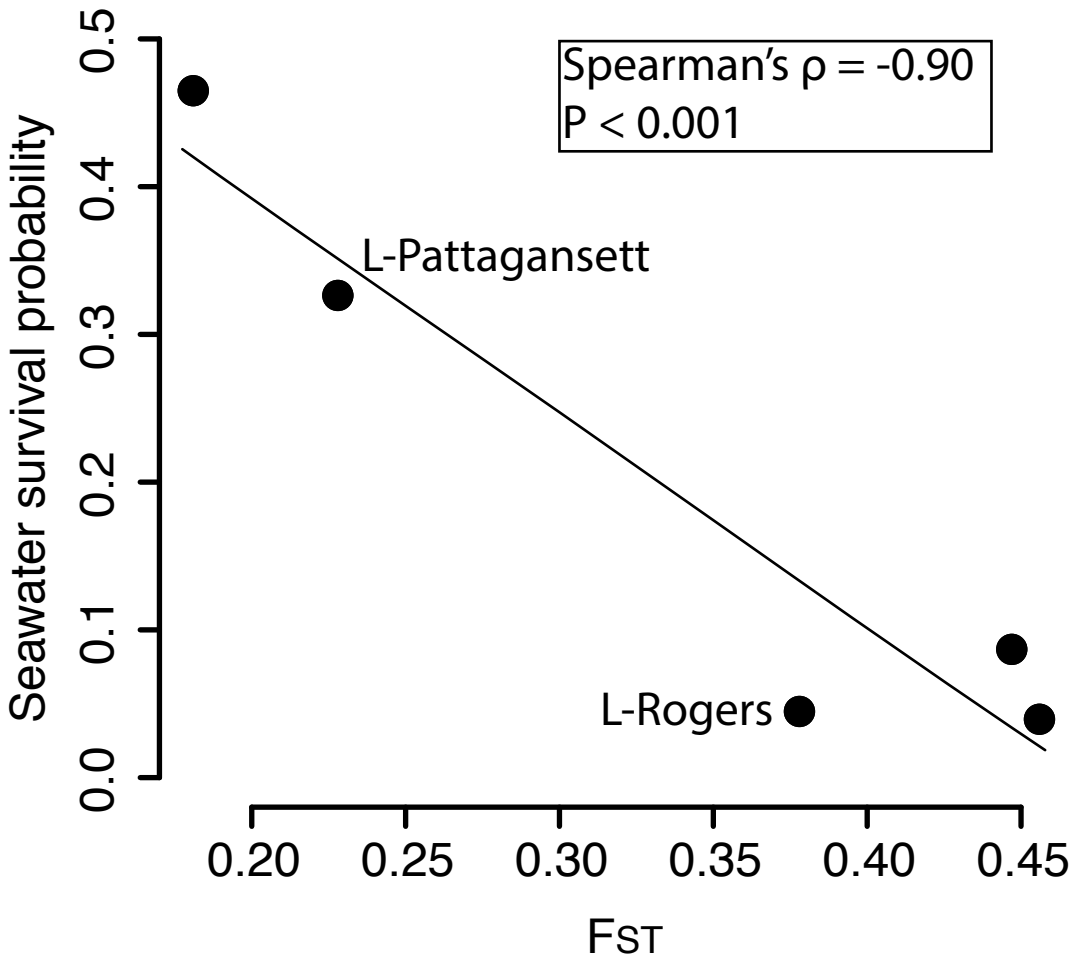


**Figure 3** Seawater survival probability among landlocked Alewife populations versus genetic differentiation (pairwise $F_{ST}$). Seawater survival probability was calculated by dividing average seawater survival and average freshwater survival of each landlocked Alewife site (results of acute seawater challenge experiment; Figure 2). Pairwise $F_{ST}$ values between each landlocked site and A-Bride were based a mitochondrial locus (control region; CR1) and obtained from Palkovacs et al. (2008). I detected a significant correlation ($\rho = -0.90$; $P < 0.001$). Values for L-Pattagansett and L-Rogers are indicated since these populations were used in laboratory-acclimation challenge experiments.

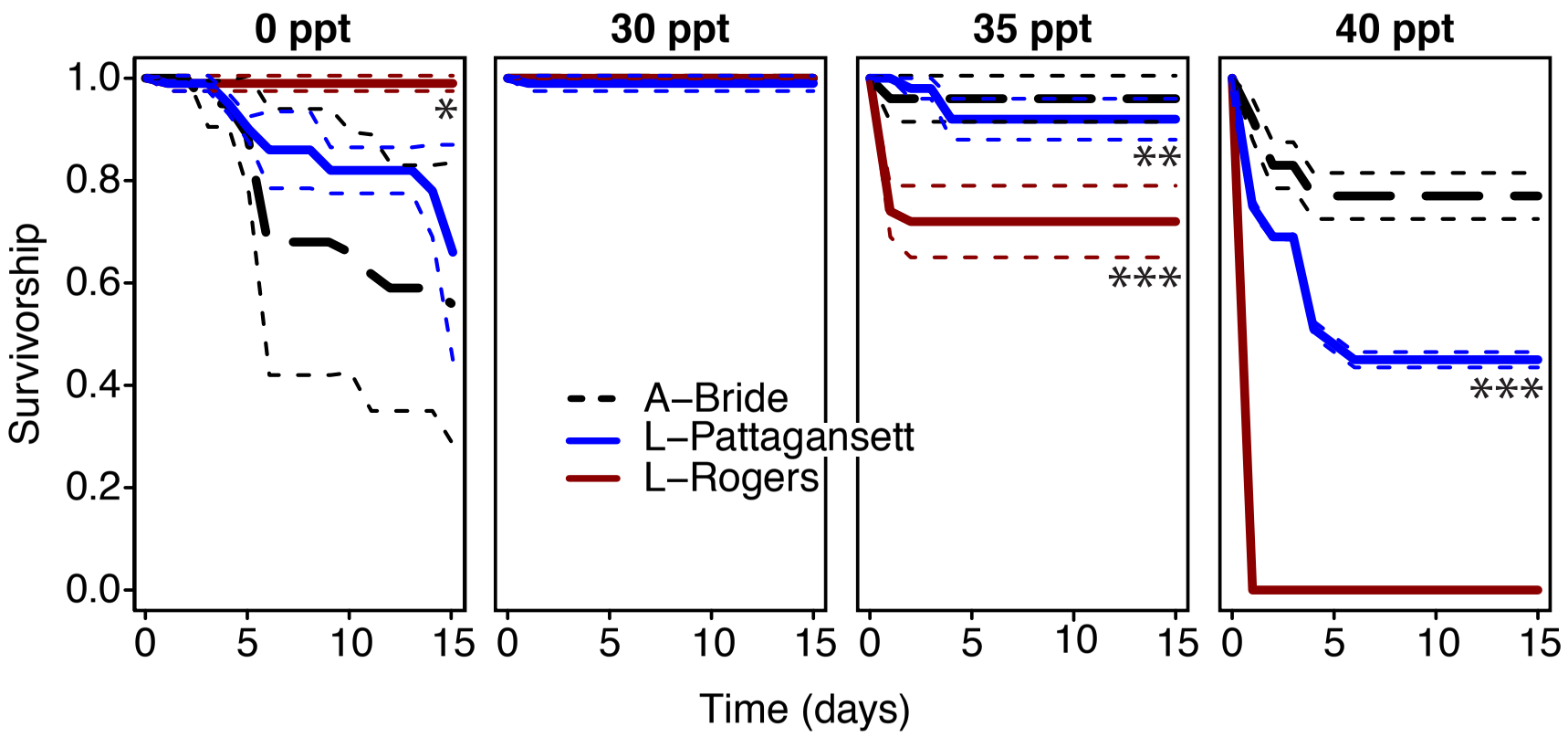


**Figure 4** Survival of anadromous (dashed line) and landlocked (solid lines) Alewives in low-ion freshwater (0 ppt) and seawater (30 ppt, 35 ppt, and 40 ppt) during two week laboratory-acclimation experiments. Short-dashed lines represent standard error of the mean. * $P < 0.05$; ** $P < 0.01$; *** $P < 0.001$ indicating significant differences in survivorship compared to A-Bride, according to a Cox proportional hazards model. See Table 3 for results of generalized linear mixed effects models.

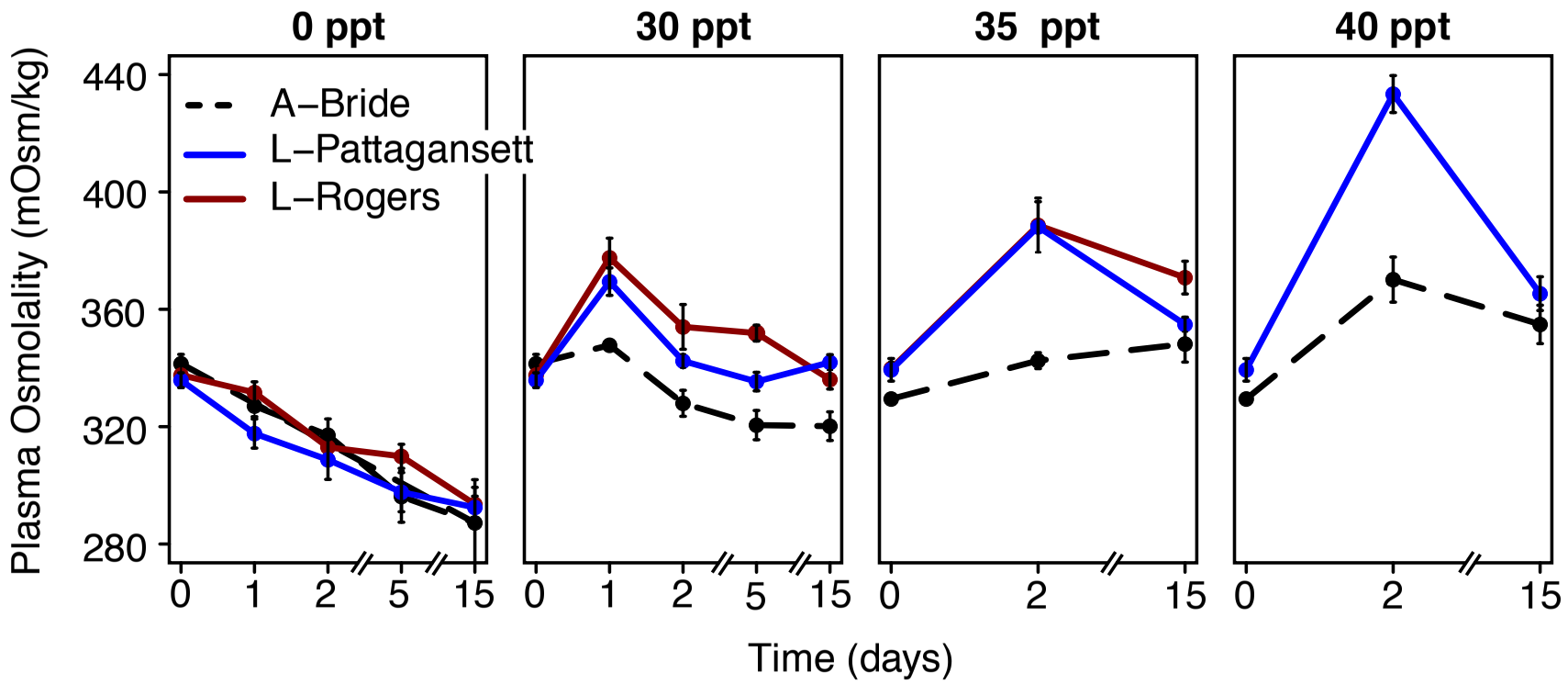


**Figure 5** Plasma osmolality of anadromous (dashed line) and landlocked (solid lines) Alewives in low-ion freshwater (0 ppt) and seawater (30 ppt, 35 ppt, and 40 ppt) during two week laboratory-acclimation challenges (n = 12 individuals per site per salinity treatment per time point). Each point is the mean value ± standard error of the mean. See Table S2 for results of linear mixed effects models.

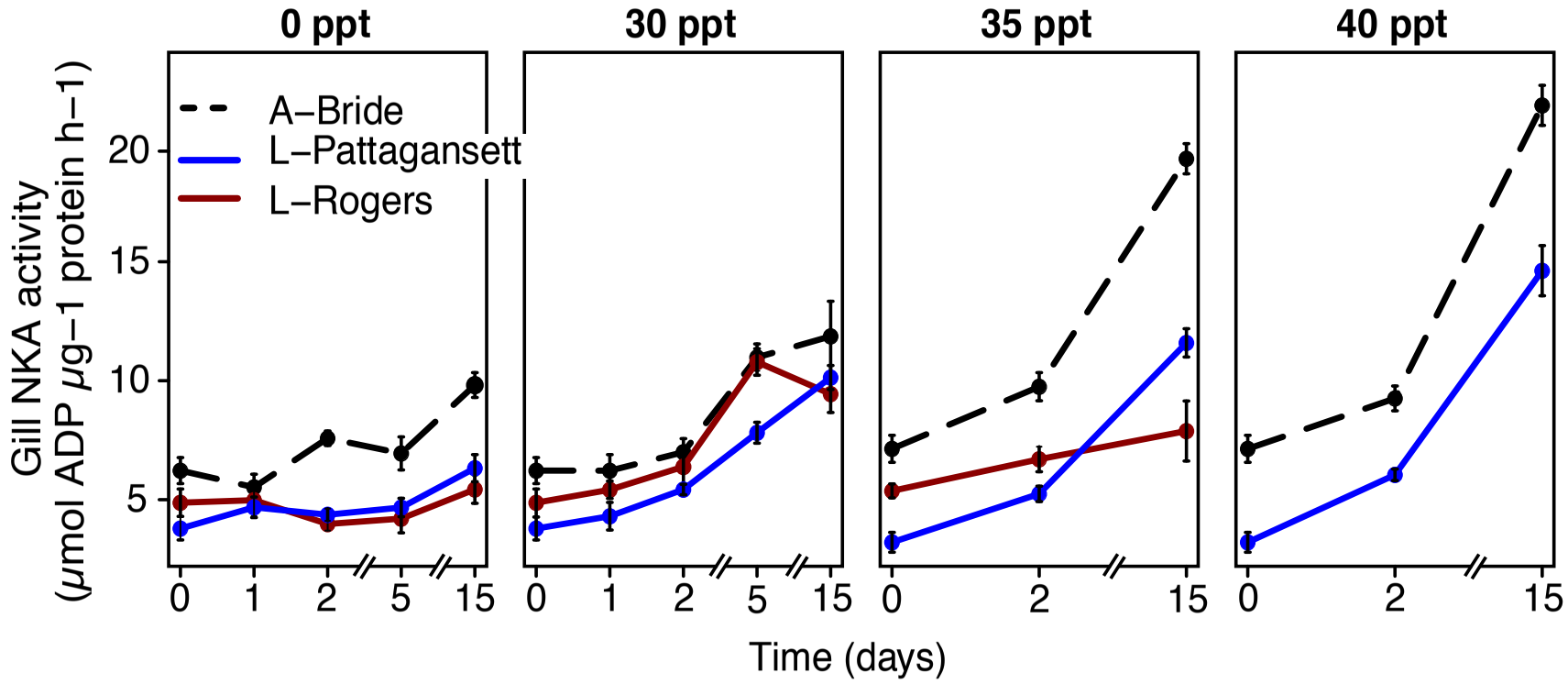


**Figure 6** $Na^+/K^+$-ATPase activity of anadromous (dashed line) and landlocked (solid lines) Alewives in low-ion freshwater (0 ppt) and seawater (30 ppt, 35 ppt, and 40 ppt) during two week laboratory-acclimation challenges (n = 12 individuals per site per salinity treatment per time point). Each point is the mean value ± standard error of the mean. See Table S2 for results of linear mixed effects models.

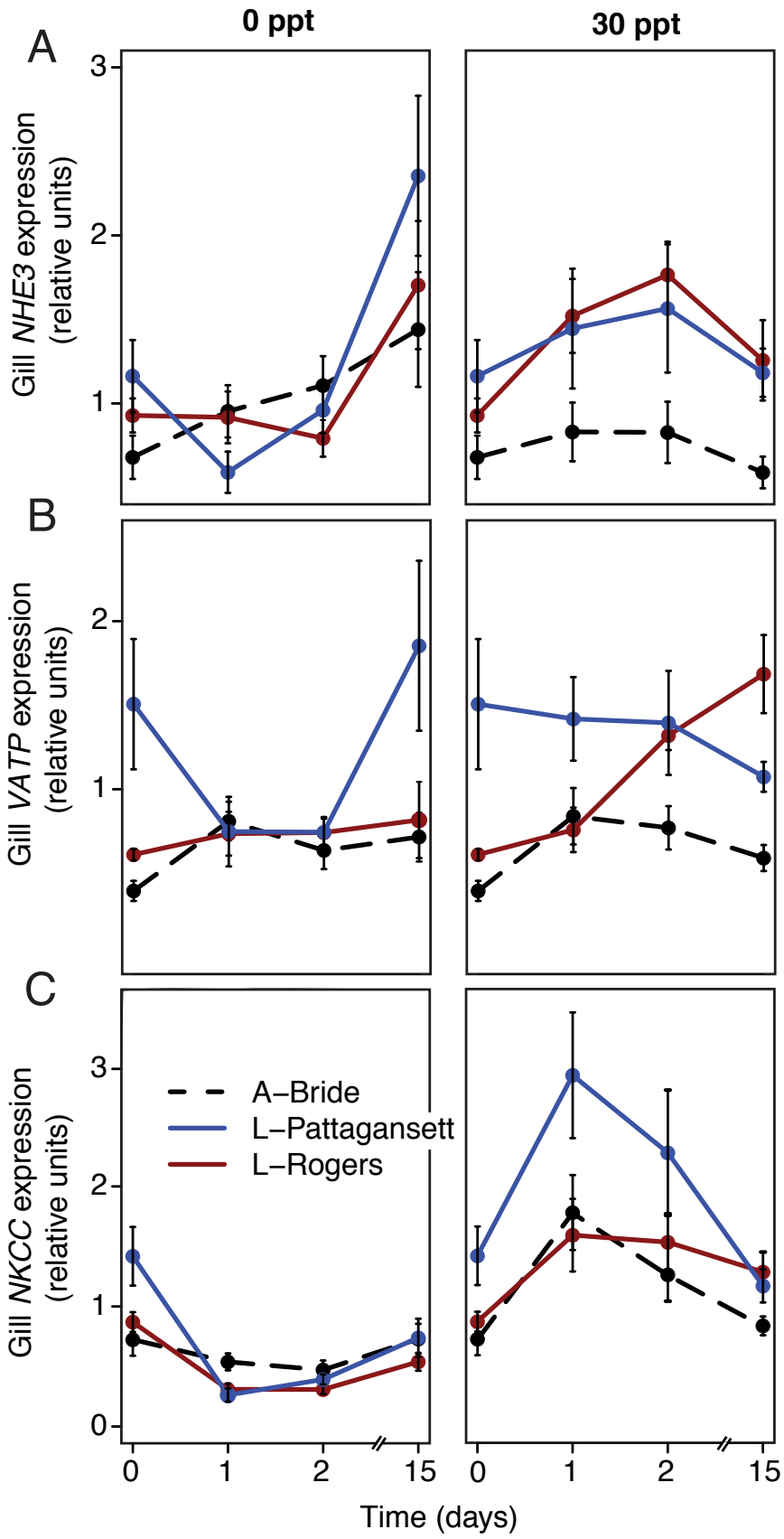
0 ppt
30 ppt
A
B
C
Gill NHE3 expression (relative units)
Gill VATP expression (relative units)
Gill NKCC expression (relative units)
A–Bride
L–Pattagansett
L–Rogers
Time (days)

**Figure 7** Gill gene expression of anadromous (dashed line) and landlocked (solid line) Alewives in low-ion freshwater (0 ppt) and seawater (30 ppt) for A) *NHE3*, B) *VATP*, and C) *NKCC*. Values were normalized to the expression of a reference gene (*EF1α*). n = 8 individuals per site per salinity treatment per time point. Each point is the mean value ± standard error of the mean. See Table S2 for results of linear mixed effects models.

**Supplementary Tables**

**Table S1** Dates of acute salinity exposure experiments. Date of transportation to University of Connecticut was one day prior to date of experiment. The L prefix denotes landlocked, the A denotes anadromous.

| Site | Date (2011) |
|---|---|
| A-Bride | 8 September |
| L-Amos | 25 September |
| L-Long | 4 September |
| L-Pattagansett | 29 August |
| L-Quonnipaug | 22 September |
| L-Rogers | 1 September |

**Table S2** Results of linear mixed effects models for plasma osmolality, gill NKA activity, and candidate gene expression data. For each response, separate models were generated for each salinity treatment. All response variables were log-transformed to meet the assumptions of normality.

**PLASMA OSMOLALITY**

**Plasma osmolality at 0 ppt**

| Fixed effect | Estimate | df | P-value | Random effect | Variance | Standard deviation |
|---|---|---|---|---|---|---|
| site - L-Pattagansett | -0.010 | 5.419 | 0.551 | tank | 1.08E-04 | 1.04E-02 |
| site - L-Rogers | -0.013 | 5.604 | 0.425 | | | |
| day 1 | -0.039 | 18.119 | ***0.037*** | | | |
| day 2 | -0.079 | 17.723 | **< 0.001** | | | |
| day 5 | -0.118 | 17.344 | **< 0.001** | | | |
| day 15 | -0.153 | 19.504 | **< 0.001** | | | |

**Plasma osmolality at 30 ppt**

| Fixed effect | Estimate | df | P-value | Random effect | Variance | Standard deviation |
|---|---|---|---|---|---|---|
| site - L-Pattagansett | -0.041 | 10.130 | 0.077 | tank | 4.84E-05 | 7.30E-03 |
| site - L-Rogers | -0.035 | 9.890 | 0.123 | | | |
| day 1 | 0.018 | 10.790 | 0.352 | | | |
| day 2 | 0.041 | 11.450 | ***0.048*** | | | |
| day 5 | 0.064 | 11.460 | ***0.005*** | | | |
| day 15 | 0.062 | 11.540 | ***0.006*** | | | |
| Length | 0.012 | 162.050 | ***0.002*** | | | |
| site-L-Pattagansett x day 1 | 0.082 | 11.220 | ***0.009*** | | | |
| site-L-Rogers x day 1 | 0.101 | 11.340 | ***0.003*** | | | |

Table S2 continued

| | | | |
|---|---|---|---|
| site-L-Pattagansett x day 2 | 0.064 | 11.500 | ***0.031*** |
| site-L-Rogers x day 2 | 0.098 | 11.880 | ***0.003*** |
| site-L-Pattagansett x day 5 | 0.065 | 11.480 | ***0.030*** |
| site-L-Rogers x day 5 | 0.121 | 12.290 | ***< 0.001*** |
| site-L-Pattagansett x day 15 | 0.079 | 11.510 | ***0.011*** |
| site-L-Rogers x day 15 | 0.066 | 11.570 | ***0.027*** |

**Plasma osmolality at 35 ppt**

| Fixed effect | Estimate | df | P-value | Random effect | Variance | Standard deviation |
|---|---|---|---|---|---|---|
| site - L-Pattagansett | -0.005 | 5.65 | 0.860 | tank | 3.00E-05 | 0.005475 |
| site - L-Rogers | 0.017 | 3.55 | 0.512 | | | |
| day 5 | 0.04 | 5.28 | 0.124 | | | |
| day 15 | 0.044 | 5.68 | 0.099 | | | |
| Length | 0.016 | 96.61 | ***0.012*** | | | |
| site-L-Pattagansett x day 2 | 0.092 | 4.9 | ***0.030*** | | | |
| site-L-Rogers x day 2 | 0.077 | 5.45 | ***0.052*** | | | |
| site-L-Pattagansett x day 15 | 0.001 | 5.27 | 0.979 | | | |
| site-L-Rogers x day 15 | 0.039 | 5.27 | 0.291 | | | |

**Plasma osmolality at 40 ppt**

| Fixed effect | Estimate | df | P-value | Random effect | Variance | Standard deviation |
|---|---|---|---|---|---|---|
| site - L-Pattagansett | 0.029 | 6.49 | 0.181 | tank | 0.00E+00 | 0.00E+00 |
| day 2 | 0.114 | 6.49 | ***< 0.001*** | | | |
| day 15 | 0.073 | 6.49 | ***0.001*** | | | |
| site-L-Pattagansett x day 2 | 0.130 | 6.49 | ***< 0.001*** | | | |
| site-L-Pattagansett x day 15 | 0.001 | 6.49 | 0.989 | | | |

Table S2 continued

**Gill NKA ACTIVITY**

**NKA activity at 0 ppt**

| Fixed effect | Estimate | df | P-value | Random effect | Variance | Standard deviation |
|---|---|---|---|---|---|---|
| site - L-Pattagansett | -0.418 | 5.59 | ***0.033*** | tank | 2.59E-02 | 1.61E-01 |
| site - L-Rogers | -0.418 | 5.81 | ***0.029*** | | | |
| day 1 | -0.026 | 8.50 | 0.860 | | | |
| day 2 | 0.093 | 8.50 | 0.527 | | | |
| day 5 | 0.047 | 8.50 | 0.748 | | | |
| day 15 | 0.370 | 8.81 | ***0.029*** | | | |

**NKA activity at 30 ppt**

| Fixed effect | Estimate | df | P-value | Random effect | Variance | Standard deviation |
|---|---|---|---|---|---|---|
| site - L-Pattagansett | -0.291 | 4.50 | ***0.016*** | tank | 9.12E-04 | 3.02E-02 |
| site - L-Rogers | -0.112 | 4.83 | 0.214 | | | |
| day 1 | 0.039 | 22.63 | 0.698 | | | |
| day 2 | 0.264 | 22.21 | ***0.013*** | | | |
| day 5 | 0.737 | 22.06 | ***< 0.001*** | | | |
| day 15 | 0.760 | 22.81 | ***< 0.001*** | | | |

**NKA activity at 35 ppt**

| Fixed effect | Estimate | df | P-value | Random effect | Variance | Standard deviation |
|---|---|---|---|---|---|---|
| site - L-Pattagansett | -0.704 | 97.97 | ***< 0.001*** | tank | 0.00E+00 | 0.00E+00 |
| site - L-Rogers | -0.269 | 97.97 | ***0.033*** | | | |
| day 2 | 0.322 | 97.97 | ***0.011*** | | | |
| day 15 | 1.022 | 97.97 | ***< 0.001*** | | | |
| site-L-Pattagansett x day 2 | 0.086 | 97.97 | 0.633 | | | |

Table S2 continued

| | | | |
|---|---|---|---|
| site-L-Rogers x day 2 | -0.120 | 97.97 | 0.499 |
| site-L-Pattagansett x day 15 | 0.182 | 97.97 | 0.310 |
| site-L-Rogers x day 15 | -0.798 | 97.97 | ***< 0.001*** |

**NKA activity at 40 ppt**

| Fixed effect | Estimate | df | P-value | Random effect | Variance | Standard deviation |
|---|---|---|---|---|---|---|
| site - L-Pattagansett | -0.704 | 65.97 | ***< 0.001*** | tank | 2.56E-18 | 1.60E-09 |
| day 2 | 0.274 | 65.97 | ***0.003*** | | | |
| day 15 | 1.130 | 65.97 | ***< 0.001*** | | | |
| site-L-Pattagansett x day 2 | 0.286 | 65.97 | **0.028** | | | |
| site-L-Pattagansett x day 15 | 0.292 | 65.97 | **0.025** | | | |

**CANDIDATE GENE EXPRESSION**

***NHE* expression at 0 ppt**

| Fixed effect | Estimate | df | P-value | Random effect | Variance | Standard deviation |
|---|---|---|---|---|---|---|
| site - L-Pattagansett | 0.108 | 5.15 | 0.659 | tank | 5.03E-02 | 2.24E-01 |
| site - L-Rogers | 0.077 | 5.22 | 0.752 | | | |
| day 1 | -0.139 | 8.02 | 0.553 | | | |
| day 2 | 0.088 | 8.19 | 0.707 | | | |
| day 15 | 0.671 | 8.63 | ***0.017*** | | | |

***NHE* expression at 30 ppt**

| Fixed effect | Estimate | df | P-value | Random effect | Variance | Standard deviation |
|---|---|---|---|---|---|---|
| site - L-Pattagansett | 0.595 | 5.11 | **0.007** | tank | 1.29E-03 | 3.59E-01 |
| site - L-Rogers | 0.693 | 5.11 | **0.004** | | | |
| day 1 | 0.229 | 15.733 | 0.162 | | | |

Table S2 continued

| | | | |
|---|---|---|---|
| day 2 | 0.343 | 15.733 | **0.043** |
| day 15 | 0.092 | 15.733 | 0.564 |

***VATP* expression at 0 ppt**

| Fixed effect | Estimate | df | P-value | Random effect | Variance | Standard deviation |
|---|---|---|---|---|---|---|
| site - L-Pattagansett | 0.348 | 4.97 | 0.229 | tank | 7.03E-02 | 2.65E-01 |
| site - L-Rogers | 0.212 | 5.01 | 0.442 | | | |
| day 1 | -0.246 | 6.77 | 0.336 | | | |
| day 2 | -0.232 | 6.79 | 0.362 | | | |
| day 15 | 0.044 | 7.09 | 0.860 | | | |

***VATP* expression at 30 ppt**

| Fixed effect | Estimate | df | P-value | Random effect | Variance | Standard deviation |
|---|---|---|---|---|---|---|
| site - L-Pattagansett | 0.625 | 109.98 | ***< 0.001*** | tank | 0.00E+00 | 0.00E+00 |
| site - L-Rogers | 0.589 | 109.98 | ***< 0.001*** | | | |
| day 1 | -0.017 | 109.98 | 0.902 | | | |
| day 2 | 0.209 | 109.98 | 0.158 | | | |
| day 15 | 0.128 | 109.98 | 0.362 | | | |

***NKCC* expression at 0 ppt**

| Fixed effect | Estimate | df | P-value | Random effect | Variance | Standard deviation |
|---|---|---|---|---|---|---|
| site - L-Pattagansett | -0.227 | 4.8 | 0.370 | tank | 5.96E-02 | 2.44E-01 |
| site - L-Rogers | -0.258 | 5.02 | 0.315 | | | |
| day 1 | -1.166 | 5.06 | ***0.001*** | | | |
| day 2 | -0.997 | 6.73 | ***0.003*** | | | |
| day 15 | -5.002 | 7.03 | 0.055 | | | |

Table S2 continued

***NKCC* expression at 30 ppt**

| Fixed effect | Estimate | df | P-value | Random effect | Variance | Standard deviation |
|---|---|---|---|---|---|---|
| site - L-Pattagansett | 0.330 | 107.98 | 0.134 | tank | 1.29E-03 | 3.59E-02 |
| site - L-Rogers | 0.182 | 107.98 | ***0.005*** | | | |
| day 1 | 0.545 | 107.98 | 0.108 | | | |
| day 2 | 0.358 | 107.98 | **< 0.001** | | | |
| day 15 | 0.006 | 107.98 | 0.964 | | | |

# Chapter 4

## Evolutionary shifts in transcription of gill ion exchange pathways underlie adaptation to freshwater in two populations of landlocked Alewife


### Abstract

Comparative approaches in physiological genomics offers an opportunity to understand the functional importance of genes involved in niche exploitation. I used populations of Alewife (*Alosa pseudoharengus*) to explore the transcriptional mechanisms that underlie adaptation to novel salinity regimes. Ancestrally anadromous Alewives have recently formed multiple, independently derived, landlocked populations, which are locally adapted to freshwater. Using an RNA-seq paradigm, I compared the gill transcriptomes of an anadromous Alewife population to two independently derived landlocked populations after a two-week challenge in freshwater (0 ppt) and seawater (35 ppt). Thousands of genes exhibiting salinity-dependent expression have differentiated between Alewife life history forms. Among these genes, I characterized the expression patterns of those with putative osmoregulatory functions. Genes involved in the gill ion secretion pathway (*NKA* $\alpha$*1b*, *NKCC*, *CFTR*, $K_{ir}$) exhibit reduced transcriptional regulation in response to seawater among landlocked Alewife populations, while several genes involved in gill ion uptake and retention (e.g., *NKA* $\alpha$*1a*, *claudin*s) exhibit enhanced freshwater expression. A substantial proportion of the genes involved in osmoregulatory functions showed parallel patterns of divergence among independently derived landlocked populations. Therefore, modifications to the expression of many well-known effectors of osmotic acclimation may underlie the evolution of osmoregulation upon adaptation to a novel salinity environment.

## Introduction

Identifying the functional role of genes involved in niche exploitation is critical to our understanding of the mechanistic basis of adaptation (Whitehead 2012). For populations that exploit novel environments, genomic elements that facilitate plasticity on acclimatory timescales may become the targets of natural selection as populations adapt to their environment over evolutionary time (Schulte 2001). Comparing transcriptional responses to environmental challenge between populations adapted to different niches is emerging as a powerful way to understand how genome-wide transcriptional regulation leads to phenotypic change. This approach offers a nuanced understanding of the gene expression patterns that contribute to adaptation (Whitehead et al 2011; Whitehead 2012). Rapid advances in genomics tools have made it possible to take a comparative genomics approach in natural populations of organisms without the need for closely related genetic models (Stapley et al 2011).

Adaptation to salinity has played an important role in the evolution and diversification of aquatic animals (Lee et al 1999; Whitehead 2010; Betancur-R 2012; Vega and Wiens 2012; Schultz and McCormick 2013). For teleost fishes, maintenance of ion and water homeostasis (i.e., osmoregulation) in either freshwater (FW) or seawater (SW) is regulated by distinct molecular and biochemical pathways (McCormick and Saunders 1986; Evans et al 2005). In particular, FW animals must actively take in ions that are lost passively from a dilute environment, while SW animals must secrete excess ions accumulated in the body (Evans et al 2005). Comparisons of populations adapted to different salinity regimes offer an opportunity to understand the mechanisms of adaptation to divergent environmental conditions. For example, studies in killifish have shown that genes regulated during acclimation to FW (e.g., the osmotic stress response) have adaptively diverged in populations native to FW compared to populations

native to brackish water (Whitehead et al 2011, 2012). Similarly, expression of genes involved in ion transport and cell volume regulation exhibit divergent responses to brackish water challenge between *Lucania parva* (a euryhaline killifish) and *L. goodei* (a freshwater specialist; Kozak et al 2013). While these studies have yielded important insights into the genomic mechanisms that underlie adaptation to salinity, research is lacking on populations that have independently adapted to novel salinity environments. Addressing this gap will help to clarify whether common or unique mechanisms of gene regulation govern repeated evolution.

I use populations of Alewife (*Alosa pseudoharengus*) to explore the genome-wide transcriptional changes associated with adaptation to a novel salinity regime. Alewives, which belong to a predominantly marine family (Clupeidae; Nelson 2006), exist in two distinct life history forms (LHF): an ancestrally anadromous form that migrates between SW and FW, and a landlocked form that is restricted to FW. Landlocked Alewives are found in multiple lakes and ponds throughout New England, where widespread dam construction during American-colonial development (circa 300-400 years ago) is thought to have been the primary mechanism of isolation. In Connecticut, several landlocked populations have evolved independently from a single genetically homogenous ancestral anadromous stock population (Palkovacs et al 2008).

Previous research has demonstrated that populations of landlocked Alewives are locally adapted to FW; landlocked Alewives are more tolerant of low-ion FW than anadromous Alewives, and are far less tolerant of – and have reduced osmotic balance in – SW (Velotta et al 2014; chapter 3). Changes in the response of several molecular pathways have evolved alongside changes in osmoregulation including lowered gill $Na^+$/ $K^+$-ATPase activity, reduced transcription of several transporters that drive gill ion exchange (Velotta et al 2014; chapter 3), and reduced expression of β-thymosin (a cytoskeletal organizing protein; Michalak et al 2014). Constitutive

differences in transcription at several loci involved in osmoregulation have been found between wild-captured Alewives from an anadromous Atlantic Ocean population and a landlocked population from Lake Michigan (Czesny et al 2012), though these differences may reflect plastic changes involved in acclimation to different salinities. In this study, I manipulated the salinity environment of laboratory-acclimated anadromous and landlocked Alewives in order to gain a functional understanding of how transcriptional regulation underlies evolution of the osmoregulatory system.

Since Alewives adapted to divergent salinity regimes exhibit pronounced differences in measures of fitness and physiological performance (Velotta et al 2014; chapter 3), analysis of the transcriptional response to salinity challenge will shed light on the functional genomic changes that underlie adaptation to salinity. I sequenced the gill transcriptomes of Alewives from one anadromous and two independently derived landlocked populations after two-week challenge in low-ion FW or SW. The gill was chosen because it is the major site of ion exchange for teleost fishes, responsible for ion uptake in freshwater and ion secretion in seawater via the coordination of suites of ion transporters (Evans et al 2005).

This design allowed me to examine several key questions regarding adaptation to FW. First, by challenging Alewives to both FW and SW I was able to differentiate between genes that contribute to adaptive evolution versus those that are evolutionarily conserved, i.e., genes responsible for osmotic acclimation that have not diverged in landlocked populations. Second, I was able to characterize reaction norms for the transcriptional response to FW and SW and identify specific patterns of divergence. Finally, the comparison of one anadromous to two independently derived landlocked populations enabled me to test whether patterns of

transcriptional differentiation have evolved in parallel or if landlocked populations employ unique solutions in adapting to FW.

Because FW and SW require opposing physiological demands, I predicted that a disproportionate number of genes exhibiting LHF divergence in salinity responsiveness would be functionally involved in gill ion exchange and osmoregulation. Among osmoregulation genes, I predicted that: 1) those that are transcriptionally responsive to SW in the ancestral, anadromous form will exhibit a reduced response in landlocked forms; while 2) those that are responsive to FW in the anadromous will exhibit an enhanced response in landlocked forms. I tested this prediction by identifying specific patterns of differentiation among putative osmoregulation genes (Figure 1): 1) reduced SW function, whereby landlocked Alewives exhibit reduced upregulation in SW compared to anadromous Alewives; 2) enhanced FW function, whereby landlocked Alewives exhibit greater upregulation in FW than anadromous Alewives. This approach allows for a more detailed understanding of the patterns of gene expression differentiation involved in evolution of the osmoregulatory system.

## Materials and Methods

### *Animals and experimental procedures*

I captured young-of-the-year Alewives of both life history forms from their natal lakes in Connecticut in October 2011 using a purse seine. Anadromous Alewives were collected from Bride Lake (hereafter A-Bride) in East Lyme, Connecticut, and landlocked Alewives were collected from Pattagansett Lake (hereafter L-Pattagansett; East Lyme, Connecticut), and Rogers Lake (hereafter L-Rogers; Old Lyme, Connecticut). Captured Alewives were immediately transported to the Conte Anadromous Fish Research Center in Turners Falls, Massachusetts in aerated 190-liter cylindrical containers at 1 ppt. Once in the laboratory, Alewives were held at 1

ppt for 1 day, after which salinity was decreased to 0.5 ppt (final rearing salinity). I segregated Alewives by site and held them in separate 1,200-liter re-circulating tanks fitted with charcoal filtration systems for one month prior to experimentation. Fish were maintained between 14.5°C – 16°C water temperature and kept on an ambient photoperiod.

Animals used in this experiment were part of a two-week salinity challenge, the details of which can be found in chapter 3. Briefly, I subjected laboratory-acclimated Alewives from each site to replicate treatments of freshwater (FW) or seawater (SW). FW treatment (0 ppt) was prepared by running filtered, de-chlorinated tap water through a resin-filled cartridge (Culligan International Company, Rosemont, IL, USA). SW treatment (35 ppt) was prepared by dissolving artificial sea salt (Crystal Sea Marine Mix, Marine Enterprises International, Baltimore, MD, USA) in filtered, de-chlorinated tap water. For each treatment, 25-35 Alewives were immediately transferred from 0.5 ppt rearing tanks to replicate 250-liter re-circulation oval tanks with charcoal filtration. Due to space constraints in the laboratory, Alewives were subjected to salinity treatments at different times; FW challenges were conducted from 16 November – 1 December 2011, while SW treatments were conducted from 20 December – 3 January 2011.

After two weeks of exposure to FW and SW, I euthanized surviving Alewives and extracted gill tissue. Fish were euthanized in 250 mg $l^{-1}$ tricaine methanesulfonate (MS-222; Argent, Redmond, WA, USA) and measured for fork length ($L_f$), total length ($L_t$) and weight. Excised gill tissue was trimmed from the bone and then placed immediately in 1 mL of RNAlater solution (Ambion, Life Technologies, Grand Island, NY, USA), incubated at 4°C overnight, and then stored at -20°C.

*Library preparation, sequencing, and* de novo *assembly*

I used massively parallel sequencing to quantify genome-wide transcriptional differences in the gills of FW and SW challenged anadromous and landlocked Alewives. Gill tissue from three individuals per population per salinity treatment was used for library preparation (18 total). I extracted gill RNA prior to sequencing using Trizol reagent following the manufacturer's instructions (Ambion, Life Technologies, USA). Illumina libraries were generated and sequenced at the Virginia Bioinformatics Institute. Using TruSeq RNA sample preparation kit (Illumina, FC-122-1001/1002), mRNA from 1 μg of total RNA with RIN ≥ 8.0 was converted into a library of template molecules suitable for subsequent cluster generation and sequencing with Illumina HiSeq 1000. The libraries generated were validated using Agilent 2100 Bioanalyzer and quantitated using Quant-iT dsDNA HS Kit (Invitrogen) and qPCR. Individually indexed cDNA libraries were pooled, clustered onto a flow cell using Illumina's TruSeq SR Cluster Kit v3 (GD-401-3001), and sequenced to 101 cycles using two TruSeq SBS Kit -HS (FC-401-1002) on HiSeq 1000. One library (A-Bride site, 0 ppt treatment) preparation failed, resulting in a total of 17 sequenced libraries.

I conducted a separate sequencing run on gill tissue pooled from three untreated L-Pattagansett fish (collected in September 2009) using a Roche 454 GS FLX Titanium sequencer (454 Life Sciences). Because 454 reads are longer than Illumina reads, these sequences improved the quality of *de novo* assembly of the gill transcriptome (see below). Gill tissue for 454 sequencing was extracted using the RNeasy Mini Kit (Qiagen, Valencia, CA, USA), and then DNase treated (TURBO DNA-free kit; Life Technologies, Grand Island, NY, USA) following the manufacturer's instructions.

Low-quality reads (Phred-scaled quality score < 35 and minimum read length of 45bp) were filtered from each library with Sickle (Joshi and Fass 2011), and adaptor sequences were removed using the FASTX-Toolkit. Two libraries were removed due to extremely low read quality (both from L-Rogers site, 35 ppt treatment; Table 1), yielding a total of 15 usable libraries. We *in silico* normalized each library prior to assembly using the insilico_read_normalization.pl function in Trinity (Haas et al 2013). Quality control of the reads and normalization yielded approximately 230 million Illumina reads and 350,000 454 reads. Trimmed read lengths averaged 68 bp among Illumina libraries, and 252 bp for the 454 library (Figure 2).

I performed *de novo* transcriptome assemblies of the Alewife gill transcriptomes with both Illumina and 454 reads, which were then clustered into a single assembly using USEARCH (UCLUST). To assemble Illumina sequenced reads, I used two publically available and top performing short-read transcriptome assembly packages -Trinity (minimum contig length of 350bp, single-end reads; Grabherr et al 2011) and SOAPdenovo (minimum contig length of 350bp, single-end reads; Luo et al 2012). I subsequently used Mira (minimum contig length of 350bp; Chevreux et al 2004) to assemble the 454 reads, since this algorithm is optimized for longer reads and lower sequencing depth. Trinity and SOAPdenovo assemblies were clustered with the Mira assembly using the UCLUST utility from the USEARCH package (95% identity and 90% coverage), producing two independent transcriptomes. Transcriptomes were similar in terms of transcript number and length (Table 2; Figure 3). I annotated (UBLAST utility in USEARCH) each hybrid assembly separately against the RefSeq protein database (NCBI) for comparison (weak E-value of .0001 and strong E-value of 1e-9). The Trinity/Mira hybrid assembly yielded a greater number of informative hits against RefSeq and an improved N50

contig length (Table 2), supporting a higher quality assembly. Subsequently, we used the Trinity/Mira assembly as a reference for RNA-seq analysis.

*Read-mapping and RNA-seq analysis*

Trimmed, non-normalized reads from individual libraries were mapped to the Alewife gill transcriptome using Bowtie (Langmead et al 2009). Across the 15 libraries, an average of 87% of reads successfully mapped to at least one transcript in the assembly. I found substantial heterogeneity among populations in the proportion of transcripts with successfully mapped reads (Table 3). Reads from A-Bride mapped to only 52% of assembled transcripts in the transcriptome, compared to 85% mapped from L-Pattagansett, and 97% from L-Rogers. There are several possible, non-mutually exclusive explanations for this observation: 1) transcription in response to FW and/or SW is higher among landlocked Alewives, yielding transcripts that are not present in A-Bride; 2) heterogeneity in post-quality control library sizes between populations (Table 3) may have contributed to a greater number of transcripts among landlocked Alewives than among individuals from A-Bride.

Because I cannot discern whether the observed heterogeneity in read mapping is biologically meaningful or the result of differences in library preparation and/or sequencing, I filtered the dataset. To do so, I retained transcripts for which at least one individual from each population (A-Bride, L-Pattagansett, and L-Rogers) and salinity treatment (FW or SW) had a successfully mapped read (i.e., a non-zero read count). This is a conservative approach, since it excludes transcripts for which zero read counts may inflate differences among populations. In general, low read counts are thought to contribute to measurement error during differential expression analysis, and transcripts with low counts are often filtered out of datasets (Robinson and Smyth 2007).

I performed RNA-seq analysis using the filtered Trinity/Mira assembly as the reference. Expression values of each transcript for each library were computed from the results of the Bowtie alignments using RSEM with default parameters via the align_and_estimate_abundance.pl function in the Trinity pipeline (Hass et al 2013). I used the Bioconductor package, edgeR (Robinson et al 2010; Robinson and Oshlack 2013), to estimate differences in gene expression between life history forms and salinity treatments in R version 3.1.0. First, the function *calcNormFactors* was used to normalize read counts among libraries. Model dispersion for each transcript was estimated separately using the function *estimateGLMTagwiseDisp* (McCarthy et al 2012). I tested for differences in transcript abundance using a generalized linear model (GLM). Factors in the model included main effects of salinity and LHF, as well as the interaction between the two. For LHF and interaction effects, each landlocked site was compared to A-Bride separately, yielding two contrasts (A-Bride vs. L-Pattagansett and A-Bride vs. L-Rogers). I controlled for multiple testing by enforcing a genome-wide false discovery rate (FDR) of 0.05 (Benjamini and Hochberg 1995).

Based on the outcome of the GLM, I categorized differentially expressed transcripts into four separate sets that reflect specific patterns of differentiation: 1) salinity-dependent - those with a significant main effect of salinity only; 2) LHF differentiated – those with a significant main effect of LHF only; 3) additive salinity and LHF differentiated – those exhibiting a salinity and LHF effect; and 4) interactive salinity and LHF differentiated – those exhibiting a significant salinity x LHF interaction.

*Annotation, enrichment analysis, and characterization of expression differentiation*

To gain substantial coverage of Gene Ontology function, process, and component terms, I annotated the reference gill transcriptome against the mouse (*Mus musculus*) protein database,

since teleost genes remain poorly characterized. We first used USEARCH (UBLAST) to obtain high confidence annotations from the mouse RefSeq database (e-value of 1e-5), and retained the best hit from these searches (Python scripts available at: https://github.com/SamGinzburg/WegrzynLab). Gene ontology (GO) terms for each hit were obtained via DAVID Bioinformatics Resources (Huang et al 2009). We used GOrilla (Eden et al 2009) to test for functional enrichment of GO terms among genes in each effect category. The filtered and annotated Trinity/Mira Alewife gill transcriptome was used as a background. Results of the enrichment analysis were visualized with REViGO (Supek et al 2011).

Since I aimed to identify genes that underlie adaptation to a novel osmotic environment, I searched for specific functional terms relating to osmoregulation among differentially expressed transcripts. I identified genes annotated with the GO terms ion transport (GO Biological Process) and tight junction (GO Cellular Component). At the gill, ion exchange in FW or SW is accomplished by suites of ion transport proteins that work in coordination (Evans et al 2005), as well as the regulation of cellular tight junctions that control permeability (e.g., Tipsmark et al 2008). I then examined ion transport and tight junction genes for specific patterns of expression differentiation (Figure 1).

Among ion transport and tight junction genes exhibiting an additive or interactive salinity and LHF differentiated pattern, I used post-hoc analyses (GLMs implemented in edgeR) to determine whether expression fit either model of differentiation (Figure 1). A genome-wide FDR $< 0.05$ was enforced. First, I examined the slopes produced by the GLM for each population to determine the direction of salinity-dependent expression within each population. I then ran a GLM within each salinity treatment to identify the direction of expression differentiation between LHFs. Genes fitting the enhanced FW function model were those with: 1) significant

upregulation in FW among landlocked populations; 2) significantly higher FW expression in landlocked compared to anadromous Alewives; and 3) non-significant difference in SW expression between LHFs. Genes fitting the reduced SW function model were those exhibiting**:** 1) significant upregulation in SW in the anadromous population; 2) significantly lower SW expression in landlocked populations compared to the anadromous; and 3) non-significant difference in FW expression between LHFs. For each analysis, we compared A-Bride to L-Pattagansett and L-Rogers separately.

**Results**

*Differentiation in gene expression between Alewife life history forms and salinity treatments*

I identified 6,034 transcripts (approximately 8% of all transcripts) in which expression was differentiated between anadromous and landlocked LHFs and/or salinity treatments according to the GLM (FDR < 0.05; Figure 4). Transcripts differentiated in a salinity-dependent manner (Figure 5A) reflect a conserved set of genes for which expression has not evolved. Salinity-dependent transcripts are a small fraction (approximately 6%) of all those differentially expressed. Approximately 60% of salinity-dependent transcripts had higher expression in FW than SW (Figure 5A). For a larger proportion of transcripts (approximately 18%), expression was LHF differentiated (Figure 5B). Among these, approximately 13% were differentiated between A-Bride and both landlocked populations (Figure 5B). The majority of differentially expressed transcripts - approximately one-third of the total - exhibited an additive (Figure 5C) or interactive (Figure 5D) salinity and LHF effect. These transcripts represent cases where expression is LHF differentiated, and where the strength of salinity-dependent expression has (interactive effect), or has not (additive effect) differentiated as well. Approximately 41% of transcripts exhibiting an additive salinity and LHF effect were differentiated between A-Bride and both landlocked sites

(Figure 5C), while less than 2% of transcripts exhibiting an interactive salinity and LHF effect were differentiated in this way (Figure 5D).

*Gill transcriptome annotation and enrichment analysis*

Approximately 40% of the Alewife gill transcriptome had informative hits to the mouse protein database, representing a total of 33,403 identified genes. Of these, 21,297 were identical (i.e., isoforms or variant transcripts of the same gene), yielding a total of 11,211 unique genes. Using GO terms obtained from informative hits, we conducted enrichment analysis for each GO category (Biology Process, Molecular Function, Cellular Component) on each set of differentially expressed transcripts (Table S1). Among genes with a salinity-dependent expression pattern, the terms sodium ion export, sodium:potassium-exchanging ATPase complex, and cation-transporting ATPase complex were enriched (GO Biological Process; Table S1). These terms included several subunits and isoforms of $Na^+/K^+$-ATPase. Among LHF differentiated transcripts, I found enrichment of the terms organic anion transport, anion transport (GO Biological Process), as well as cell junction and cell-cell junction (GO Cellular Component; Table S1). Genes in this category included several solute carrier family genes, as well genes with known osmoregulatory roles: $Na^+/K^+$-ATPase $\alpha$1 (*NKA$\alpha$1*), potassium inwardly-rectifying channel ($K_{ir}$), $Na^+/K^+/2Cl^-$ cotransporter (*NKCC*), and several *claudins*. Genes exhibiting an interactive salinity and LHF effect were enriched for several terms involved in post-transcriptional modification, including the Biological Process terms translation and mRNA processes. No ion transport or tight junction regulation terms were enriched among additive or interactive salinity and LHF differentiated genes (Table S1).

*Patterns of expression differentiation of osmoregulatory genes*

I identified transcripts with potential functional roles in osmoregulation by extracting those annotated with ion transport (GO Biological Process) and tight junction assembly (GO Cellular Component) terms (Tables 4-7). These GO terms were not enriched among sets of differentially expressed genes. However, I considered them for this analysis since: 1) the primary goal was to identify genes that underlie evolutionary shifts in osmoregulation; 2) many of these genes were included in lower GO terms that were found to be enriched in several categories of expression differentiation (e.g., sodium transport and anion transport; see above and Table S1).

Among genes with ion transport and tight junction assembly functions, the majority exhibited an interactive salinity and LHF differentiated pattern, in which differentiation was significant between A-Bride and either L-Pattagansett or L-Rogers, but not both (Table 7). A single gene (*NKCC*) exhibiting a significant interaction effect was differentiated between A-Bride and both landlocked populations. Several genes involved in ion transport exhibited an additive salinity and LHF effect (Table 6), all of which have putative roles in osmoregulation. All genes in this effect category were significantly differentiated between A-Bride and both landlocked populations in the same direction and magnitude, i.e., a common pattern of differentiation.

I conducted a post-hoc analysis among salinity-dependent and LHF differentiated transcripts in order to test predictions regarding the pattern and direction of differentiation (Figure 1). Twenty-five out of 89 transcripts (28%) exhibited patterns of differentiation that met the expectation of one of two predicted models (Tables 6-7). Of the 25 transcripts, two exhibited a pattern consistent with the enhanced FW function model (*NKA $\alpha$1* and *glutamate receptor AMPA4*; Table 6-7). I identified the *NKA $\alpha$1* transcript fitting the enhanced FW function model

as *NKA α1a* (Figure 7), a paralog of *NKA α1* for which expression is upregulated in FW in several species of fish (see Discussion), based on several lines of evidence: 1) BLAST results against NCBI's nr database revealed that its closest match is *Danio rerio NKA α1a*; 2) it is more highly expressed in FW than SW among all Alewife populations (Figure 7); and 3) a separate study using quantitative real time PCR reveals that this transcript is upregulated in response to freshwater and downregulated in response to SW over a two-week salinity challenge period (Velotta, McCormick, and Schultz, unpublished data). Subsequently, I identified *NKA α1b*, a paralog of *NKA α1* associated with SW ion secretion, in my dataset. Expression of this transcript shows strong upregulation in SW among anadromous Alewives, and weak upregulation in both populations of landlocked Alewives (fitting the reduced SW model; Figure 7), though only nominal P-values were significant ($P < 0.05$) for the interaction between A-Bride and both landlocked sites.

Twenty-three ion transport/tight junction regulation transcripts fit the reduced SW function model (Tables 6-7). Many of these transcripts have well-established roles in gill ion exchange including *NKCC*, cystic fibrosis transmembrane conductance regulator (*CFTR*), and $K_{ir}$ (Figure 6). Eighteen transcripts fit a pattern of differentiation that was similar to either of the two proposed models (but for which reaction norms for expression cross (i.e., the landlocked response to both FW and SW has differentiated). In all cases, expression is significantly higher in FW and significantly lower in SW for landlocked compared to anadromous Alewives. (reciprocal expression differentiation)

**Discussion**

The results of this study reveal that the transition to an exclusively FW life history has led to shifts in transcription of thousands of genes in the gill. Among landlocked Alewives, many genes that function to maintain hypoosmotic balance exhibited reduced expression in SW, while a single gene that functions to maintain hyperosmotic balance exhibited enhanced expression in FW. This suggests that shifts in the limits of FW and SW tolerance among landlocked Alewives may reflect changes in transcriptional regulation of gill ion exchange pathways. For many of these genes, expression differentiation has evolved in a common pattern in both independently derived landlocked populations, suggesting that changes in transcription at these loci may be an adaptive response to an exclusively freshwater life history. Yet the vast majority of transcripts are differentiated between A-Bride and only a single landlocked site, indicating that there may be independent mechanisms by which Alewives adapt to FW. This study provides insight into the ways in which fish have adapted to novel osmotic environments - through shifts in the regulation of ion uptake and ion secretion at the gill – and characterizes evolved expression patterns of many of the well-known effectors of osmotic acclimation.

I identified several thousand transcripts that are differentially expressed between salinity treatments, Alewife LHFs, or both, and classified these into four categories of differentiation according to the results of a GLM: 1) salinity-dependent, 2) LHF differentiated, 3) additive salinity and LHF differentiated, and 4) interactive salinity and LHF differentiated (Figures 4 and 5). Several hundred differentially expressed transcripts showed a salinity-dependent pattern of expression, which reflect the set of transcripts that have a conserved role in acclimation to FW or SW. Among this set, I found enrichment of the GO term sodium ion transport (Table S1), which includes genes with established roles in gill ion exchange: $Na^+$/ $K^+$-ATPase (*NKA*) $\alpha 1$ and $\alpha 3$

(both upregulated in FW). NKA, a membrane-bound ion pump, plays a critical role in gill ion exchange, establishing and maintaining an electrochemical gradient within ionocytes (McCormick et al 2003; Evans et al 2005). Thus, it is not surprising that the expression of NKA α transcripts appear to have a conserved function. Several other transcripts of NKAα1, however, do show patterns of LHF differentiation (see below), suggesting that some isoforms of this enzyme may be more evolutionary labile than others.

Among genes with salinity and LHF differentiated expression patterns (Figure 2 B-D), I detected enrichment of several GO terms with putative functions in gill ion exchange and osmoregulation, including anion transport, sodium ion transport, and cell junction. This suggests that a high proportion of genes with ion exchange/osmoregulatory functions have experienced shifts in transcription in landlocked forms. I also detected enrichment of many GO functions that have no direct role in ion exchange. These include the terms mRNA processing, mRNA metabolic processes, and translation (Table S1). Enrichment of these terms among genes exhibiting a significant interaction may reflect an increase in transcription rate in response to FW or SW; this is particularly likely in SW-treated landlocked Alewives, which experienced severe osmotic perturbations in response to SW (chapter 3, Figure 4).

The vast majority of salinity and LHF differentiated transcripts (additive and interactive) were between the anadromous and a single landlocked population, L-Rogers. Forty-five times as many transcripts exhibited a significant interaction between A-Bride and L-Rogers than between A-Bride and L-Pattagansett (Figure 2D). This result suggests that L-Rogers is more highly diverged from the anadromous ancestor than L-Pattagansett, which is consistent with results of previous work: L-Rogers Alewives exhibit lower SW tolerance and higher FW tolerance than L-Pattagansett fish (chapter 3), and are more genetically differentiated from A-Bride at neutral loci

(Palkovacs et al 2008; chapter 3). Differences in the strength of expression differentiation among landlocked Alewife sites may be due to differences in the length of time landlocked populations have been established (greater genetic differentiation ($F_{ST}$) at neutral loci suggests that L-Rogers was landlocked earlier than L-Pattagansett), or may reflect differences in effective population sizes ($N_e$). Between A-Bride and L-Pattagansett, many genes exhibit significant nominal (uncorrected) P-values ($P < 0.05$) for the interaction effect. This suggests that many more genes may be commonly differentiated than the analysis has the power to detect.

*Transcriptional evolution of gill ion exchange genes*

I identified salinity and LHF differentiated genes with putative roles in osmoregulation as those annotated with ion transport or tight junction assembly GO terms (Tables 6-7). To characterize the direction of differentiation among landlocked Alewives, I determined whether osmoregulation genes fit either a reduced SW or an enhanced FW function pattern of differentiation (Figure 1). Among euryhaline species, transcription of genes thought to regulate FW ion uptake tend to be upregulated in FW and downregulated in SW. By contrast, genes that drive SW ion secretion exhibit the opposite pattern: upregulation in SW and downregulation in FW (Hwang and Lee 2007). Furthermore, several studies have demonstrated that transcription of FW ion uptake genes is more highly upregulated among FW populations (Scott et al 2004; Lee et al 2011; Whitehead et al 2012), while ion secretion genes exhibit reduced SW upregulation among individuals from FW populations (Velotta et al 2014, Scott and Schulte 2005). Thus, I predicted that genes with putative roles in osmoregulation that exhibit a salinity-dependent and LHF differentiated response would fit either of these two models of differentiation.

Approximately 30% of salinity and LHF differentiated transcripts with ion transport or tight junction assembly functions fit into one of the two models of differentiation, and many of

these transcripts are well known effectors of osmotic acclimation. The vast majority of genes fit the reduced SW model (23 of 25; Table 6-7), with only two transcripts (*NKA* $\alpha$*1*, and *glutamate receptor*; Tables 6-7) fitting the enhanced FW function model. Among transcripts fitting either model, three (*NKA*$\alpha$*1*, $K_{ir}$, and *NKCC*; Tables 6-7) are significantly (FDR < 0.05) differentiated between A-Bride and both landlocked sites, indicating that transcriptional regulation of these genes has evolved independently and in parallel.

Eighteen LHF differentiated ion transport or tight junction assembly genes show a pattern of expression that I did not predict *a priori*. For this set of genes, which I have termed reciprocal expression differentiation, I detected significantly higher expression in FW and lower expression in SW for landlocked compared to anadromous Alewives (reaction norms for gene expression cross; Table 7). I did not predict this pattern of differentiation since it represents cases in which the direction of salinity-dependent transcription is opposite between LHFs. Genes exhibiting this pattern may reflect those that have evolved via a trade-off, whereby an increase in expression in one salinity leads to the reduction of expression in the other (e.g., via an antagonistic pleiotropy; Levins 1968; Elena and Sanjuan 2003, Kawecki and Ebert 2004). Many genes exhibiting this pattern of differentiation have no known roles in osmoregulation, with the exception a single transcript of *NKCC* and *claudin 8* (Table 7).

*Reduced function of seawater ion secretion pathways*

I detected evolutionary shifts in gene expression of the major transporters that contribute to ion secretion in the teleost gill. SW ion secretion is accomplished by the coordination of several ion transport proteins (NKA, NKCC, CFTR, and $K_{ir}$) within highly specialized cells of the branchial epithelium known as ionocytes (Evans et al 2005). Basolaterally located NKA

generates an electrochemical gradient that drives ion secretion via the exchange of 2 $K^+$ for 3 $Na^+$ ions. Using the electrochemical gradient established by NKA, NKCC passively transports $Cl^-$ into ionocytes via co-transport with $Na^+$ and $K^+$. $Cl^-$ is then secreted through CFTR, an apical ion channel, while $Na^+$ is secreted paracellularly through leaky tight junctions between ionocytes and accessory cells (McCormick 1995; Evans et al 2005; Marshall and Grosell 2006; Hwang and Lee 2007). The $K^+$ inwardly-rectifying channel ($K_{ir}$) is responsible for recycling excess $K^+$ ions that build up in ionocytes as a result of the action of NKA (Suzuki et al 1999). Previous research has shown that anadromous Alewives are able to acclimate to SW in part by upregulating NKA, NKCC, and CFTR at the gill (protein expression: Christensen et al 2012; gene expression and gill NKA activity: Velotta et al 2014, chapter 3).

I found that seawater expression of *NKCC*, *$K_{ir}$ subfamily J member 1*, *CFTR*, and *NKA $\alpha$1b* is strongly upregulated in anadromous Alewives, but weakly or not at all upregulated among landlocked Alewives (Figure 6). This result is consistent with previous work demonstrating that gene expression of *NKCC*, *CFTR*, and the enzymatic activity of gill NKA is reduced in SW in landlocked Alewives (Velotta et al 2014; though see chapter 3 for contradictory results for *NKCC* expression). Here, I add to this finding by demonstrating that gene expression of these ion transporters has differentiated in parallel between two independently derived landlocked populations, and add *$K_{ir}$* and *NKA $\alpha$1b* to the list of transporters for which expression has differentiated. *$K_{ir}$* and *NKA $\alpha$1b* may be under direct positive selection in the transition to FW since these genes bear signatures of positive selection in several landlocked populations of Threespine Stickleback (*Gasterosteus aculeatus*; Shimada et al 2010; DeFaveri et al 2011; Jones et al 2013). Thus, both gene sequence and transcriptional regulation appear to be under selection in the transition to FW for several genes involved in salt secretion at the gill.

Expression of *prostaglandin receptor E* is more highly upregulated in SW in A-Bride compared to L-Rogers (expression appears undifferentiated in L-Pattagansett; Figure 6). Prostaglandins are thought to inhibit salt extrusion in the SW gill (Evans et al 2005), and may therefore modulate fine control of ion secretion. The apparent decrease in *prostaglandin receptor E* expression among L-Rogers Alewives may be the result of result of accumulation of deleterious alleles on genes that control transcription of this receptor. In addition, genes involved in gill ion uptake (Rhesus blood group-associated A glycoprotein (*Rhcg1*; Hsu et al 2014) and anion exchanger (*AE4*, a putative $Cl^-$ mechanism for $Cl^-$ uptake; Evans 2008) exhibit reduced SW patterns of differentiation (Figure 6).

My results suggest that reductions in SW tolerance and hypoosmoregulatory function among landlocked Alewives (Velotta et al 2014, chapter 3) are in part the result of reductions in the transcriptional response to SW of gill ion secretion genes. That landlocked populations evolved relatively recently (300-400 years; Palkovacs et al 2008), and that changes in gene expression occur in parallel, suggests that reduced transcription of genes central to the maintenance of hypoosmotic homeostasis is under selection upon transition to FW. The removal of SW as a source of selection should reduce or eliminate traits for SW osmoregulatory function by either neutral or non-neutral processes (relaxed selection; Lahti et al 2009). Reduced transcriptional responses to SW among landlocked Alewives may be the result of selection if regulation of SW osmoregulation genes is constitutively costly (e.g., an energetic cost of the regulatory systems needed to detect and respond to SW; Auld et al 2010) or if there are negative genetic correlations with traits under selection in FW. The possibility exists, however, that reduced transcriptional responses to SW are a function of deterioration via accumulation of deleterious mutations (i.e., genetic drift; Lahti et al 2009).

*Enhanced function of freshwater ion uptake pathways*

Several gill ion uptake pathways appear to be under strong positive selection among landlocked Alewives. Expression of *NKA α1a* (Figure 7), several *claudin* genes, and *Rho GTPase 17* (Figure 8) are more sharply upregulated in FW in both populations of landlocked Alewife compared to the anadromous. Although *NKA α1a* is the only of these to fit the enhanced FW function model of differentiation, reaction norms for *claudin 3*, *claudin 8*, and a single transcript of *Rho GTPase 17* clearly indicate enhanced FW expression among landlocked Alewives; significant interactions were detected for *claudin 8* and *Rho GTPase 17*, which fit the reciprocal expression model of differentiation (Table 7), while a significant LHF effect was detected for *claudin 3* (Table 5).

Claudins comprise a main component of tight junction strands that regulate ion permeability at cellular junctions (Sonoda et al 1999), and several paralogs have salinity-dependent expression at the teleost gill (Tipsmark et al 2008; Whitehead 2011, 2012). The regulation of claudins is thought to limit ion permeability in the FW gill (Karnaky 1991), a key process by which fishes maintain hyperosmotic balance. I found the transcription of *claudin 8* and *claudin 3* (Figure 8) is weakly upregulated in SW among anadromous Alewives, but strongly upregulated in FW in both populations of the landlocked form. This pattern of expression differentiation is also evident in *Rho GTPase* (Figure 8), a molecular switch that triggers cytoskeletal remodeling (Di Ciano-Oliceira 2006) and likely accommodates cell volume changes during osmotic acclimation (Evans and Somero 2008). The enhanced expression of *claudin 8, claudin 3,* and *Rho GTPase* in FW among landlocked Alewives suggests that their regulation is under positive selection in the transition to FW, and may facilitate improved hyperosmoregulatory ability via enhanced regulation of ion permeability at the gill. Several

claudin genes (*claudin 4*, *claudin 10*, and *claudin* 17) bear signatures of natural selection in FW populations of the euryhaline killifish *Lucania parva* (Kozak et al 2013), and a Rho GTPase gene (*RHOGTP8*) has been shown to be under selection in FW Threespine Stickleback (DeFaveri et al 2011).

I identified the $Na^+/Cl^-$ cotransporter (*NCC*; Figure 9) among the set of salinity and LHF differentiated genes (Table 7). NCC is a gill ion transporter that regulates $Na^+$ and $Cl^-$ import in several species (Hiroi et al 2008) and was thought to be absent from clupeids (based on immunohistochemical evidence; McCormick and Hiroi 2012). Although individual-level variance is substantial, I found that *NCC* transcription is upregulated in FW, consistent with its role in ion uptake. Transcription of *NCC* does not fit the enhanced FW model, although upregulation is stronger among landlocked Alewives, suggesting that regulation of its expression has evolved in parallel. A higher rate of transcription may confer an adaptive advantage in FW where ions are scarce. In addition, population genetic studies in Threespine Stickleback have found signatures of selection on *NCC* nucleotide sequence (DeFaveri et al 2011). Together with these results, the available data suggest that *NCC* may be a target of selection upon adaptation to freshwater.

*Evolution of gill $Na^+/K^+$-ATPase transcription*

Modulation of *NKA* expression and activity is central to the remodeling of the fish gill upon changes in salinity (Evans et al 2005), and may be directly linked to salinity tolerance (e.g., McCormick et al 2013). I demonstrated that two paralogs of *NKA α1 – NKA α1a* and *NKA α1b* – exhibit a salinity and LHF differentiated pattern of expression. These two *NKA α1* paralogs (also known as isoforms) have recently been identified in several species of fish, and have been shown

to exhibit salinity-dependent expression (termed 'isoform switching'); the *NKA$\alpha$1a* paralog is highly upregulated in FW, while the *$\alpha$1b* paralog is expressed more highly in SW (Richards et al 2003; Shrimpton et al 2005, Bystriansky et al 2006; Nilsen et al 2007; Larsen et al 2008; Madsen et al 2009; Tipsmark et al 2011; Urbina et al 2012; McCormick et al 2009, 2013; Dalziel et al 2014). One study has identified distinctive electrochemical properties between NKA $\alpha$1a and $\alpha$1b, which are thought to maximize ion exchange efficiency in either FW or SW, respectively. For example, NKA $\alpha$1a substitutions are may lead to more efficient $Na^+$ binding, reducing the energy required to transport it from FW to the blood (Jorgensen et al 2008). Thus, switching of NKA $\alpha$1 isoforms may facilitate euryhalinity.

My results indicate that, among landlocked Alewives, expression of *NKA $\alpha$1a* is enhanced in FW, while expression of *NKA $\alpha$1b* is reduced in SW. This is the first study to demonstrate that transcription of *NKA $\alpha$1* paralogs in response to FW and SW evolves in parallel among FW-restricted populations, and adds to the growing body of literature suggesting that paralogs of *NKA $\alpha$1* have evolved in multiple unrelated lineages (Dalziel et al 2014). Failure to upregulate *NKA $\alpha$1b* in SW may account, in part, for reduced SW tolerance of landlocked Alewives (Velotta et al 2014; chapter 3), as has been demonstrated for salmonids (Bystriansky et al 2007, Nilsen et al 2007). Furthermore, enhanced FW expression of *NKA $\alpha$1a* may lead to improved FW tolerance among landlocked Alewives (see chapter 3). This result is consistent with Nilsen et al (2007), who demonstrated that gene expression of gill *NKA $\alpha$1a* remains elevated in landlocked Atlantic salmon compared to an anadromous population. Previous studies have indicated that gill NKA activity is constitutively lower among FW-restricted populations (Velotta et al 2014; chapter 3; Lee et al 2011), and that NKA $\alpha$ may under positive selection upon transition to FW (Shimada et al 2010; DeFaveri et al 2011; Jones et al 2013). Here, I

provide evidence that selection on increased transcriptional regulation of *NKA α1a* in response to FW, and decreased transcription of *NKA α1b* in response to SW has occurred in parallel. Since NKA is the major driver of ion exchange at the gill in both FW and SW, evolved differences in transcriptional regulation may be a primary way by which fish have adapted to FW.

*Conclusions*

The transition to a fully FW life cycle results in a trade-off in salinity tolerance, which may occur by changes in the regulation of genes for ion exchange. Enhanced transcriptional regulation of *NKA α1a*, claudins, and Rho GTPase in FW may lead to improved tolerance among landlocked Alewives via a more efficient ion uptake system. Conversely, lowered transcription of *NKA α1b, CFTR*, *NKCC*, $K_{ir}$, and *prostaglandin E receptor* may limit the efficiency of SW ion secretion among landlocked Alewives. Though many more genes exhibit unique rather than common patterns of expression differentiation, a substantial proportion of the genes involved in osmoregulatory function show parallel patterns of divergence. Thus, modifications to the expression of many well-known osmoregulatory pathways may underlie the evolution of osmoregulatory function upon adaptation to freshwater.

**Acknowledgements**

I am indebted to Pawel Michalak and the staff of the Virginia Bioinformatics Institute for conducting Illumina sequencing. Thanks to Jill Wegrzyn, Nathanial Jue, and Lin Kang for significant assistance with bioinformatics and data analysis. Thanks to Emily Funk, Grace Casselberry, Jeffrey Divino, and Andrew Jones for help collecting Alewives. Special thanks to Amy Regish and Mike O'Dea (1962-2014) for their assistance with fish rearing and care.

Funding for Illumina sequencing was provided by a grant from State of Illinois Department of Natural Resources (#CAFWS-74) to Pawel Michalak and colleagues.

**References**

Auld, J.R., Agrawal, A.A., and Relyea, R.A. (2010). Re-evaluating the costs and limits of adaptive phenotypic plasticity. Proc. R. Soc. B *277*, 503–511.

Benjamini, Y., and Hochberg, Y. (1995). Controlling the false discovery rate: a practical and powerful approach to multiple testing. J. Roy. Stat. Soc. B. Met. *57*, 289–300.

Betancur-R., R., Ortí, G., Stein, A.M., Marceniuk, A.P., and Alexander Pyron, R. (2012). Apparent signal of competition limiting diversification after ecological transitions from marine to freshwater habitats. Ecol. Lett. *15*, 822–830.

Bystriansky, J.S., Richards, J.G., Schulte, P.M., and Ballantyne, J.S. (2006). Reciprocal expression of gill $Na^+/K^+$-ATPase α -subunit isoforms α1a and α1b during seawater acclimation of three salmonid fishes that vary in their salinity tolerance. J. Exp. Biol. *209*, 1848–1858.

Bystriansky, J.S., Frick, N.T., Richards, J.G., Schulte, P.M., and Ballantyne, J.S. (2007). Failure to up-regulate gill $Na^+,K^+$-ATPase α-subunit isoform α1b may limit seawater tolerance of land-locked Arctic char (*Salvelinus alpinus*). Comp. Biochem. Phys. A *148*, 332–338.

Chevreux, B., Pfisterer, T., Drescher, B., Driesel, A.J., Müller, W.E.G., Wetter, T., and Suhai, S. (2004). Using the miraEST Assembler for Reliable and Automated mRNA Transcript Assembly and SNP Detection in Sequenced ESTs. Genome Res. *14*, 1147–1159.

Christensen, A.K., Hiroi, J., Schultz, E.T., and McCormick, S.D. (2012). Branchial ionocyte organization and ion-transport protein expression in juvenile alewives acclimated to freshwater or seawater. J. Exp. Biol. *215*, 642–652.

Di Ciano-Oliveira, C., Thirone, A.C.P., Szászi, K., and Kapus, A. (2006). Osmotic stress and the cytoskeleton: the R(h)ole of Rho GTPases. Acta Physiologica *187*, 257–272.

Czesny, S., Epifanio, J., and Michalak, P. (2012). Genetic divergence between freshwater and marine morphs of alewife (Alosa pseudoharengus): A "next-generation" sequencing analysis. PLoS ONE *7*, e31803.

Dalziel, A.C., Bittman, J., Mandic, M., Ou, M., and Schulte, P.M. (2014). Origins and functional diversification of salinity-responsive $Na^+$, $K^+$ATPase α1 paralogs in salmonids. Mol. Ecol. *23*, 3483–3503.

DeFaveri, J., Shikano, T., Shimada, Y., Goto, A., and Merilä, J. (2011). Global analysis of genes involved in freshwater adaptation in threespine sticklebacks (*Gasterosteus aculeatus*). Evolution *65*, 1800–1807.

Eden, E., Navon, R., Steinfeld, I., Lipson, D., and Yakhini, Z. (2009). GOrilla: a tool for discovery and visualization of enriched GO terms in ranked gene lists. BMC Bioinformatics *10*, 48.

Elena, S.F., and Sanjuán, R. (2003). Climb every mountain? Science *302*, 2074–2075.

Evans, D.H. (2008). Teleost fish osmoregulation: what have we learned since August Krogh, Homer Smith, and Ancel Keys. Am. J. Physiol-Reg. I. *295*, R704–R713.

Evans, T.G., and Somero, G.N. (2008). A microarray-based transcriptomic time-course of hyper- and hypo-osmotic stress signaling events in the euryhaline fish *Gillichthys mirabilis*: osmosensors to effectors. J. Exp. Biol. *211*, 3636–3649.

Evans, D.H., Piermarini, P.M., and Choe, K.P. (2005). The multifunctional fish gill: dominant site of gas exchange, osmoregulation, acid-base regulation, and excretion of nitrogenous waste. Physiol. Rev. *85*, 97–177.

Grabherr, M.G., Haas, B.J., Yassour, M., Levin, J.Z., Thompson, D.A., Amit, I., Adiconis, X., Fan, L., Raychowdhury, R., Zeng, Q., et al. (2011). Full-length transcriptome assembly from RNA-Seq data without a reference genome. Nat. Biotech. *29*, 644–652.

Haas, B.J., Papanicolaou, A., Yassour, M., Grabherr, M., Blood, P.D., Bowden, J., Couger, M.B., Eccles, D., Li, B., Lieber, M., et al. (2013). De novo transcript sequence reconstruction from RNA-seq using the Trinity platform for reference generation and analysis. Nat. Protocols *8*, 1494–1512.

Hiroi, J., and McCormick, S.D. (2012). New insights into gill ionocyte and ion transporter function in euryhaline and diadromous fish. Resp. Physiol. Neurobi. *184*, 257–268.

Hiroi, J., Yasumasu, S., McCormick, S.D., Hwang, P.-P., and Kaneko, T. (2008). Evidence for an apical Na–Cl cotransporter involved in ion uptake in a teleost fish. J. Exp. Biol. *211*, 2584–2599.

Hsu, H.-H., Lin, L.-Y., Tseng, Y.-C., Horng, J.-L., and Hwang, P.-P. (2014). A new model for fish ion regulation: identification of ionocytes in freshwater- and seawater-acclimated medaka (*Oryzias latipes*). Cell. Tissue Res. *357*, 225–243.

Huang, D.W., Sherman, B.T., and Lempicki, R.A. (2008). Systematic and integrative analysis of large gene lists using DAVID bioinformatics resources. Nat. Protocols *4*, 44–57.

Hwang, P.-P., and Lee, T.-H. (2007). New insights into fish ion regulation and mitochondrion-rich cells. Comp. Biochem. Phys. A *148*, 479–497.

Jones, F.C., Grabherr, M.G., Chan, Y.F., Russell, P., Mauceli, E., Johnson, J., Swofford, R., Pirun, M., Zody, M.C., White, S., et al. (2012). The genomic basis of adaptive evolution in threespine sticklebacks. Nature *484*, 55–61.

Jorgensen, P.L. (2008). Importance for absorption of $Na^+$ from freshwater of lysine, valine and serine substitutions in the α1a-isoform of $Na^+$,$K^+$-ATPase in the Gills of Rainbow Trout (*Oncorhynchus mykiss*) and Atlantic Salmon (*Salmo salar*). J. Membrane Biol. *223*, 37–47.

Joshi, N.A., and Foss, J.N. (2011). Sickle: A sliding-window, adaptive, quality-based trimming tool for FastQ files (Version 1.33) [Software]. Available at https://github.com/najoshi/sickle

Karnaky Jr., K.J. (1991). Teleost osmoregulation: changes in the tight junction in response to the salinity of the environment. In The Tight Junction, (CRC Press), pp. 175–185.

Kawecki, T.J., and Ebert, D. (2004). Conceptual issues in local adaptation. Ecol. Lett. *7*, 1225–1241.

Kozak, G.M., Brennan, R.S., Berdan, E.L., Fuller, R.C., and Whitehead, A. (2014). Functional and population genomic divergence within and between two species of killifish adapted to different osmotic niches. Evolution *68*, 63–80.

Lahti, D.C., Johnson, N.A., Ajie, B.C., Otto, S.P., Hendry, A.P., Blumstein, D.T., Coss, R.G., Donohue, K., and Foster, S.A. (2009). Relaxed selection in the wild. Trends Ecol. Evol. *24*, 487–496.

Langmead, B., Trapnell, C., Pop, M., and Salzberg, S. (2009). Ultrafast and memory-efficient alignment of short DNA sequences to the human genome. Genome Biol. *10*, R25–10.

Larsen, P.F., Nielsen, E.E., Koed, A., Thomsen, D.S., Olsvik, P.A., and Loeschcke, V. (2008). Interpopulation differences in expression of candidate genes for salinity tolerance in winter migrating anadromous brown trout (*Salmo trutta* L.). BMC Genetics *9*, 12.

Lee, C.E., Bell, M.A., Lee, C.E., and Bell, M.A. (1999). Causes and consequences of recent freshwater invasions by saltwater animals. Trends Ecol. Evol. *14*, 284–288.

Lee, C.E., Kiergaard, M., Gelembiuk, G.W., Eads, B.D., and Posavi, M. (2011). Pumping ions: rapid parallel evolution of ionic regulation following habitat invasions. Evolution *65*, 2229–2244.

Levins, R. (1968). Evolution in Changing Environments: Some Theoretical Explorations (Princeton University Press).

Madsen, S.S., Kiilerich, P., and Tipsmark, C.K. (2009). Multiplicity of expression of $Na^+$,$K^+$–ATPase α -subunit isoforms in the gill of Atlantic salmon (*Salmo salar*): cellular localisation and absolute quantification in response to salinity change. J. Exp. Biol. *212*, 78–88.

Marshall, W.S., and Grosell, M. (2006). Ion transport, osmoregulation, and acid-base balance. In The Physiology of Fishes, (CRC Press), pp. 177–230.

McCarthy, D.J., Chen, Y., and Smyth, G.K. (2012). Differential expression analysis of multifactor RNA-Seq experiments with respect to biological variation. Nucl. Acids Res. *40*, 4288–4297.

McCormick, S.D. (1995). Hormonal control of gill $Na^+$,$K^+$-ATPase and chloride cell function. In Fish Physiology, Chris M. Wood and Trevor J. Shuttleworth, ed. (Academic Press), pp. 285–315.

McCormick, S.D., and Saunders, R.L. (1986). Preparatory physiological adaptations for marine life of salmonids: osmoregulation, growth, and metabolism. American Fisheries Society Symposium *1*, 229.

McCormick, S.D., Sundell, K., Björnsson, B.T., Brown, C.L., and Hiroi, J. (2003). Influence of salinity on the localization of $Na^+/K^+$-ATPase, $Na^+/K^+/2Cl^-$ cotransporter (NKCC) and CFTR anion channel in chloride cells of the Hawaiian goby (*Stenogobius hawaiiensis*). J. Exp. Biol. *206*, 4575–4583.

McCormick, S.D., Regish, A.M., and Christensen, A.K. (2009). Distinct freshwater and seawater isoforms of $Na^+/K^+$-ATPase in gill chloride cells of Atlantic salmon. J Exp Biol *212*, 3994–4001.

McCormick, S.D., Regish, A.M., Christensen, A.K., and Björnsson, B.T. (2013). Differential regulation of sodium–potassium pump isoforms during smolt development and seawater exposure of Atlantic salmon. J. Exp. Biol. *216*, 1142–1151.

Michalak, K., Czesny, S., Epifanio, J., Snyder, R.J., Schultz, E.T., Velotta, J.P., McCormick, S.D., Brown, B.L., Santopietro, G., and Michalak, P. (2014). Beta-thymosin gene polymorphism associated with freshwater invasiveness of alewife (*Alosa pseudoharengus*). J. Exp. Zool *321*, 233–240.

Nelson, J.S. (2006). Fishes of the World (John Wiley & Sons).

Nilsen, T.O., Ebbesson, L.O.E., Madsen, S.S., McCormick, S.D., Andersson, E., Björnsson, B.T., Prunet, P., and Stefansson, S.O. (2007). Differential expression of gill $Na^+$,$K^+$-ATPase α - and β-subunits, $Na^+$,$K^+$,2Cl- cotransporter and CFTR anion channel in juvenile anadromous and landlocked Atlantic salmon *Salmo salar*. J. Exp. Biol. *210*, 2885–2896.

Palkovacs, E.P., Dion, K.B., Post, D.M., and Caccone, A. (2008). Independent evolutionary origins of landlocked alewife populations and rapid parallel evolution of phenotypic traits. Mol. Ecol. *17*, 582–597.

Richards, J.G., Semple, J.W., Bystriansky, J.S., and Schulte, P.M. (2003). $Na^+/K^+$-ATPase α-isoform switching in gills of rainbow trout (*Oncorhynchus mykiss*) during salinity transfer. J. Exp. Biol. *206*, 4475–4486.

Robinson, M.D., and Smyth, G.K. (2007). Moderated statistical tests for assessing differences in tag abundance. Bioinformatics *23*, 2881–2887.

Robinson, M., and Oshlack, A. (2010). A scaling normalization method for differential expression analysis of RNA-seq data. Genome Biol. *11*, R25.

Robinson, M.D., McCarthy, D.J., and Smyth, G.K. (2010). edgeR: a Bioconductor package for differential expression analysis of digital gene expression data. Bioinformatics *26*, 139–140.

Schulte, P.M. (2001). Environmental adaptations as windows on molecular evolution. Comp. Biochem. Phys. B *128*, 597–611.

Schultz, E.T., and McCormick, S.D. (2013). Euryhalinity in an evolutionary context. In: McCormick SD, Farrell AP, Brauner CJ (eds) Fish Physiology, vol 32. Academic Press

Scott, G.R., and Schulte, P.M. (2005). Intraspecific variation in gene expression after seawater transfer in gills of the euryhaline killifish *Fundulus heteroclitus*. Comp. Biochem. Phys. A *141*, 176–182.

Scott, G.R., Rogers, J.T., Richards, J.G., Wood, C.M., and Schulte, P.M. (2004). Intraspecific divergence of ionoregulatory physiology in the euryhaline teleost *Fundulus heteroclitus*: possible mechanisms of freshwater adaptation. J. Exp. Biol. *207*, 3399–3410.

Shimada, Y., Shikano, T., and Merilä, J. (2011). A high incidence of selection on physiologically important genes in the three-spined stickleback, *Gasterosteus aculeatus*. Mol. Biol. Evol. *28*, 181–193.

Shrimpton, J.M., Patterson, D.A., Richards, J.G., Cooke, S.J., Schulte, P.M., Hinch, S.G., and Farrell, A.P. (2005). Ionoregulatory changes in different populations of maturing sockeye salmon *Oncorhynchus nerka* during ocean and river migration. J. Exp. Biol. *208*, 4069–4078.

Sonoda, N., Furuse, M., Sasaki, H., Yonemura, S., Katahira, J., Horiguchi, Y., and Tsukita, S. (1999). *Clostridium perfringens* enterotoxin fragment removes specific claudins from tight junction strands evidence for direct involvement of claudins in tight junction barrier. J. Cell Biol. *147*, 195–204.

Stapley, J., Reger, J., Feulner, P.G.D., Smadja, C., Galindo, J., Ekblom, R., Bennison, C., Ball, A.D., Beckerman, A.P., and Slate, J. (2010). Adaptation genomics: the next generation. Trends Ecol. Evol. *25*, 705–712.

Supek, F., Bošnjak, M., Škunca, N., and Šmuc, T. (2011). REVIGO Summarizes and Visualizes Long Lists of Gene Ontology Terms. PLoS ONE *6*, e21800.

Suzuki, Y., Itakura, M., Kashiwagi, M., Nakamura, N., Matsuki, T., Sakuta, H., Naito, N., Takano, K., Fujita, T., and Hirose, S. (1999). Identification by differential display of a hypertonicity-inducible inward rectifier potassium channel highly expressed in chloride cells. J. Biol. Chem. *274*, 11376–11382.

Tipsmark, C.K., Baltzegar, D.A., Ozden, O., Grubb, B.J., and Borski, R.J. (2008). Salinity regulates claudin mRNA and protein expression in the teleost gill. Am. J. Physiol-Reg. I. *294*, R1004–R1014.

Tipsmark, C.K., Breves, J.P., Seale, A.P., Lerner, D.T., Hirano, T., and Grau, E.G. (2011). Switching of $Na^+$, $K^+$-ATPase isoforms by salinity and prolactin in the gill of a cichlid fish. J. Endocrinol. *209*, 237–244.

Urbina, M.A., Schulte, P.M., Bystriansky, J.S., and Glover, C.N. (2013). Differential expression of $Na^+$, $K^+$-ATPase α-1 isoforms during seawater acclimation in the amphidromous galaxiid fish *Galaxias maculatus*. J. Comp. Physiol. B *183*, 345–357.

Vega, G.C., and Wiens, J.J. (2012). Why are there so few fish in the sea? Proc. R. Soc. B *279*, 2323–2329.

Velotta, J.P., McCormick, S.D., O'Neill, R.J., and Schultz, E.T. (2014). Relaxed selection causes microevolution of seawater osmoregulation and gene expression in landlocked Alewives. Oecologia *175*, 1081–1092.

Whitehead, A. (2010). The evolutionary radiation of diverse osmotolerant physiologies in Killifish (*Fundulus sp.).* Evolution *64*, 2070–2085.

Whitehead, A. (2012). Comparative genomics in ecological physiology: toward a more nuanced understanding of acclimation and adaptation. J. Exp. Biol. *215*, 884–891.

Whitehead, A., Roach, J.L., Zhang, S., and Galvez, F. (2011). Genomic mechanisms of evolved physiological plasticity in killifish distributed along an environmental salinity gradient. PNAS *108*, 6193–6198.

Xie, Y., Wu, G., Tang, J., Luo, R., Patterson, J., Liu, S., Huang, W., He, G., Gu, S., Li, S., et al. (2014). SOAPdenovo-Trans: de novo transcriptome assembly with short RNA-Seq reads. Bioinformatics *30*, 1660–1666.

**Tables**

**Table 1** Details of each library used in RNA-seq analysis, including library size after quality control. * denotes libraries that were not used in RNA-seq analysis due to extremely low size.

| Library name | Site | Life history form | Salinity (ppt) | Library size (number of reads in bp) |
|---|---|---|---|---|
| B1 | A-Bride | Anadromous | 0 | 4,505,858 |
| B2 | A-Bride | Anadromous | 0 | 4,103,306 |
| B3 | A-Bride | Anadromous | 35 | 5,134,240 |
| B4 | A-Bride | Anadromous | 35 | 26,088,843 |
| B5 | A-Bride | Anadromous | 35 | 27,966,280 |
| P1 | L-Pattagansett | Landlocked | 0 | 57,869,321 |
| P2 | L-Pattagansett | Landlocked | 0 | 53,490,293 |
| P3 | L-Pattagansett | Landlocked | 0 | 50,434,237 |
| P4 | L-Pattagansett | Landlocked | 35 | 28,259,630 |
| P5 | L-Pattagansett | Landlocked | 35 | 16,779,296 |
| P6 | L-Pattagansett | Landlocked | 35 | 35,675,336 |
| R1 | L-Rogers | Landlocked | 0 | 39,801,588 |
| R2 | L-Rogers | Landlocked | 0 | 30,391,132 |
| R3 | L-Rogers | Landlocked | 0 | 46,521,267 |
| R4 | L-Rogers | Landlocked | 35 | 32,836,068 |
| R5* | L-Rogers | Landlocked | 35 | 859,994 |
| R6* | L-Rogers | Landlocked | 35 | 108,162 |

**Table 2** Statistics for *de novo* assembled Alewife gill transcriptomes. Illumina sequenced reads were assembled using Trinity and SOAPdenovo, then each was clustered with a separate assembly using 454 reads (via Mira). See text for details. The statistics in the table represent these combined assemblies. Each assembly was annotated against the RefSeq (NCBI) protein database for comparison. The Trinity/Mira hybrid assembly was used in RNA-seq analysis since a larger proportion of transcripts mapped to the RefSeq database.

| | **# transcripts** | **Avg. transcript length (bp)** | **Transcript length range (bp)** | **N50 transcript length (bp)** | **Percentage of transcripts with ≥ 1 informative RefSeq hit** |
|---|---|---|---|---|---|
| Trinity/Mira | 221,475 | 907 | 350 – 19,607 | 1,130 | 40% |
| SOAPdenovo/Mira | 205,423 | 782 | 350 – 12,697 | 870 | 38% |

**Table 3** Table of the percentage of transcripts with non-zero read counts for each site. Substantial heterogeneity among sites in the proportion of transcripts with successfully mapped reads was found.

| Site | Life history form | # of transcripts | Percentage of transcripts with non-zero read count |
|---|---|---|---|
| A-Bride | Anadromous | 221,475 | 52% |
| L-Pattagansett | Landlocked | 221,475 | 85% |
| L-Rogers | Landlocked | 221,475 | 97% |

**Table 4** Table of genes involved in ion transport functions exhibiting a significant salinity-dependent effect (main effect of salinity only) according to a GLM. Log-fold change (logFC), nominal P-Value (P), and False Discovery Rate corrected P-value (FDR) are presented. SW expression was compared to FW expression in the GLM, and as such, a negative log-fold change indicates higher expression in FW than SW.

| Gene | Function | logFC | P | FDR | Upregulated in FW or SW? |
|---|---|---|---|---|---|
| ATPase, Na+/K+ transporting, alpha 1 polypeptide (NKA α1) | ion transport | -8.516 | < 0.001 | < 0.001 | FW |
| ATPase, Na+/K+ transporting, alpha 3 polypeptide (NKA α3) | ion transport | -7.648 | < 0.001 | 0.001 | FW |
| cyclin M2 | ion transport | -2.979 | < 0.001 | 0.002 | FW |
| ferritin heavy chain 1 | ion transport | -2.285 | < 0.001 | 0.001 | FW |
| inositol 1,4,5-triphosphate receptor 3 | ion transport | 1.893 | 0.001 | 0.046 | SW |
| solute carrier family 20, member 1 | ion transport | -2.579 | < 0.001 | < 0.001 | FW |
| solute carrier family 38, member 3 | ion transport | -1.968 | < 0.001 | 0.005 | FW |
| solute carrier family 44, member | ion transport | -4.873 | 0.001 | 0.046 | FW |

**Table 5** Genes involved in ion transport or tight junction assembly functions exhibiting a significant LHF differentiated effect (main effect of LHF only) according to a GLM. Log fold change (logFC), nominal P-Value (P), and False Discovery Rate corrected P-value (FDR) are presented for each comparison (A-Bride vs. L-Pattagansett; A-Bride vs. L-Rogers). Whether significant differentiation was found between A-Bride and both landlocked populations (common) or between A-Bride and either L-Pattagansett or L-Rogers (unique) is included.

| | | A-Bride vs. L-Pattagansett | | | A-Bride vs. L-Rogers | | | |
|---|---|---|---|---|---|---|---|---|
| **Gene** | **Function** | **logFC** | **P** | **FDR** | **logFC** | **P** | **FDR** | **Differentiation common or unique** |
| ATPase, H+ transporting, lysosomal V0 (VATP) subunit C, pseudogene 2 | ion transport | -3.865 | < 0.001 | < 0.001 | -0.507 | 0.463 | 0.896 | unique |
| claudin 15 | tight junction | -2.548 | < 0.001 | 0.022 | -1.207 | 0.075 | 0.572 | unique |
| claudin 15 | tight junction | -2.548 | < 0.001 | 0.022 | -1.207 | 0.075 | 0.572 | unique |
| claudin 15 | tight junction | -2.548 | < 0.001 | 0.022 | -1.207 | 0.075 | 0.572 | unique |
| ferritin heavy chain 1 | ion transport | 4.891 | 0.001 | 0.049 | 3.517 | 0.010 | 0.251 | unique |
| inositol 1,4,5-triphosphate receptor 1 | ion transport | 5.013 | < 0.001 | 0.015 | 4.221 | 0.001 | 0.065 | unique |
| potassium inwardly-rectifying channel ($K_{ir}$), subfamily J, member 1 | ion transport | -2.247 | < 0.001 | 0.021 | -1.458 | 0.014 | 0.300 | unique |
| protein tyrosine phosphatase, receptor type, C | ion transport | 0.988 | 0.126 | 0.602 | 2.803 | < 0.001 | 0.014 | unique |
| Rhesus blood group-associated B glycoprotein | ion transport | -5.158 | < 0.001 | < 0.001 | -4.386 | < 0.001 | < 0.001 | common |
| sideroflexin 3 | ion transport | 6.632 | < 0.001 | 0.030 | 6.297 | 0.001 | 0.059 | unique |
| solute carrier family 12, member 6 ($K^+$, $Cl^-$ cotransporter) | ion transport | 5.279 | < 0.001 | 0.011 | 4.722 | < 0.001 | 0.034 | common |
| solute carrier family 16 (monocarboxylic acid transporters), member 3 | ion transport | 2.925 | 0.001 | 0.039 | 0.595 | 0.450 | 0.895 | unique |
| solute carrier family 25 (mitochondrial carrier, glutamate), member 22 | ion transport | 1.153 | 0.022 | 0.301 | 1.883 | < 0.001 | 0.037 | unique |

Table 5 continued

| | | | | | | | | |
|---|---|---|---|---|---|---|---|---|
| solute carrier family 4 (anion exchanger; AE), member 3 | ion transport | 5.663 | 0.001 | 0.049 | 5.404 | 0.001 | 0.091 | unique |
| solute carrier family 6 (neurotransmitter transporter, creatine), member 8 | ion transport | 3.341 | < 0.001 | 0.017 | 1.806 | 0.029 | 0.401 | unique |
| solute carrier family 8 (sodium/calcium exchanger), member 1 | ion transport | -2.991 | 0.001 | 0.047 | -0.476 | 0.574 | 0.928 | unique |
| solute carrier organic anion transporter family, member 1c1 | ion transport | -0.035 | 0.980 | 0.999 | 6.016 | < 0.001 | 0.009 | unique |
| transferrin | ion transport | 5.875 | < 0.001 | 0.019 | 1.995 | 0.168 | 0.720 | unique |

**Table 6** Genes involved in ion transport or tight junction assembly functions exhibiting a significant additive salinity and LHF effect (main effects of salinity and LHF) according to a GLM. Log fold change (logFC), nominal P-Value (P), and False Discovery Rate corrected P-value (FDR) are presented for each comparison (A-Bride vs. L-Pattagansett; A-Bride vs. L-Rogers). Whether significant differentiation was found between A-Bride and both landlocked populations (common) or between A-Bride and either L-Pattagansett or L-Rogers (unique) is included. The pattern of expression differentiation between anadromous and landlocked forms was assigned to a reduced SW function model, enhanced FW function model (Figure 1), reciprocal expression model, or no model (none).

| | | A-Bride vs. L-Pattagansett | | | A-Bride vs. L-Rogers | | | | |
|---|---|---|---|---|---|---|---|---|---|
| **Gene** | **Function** | **logFC** | **P** | **FDR** | **logFC** | **P** | **FDR** | **Differentiation common or unique** | **Model of differentiation** |
| ATPase, Ca++ transporting, plasma membrane 1 | ion transport | 2.173 | < 0.001 | 0.022 | 2.273 | < 0.001 | 0.022 | common | none |
| ATPase, H+ transporting, lysosomal V1 (VATP) subunit B1 | ion transport | 5.772 | < 0.001 | < 0.001 | 4.661 | < 0.001 | 0.010 | common | none |
| ATPase, Na+/K+ transporting, alpha 1 polypeptide (NKA $\alpha$1) | ion transport | 3.003 | < 0.001 | 0.016 | 3.039 | < 0.001 | 0.021 | common | enhanced FW |
| potassium inwardly-rectifying channel ($K_{ir}$), subfamily J, member 1 | ion transport | -4.438 | < 0.001 | < 0.001 | -3.205 | < 0.001 | 0.006 | common | reduced SW |

**Table 7** Genes involved in ion transport or tight junction assembly functions exhibiting a significant interactive salinity and LHF effect (salinity x LHF interaction) according to a GLM. Log fold change (logFC), nominal P-Value (P), and False Discovery Rate corrected P-value (FDR) are presented for each comparison (A-Bride vs. L-Pattagansett; A-Bride vs. L-Rogers). Whether significant differentiation was found between A-Bride and both landlocked populations (common) or between A-Bride and either L-Pattagansett or L-Rogers (unique) is included. The pattern of expression differentiation between anadromous and landlocked forms was assigned to a reduced SW function model, enhanced FW function model (Figure 1), reciprocal expression model, or no model (none).

| | | A-Bride vs. L-Pattagansett | | | A-Bride vs. L-Rogers | | | | |
|---|---|---|---|---|---|---|---|---|---|
| **Gene** | **Function** | **logFC** | **P** | **FDR** | **logFC** | **P** | **FDR** | **Differentiation common or unique** | **Model of differentiation** |
| ADP-ribosylation factor-like 6 interacting protein 5 | ion transport | 0.336 | 0.558 | 0.998 | 2.602 | < 0.001 | 0.004 | unique | none |
| ATP synthase, H+ transporting, mitochondrial F0 complex, subunit F pseudogene | ion transport | -0.160 | 0.833 | 1.000 | 3.266 | < 0.001 | 0.007 | unique | none |
| ATP synthase, H+ transporting, mitochondrial F1F0 complex, subunit e | ion transport | 0.034 | 0.975 | 1.000 | 3.741 | 0.002 | 0.041 | unique | none |
| ATP synthase, H+ transporting, mitochondrial FO complex, subunit G2, pseudogene | ion transport | -0.366 | 0.628 | 0.999 | 2.633 | 0.002 | 0.044 | unique | none |
| ATPase, Ca++ transporting, cardiac muscle, fast twitch 1 | ion transport | 1.398 | 0.130 | 0.863 | -5.759 | < 0.001 | 0.003 | unique | none |
| ATPase, Ca++ transporting, cardiac muscle, fast twitch 1 | ion transport | 0.669 | 0.353 | 0.979 | -3.474 | 0.001 | 0.027 | unique | reduced SW |
| ATPase, Ca++ transporting, cardiac muscle, slow twitch | ion transport | -7.517 | < 0.001 | 0.056 | -10.084 | 0.001 | 0.020 | unique | reciprocal expression |
| ATPase, Ca++ transporting, plasma membrane 1 | ion transport | -1.068 | 0.159 | 0.895 | -3.525 | 0.001 | 0.024 | unique | reduced SW |
| ATPase, H+ transporting, lysosomal V1 (VATP) subunit C | ion transport | 1.016 | 0.148 | 0.885 | 3.689 | < 0.001 | < 0.001 | unique | none |

Table 7 continued

| | | | | | | | | | |
|---|---|---|---|---|---|---|---|---|---|
| ATPase, H+ transporting, lysosomal V1 (VATP) subunit F | ion transport | 0.346 | 0.671 | 0.999 | 4.563 | < 0.001 | < 0.001 | unique | none |
| ATPase, H+ transporting, lysosomal V1 (VATP) subunit G1 | ion transport | 0.280 | 0.772 | 1.000 | 3.378 | 0.002 | 0.043 | unique | none |
| ATPase, Na+/K+ transporting, alpha 1 polypeptide (NKA α1) | ion transport | 4.910 | < 0.001 | 0.005 | 1.147 | 0.342 | 0.640 | unique | none |
| ATX1 (antioxidant protein 1) homolog 1 (yeast) | ion transport | 1.237 | 0.051 | 0.708 | 2.258 | 0.002 | 0.039 | unique | none |
| calcium channel, voltage-dependent, R type, alpha 1E subunit | ion transport | 0.133 | 0.877 | 1.000 | 3.456 | < 0.001 | 0.015 | unique | none |
| calcium/calmodulin-dependent protein kinase II gamma | ion transport | -0.231 | 0.741 | 1.000 | -2.915 | 0.001 | 0.029 | unique | reduced SW |
| caveolin 1, caveolae protein | ion transport | -0.043 | 0.962 | 1.000 | 4.461 | < 0.001 | 0.001 | unique | none |
| chloride intracellular channel 1 | ion transport | -1.503 | 0.057 | 0.732 | -3.663 | < 0.001 | 0.013 | unique | reciprocal expression |
| claudin 10 | tight junction | -0.374 | 0.668 | 0.999 | 3.360 | 0.001 | 0.020 | unique | none |
| claudin 4 | tight junction | 1.307 | 0.060 | 0.740 | 3.220 | < 0.001 | 0.003 | unique | none |
| claudin 8 | tight junction | -1.946 | 0.051 | 0.708 | -3.998 | 0.003 | 0.048 | unique | reciprocal expression |
| cystic fibrosis transmembrane conductance regulator homolog (CFTR) | ion transport | -1.612 | 0.015 | 0.489 | -2.915 | 0.001 | 0.019 | unique | reduced SW |
| ferritin heavy chain 1 | ion transport | 0.007 | 0.991 | 1.000 | 2.091 | 0.002 | 0.045 | unique | none |
| ferritin light chain 2 | ion transport | 1.925 | 0.002 | 0.222 | 2.904 | < 0.001 | 0.003 | unique | none |
| FXYD domain-containing ion transport regulator 1 | ion transport | -0.221 | 0.856 | 1.000 | 4.281 | 0.002 | 0.038 | unique | none |
| FXYD domain-containing ion transport regulator 2 | ion transport | 2.817 | < 0.001 | 0.075 | 6.159 | < 0.001 | < 0.001 | unique | none |
| glutamate receptor, ionotropic, AMPA2 (alpha 2) | ion transport | -5.474 | < 0.001 | 0.043 | -4.896 | 0.006 | 0.075 | unique | enhanced FW |
| glutamate receptor, ionotropic, AMPA4 (alpha 4) | ion transport | 6.724 | < 0.001 | 0.045 | 4.858 | 0.016 | 0.136 | unique | none |
| glutamate receptor, ionotropic, kainate 2 (beta 2) | ion transport | -1.727 | 0.045 | 0.681 | -3.386 | 0.003 | 0.049 | unique | reduced SW |
| hephaestin-like 1 | ion transport | -0.117 | 0.856 | 1.000 | -2.546 | 0.002 | 0.044 | unique | reduced SW |
| huntingtin | ion transport | -1.783 | 0.106 | 0.829 | -5.142 | < 0.001 | 0.008 | unique | reciprocal expression |
| inositol 1,4,5-triphosphate receptor 1 | ion transport | -1.248 | 0.081 | 0.790 | -2.803 | 0.002 | 0.037 | unique | reciprocal expression |

Table 7 continued

| | | | | | | | | | |
|---|---|---|---|---|---|---|---|---|---|
| inositol 1,4,5-triphosphate receptor 3 | ion transport | -0.902 | 0.344 | 0.976 | 4.227 | < 0.001 | 0.009 | unique | none |
| junction adhesion molecule 2 | tight junction | -1.397 | 0.070 | 0.765 | -2.933 | 0.002 | 0.042 | unique | reciprocal expression |
| membrane associated guanylate kinase, WW and PDZ domain containing 3 | tight junction | -4.198 | < 0.001 | 0.063 | -5.131 | < 0.001 | 0.009 | unique | reciprocal expression |
| nicotinamide nucleotide transhydrogenase | ion transport | -1.515 | 0.043 | 0.673 | -3.180 | 0.001 | 0.023 | unique | reciprocal expression |
| nicotinamide nucleotide transhydrogenase | ion transport | -1.516 | 0.077 | 0.782 | -3.549 | 0.001 | 0.031 | unique | reduced SW |
| potassium channel tetramerisation domain containing 14 | ion transport | -0.244 | 0.688 | 0.999 | 3.043 | < 0.001 | 0.001 | unique | none |
| potassium channel, subfamily K, member 10 | ion transport | -1.731 | 0.055 | 0.723 | -4.507 | < 0.001 | 0.013 | unique | reduced SW |
| potassium inwardly-rectifying channel ($K_{ir}$), subfamily J, member 2 | ion transport | -2.383 | 0.020 | 0.540 | -4.124 | 0.003 | 0.049 | unique | reciprocal expression |
| prostaglandin E receptor 3 (subtype EP3) | ion transport | 0.778 | 0.362 | 0.981 | -3.505 | 0.003 | 0.048 | unique | reduced SW |
| purinergic receptor P2X, ligand-gated ion channel 4 | ion transport | 0.302 | 0.628 | 0.999 | 2.992 | < 0.001 | 0.002 | unique | none |
| purinergic receptor P2X, ligand-gated ion channel 4 | ion transport | -0.224 | 0.825 | 1.000 | -6.792 | < 0.001 | 0.015 | unique | reduced SW |
| pyrimidinergic receptor P2Y, G-protein coupled, 6 | ion transport | 1.402 | 0.195 | 0.924 | 3.675 | 0.002 | 0.046 | unique | none |
| Rhesus blood group-associated A glycoprotein | ion transport | -1.412 | 0.090 | 0.806 | -3.680 | 0.001 | 0.025 | unique | reduced SW |
| Rho GTPase activating protein 17 | tight junction | -2.317 | 0.033 | 0.623 | -3.573 | 0.002 | 0.041 | unique | reciprocal expression |
| Rho GTPase activating protein 17 | tight junction | -0.004 | 0.996 | 1.000 | -5.216 | < 0.001 | 0.001 | unique | reduced SW |
| rho/rac guanine nucleotide exchange factor (GEF) 2 | tight junction | -2.046 | 0.006 | 0.343 | -2.855 | 0.002 | 0.039 | unique | reciprocal expression |
| SCO cytochrome oxidase deficient homolog 1 (yeast) | ion transport | 0.129 | 0.828 | 1.000 | 2.148 | 0.002 | 0.036 | unique | none |
| similar to solute carrier family 12, member 2 (NKCC) | ion transport | -3.193 | < 0.001 | 0.010 | -6.069 | < 0.001 | < 0.001 | common | reciprocal expression |
| similar to solute carrier family 12, member 2 (NKCC) | ion transport | -2.723 | 0.002 | 0.226 | -4.629 | < 0.001 | 0.006 | unique | reduced SW |
| similar to solute carrier family 30, member 2 | ion transport | 0.477 | 0.469 | 0.993 | 3.427 | < 0.001 | 0.001 | unique | none |
| six transmembrane epithelial antigen of prostate 2 | ion transport | -3.143 | 0.002 | 0.207 | -4.273 | < 0.001 | 0.013 | unique | reciprocal expression |
| sodium channel, voltage-gated, type I, beta | ion transport | 0.344 | 0.664 | 0.999 | 3.231 | < 0.001 | 0.010 | unique | none |
| sodium channel, voltage-gated, type II, alpha 1 | ion transport | -2.637 | 0.016 | 0.498 | -5.784 | < 0.001 | 0.011 | unique | reciprocal expression |

Table 7 continued

| | | | | | | | | | |
|---|---|---|---|---|---|---|---|---|---|
| sodium channel, voltage-gated, type VIII, alpha | ion transport | -0.936 | 0.260 | 0.954 | -3.656 | 0.001 | 0.033 | unique | reduced SW |
| solute carrier family 12, member 3 (NCC) | ion transport | -3.745 | 0.002 | 0.220 | -5.767 | 0.001 | 0.021 | unique | none |
| solute carrier family 16 (monocarboxylic acid transporters), member 7 | ion transport | -1.679 | 0.032 | 0.617 | -3.475 | 0.001 | 0.019 | unique | reciprocal expression |
| solute carrier family 20, member 1 | ion transport | -2.718 | 0.026 | 0.584 | -4.634 | 0.001 | 0.024 | unique | reciprocal expression |
| solute carrier family 22 (organic anion transporter), member 6 | ion transport | 0.757 | 0.446 | 0.990 | 3.830 | 0.001 | 0.020 | unique | none |
| solute carrier family 22 (organic cation transporter), member 5 | ion transport | 1.437 | 0.112 | 0.840 | 3.727 | < 0.001 | 0.011 | unique | none |
| solute carrier family 23 (nucleobase transporters), member 1 | ion transport | 0.204 | 0.744 | 1.000 | 3.623 | < 0.001 | < 0.001 | unique | none |
| solute carrier family 24 (sodium/potassium/calcium exchanger), member 3 | ion transport | -1.282 | 0.084 | 0.799 | -2.916 | 0.003 | 0.048 | unique | reduced SW |
| solute carrier family 38, member 10 | ion transport | -0.710 | 0.448 | 0.990 | -3.931 | 0.002 | 0.037 | unique | reduced SW |
| solute carrier family 38, member 4 | ion transport | -0.935 | 0.152 | 0.888 | -2.703 | 0.001 | 0.030 | unique | reciprocal expression |
| solute carrier family 38, member 4 | ion transport | -0.272 | 0.710 | 0.999 | -2.965 | 0.002 | 0.041 | unique | reduced SW |
| solute carrier family 4 (anion exchanger; AE), member 1 | ion transport | -2.317 | 0.008 | 0.372 | -3.743 | 0.001 | 0.027 | unique | reduced SW |
| solute carrier family 5 (choline transporter), member 7 | ion transport | -2.079 | 0.002 | 0.198 | -3.152 | < 0.001 | 0.009 | unique | reciprocal expression |
| solute carrier family 9 (sodium/hydrogen exchanger; NHE), member 6 | ion transport | -0.941 | 0.173 | 0.908 | -2.769 | 0.002 | 0.037 | unique | reduced SW |
| sorcin | ion transport | 0.290 | 0.701 | 0.999 | 2.822 | 0.001 | 0.027 | unique | none |
| thiosulfate sulfurtransferase, mitochondrial | ion transport | -1.039 | 0.124 | 0.855 | -3.030 | 0.001 | 0.017 | unique | reduced SW |
| transient receptor potential cation channel, subfamily M, member 6 | ion transport | -2.182 | 0.002 | 0.207 | -3.349 | < 0.001 | 0.007 | unique | reciprocal expression |
| translocase of outer mitochondrial membrane 40 homolog-like (yeast) | ion transport | 0.899 | 0.245 | 0.950 | 4.226 | < 0.001 | < 0.001 | unique | none |

**Figures**

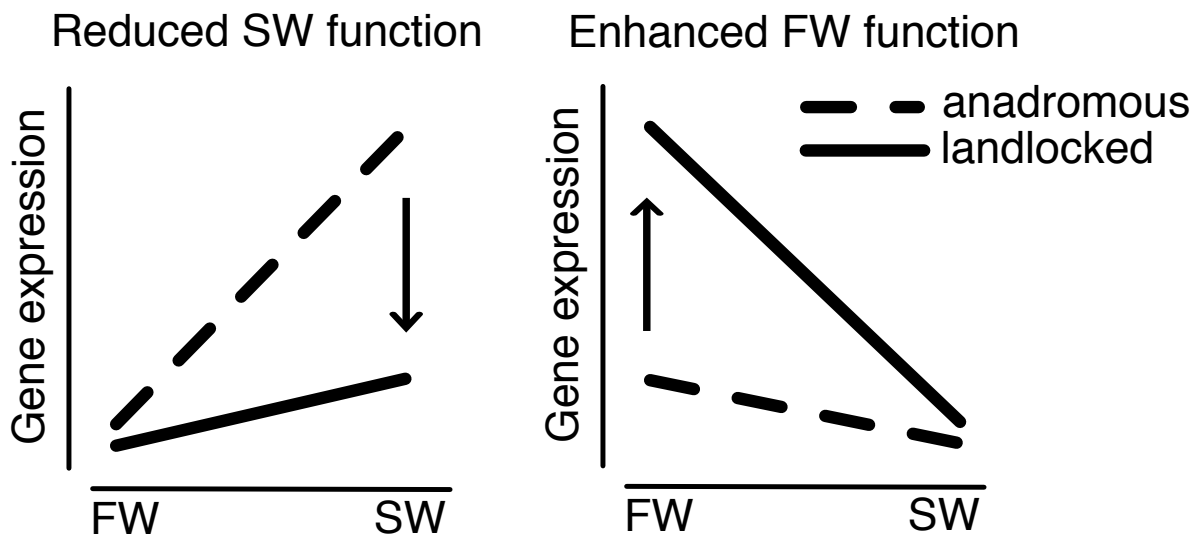


**Figure 1** Schematic plots of two predicted patterns of differentiation among putative osmoregulation genes. Dashed lines indicate anadromous Alewife reaction norms, solid lines indicate landlocked. The direction of the arrow represents the direction of differentiation in landlocked compared to anadromous Alewives. Reduced SW function model: landlocked Alewives exhibit reduced upregulation in SW compared to anadromous forms. Enhanced FW function model: landlocked Alewives exhibit greater upregulation in FW than anadromous forms.

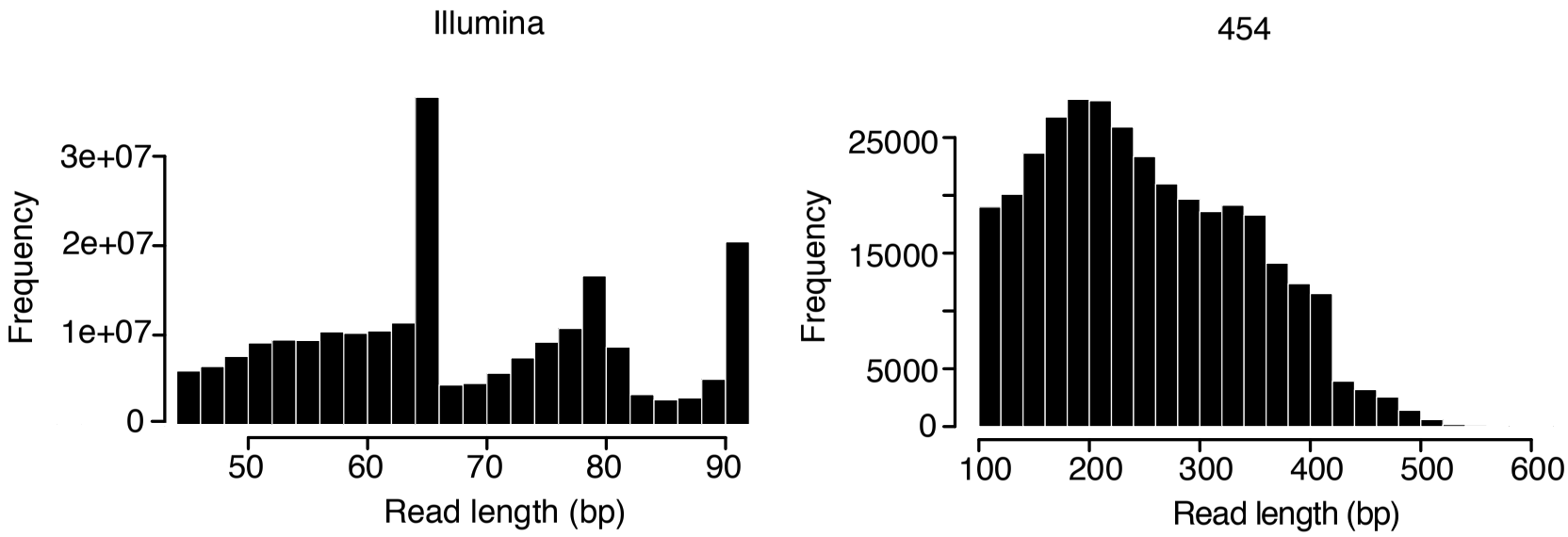


**Figure 2** Frequency histograms of read lengths (base pairs; bp) for Illumina and 454 libraries.

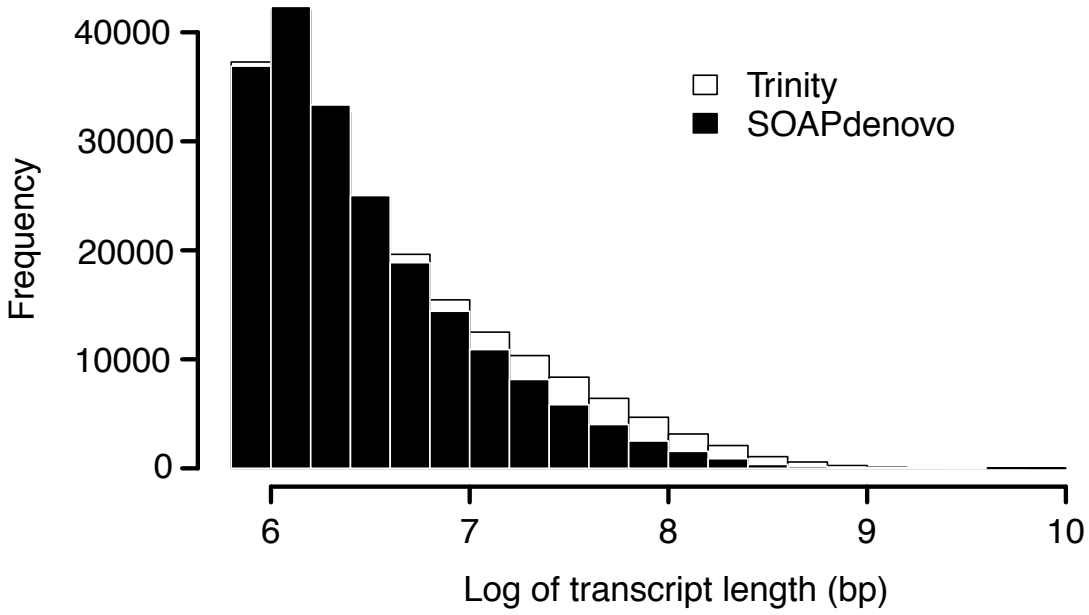


**Figure 3** Frequency histogram of transcript lengths of Trinity/Mira and SOAPdenovo/Mira hybrid assemblies. Transcript lengths (base pairs; bp) were natural log transformed.

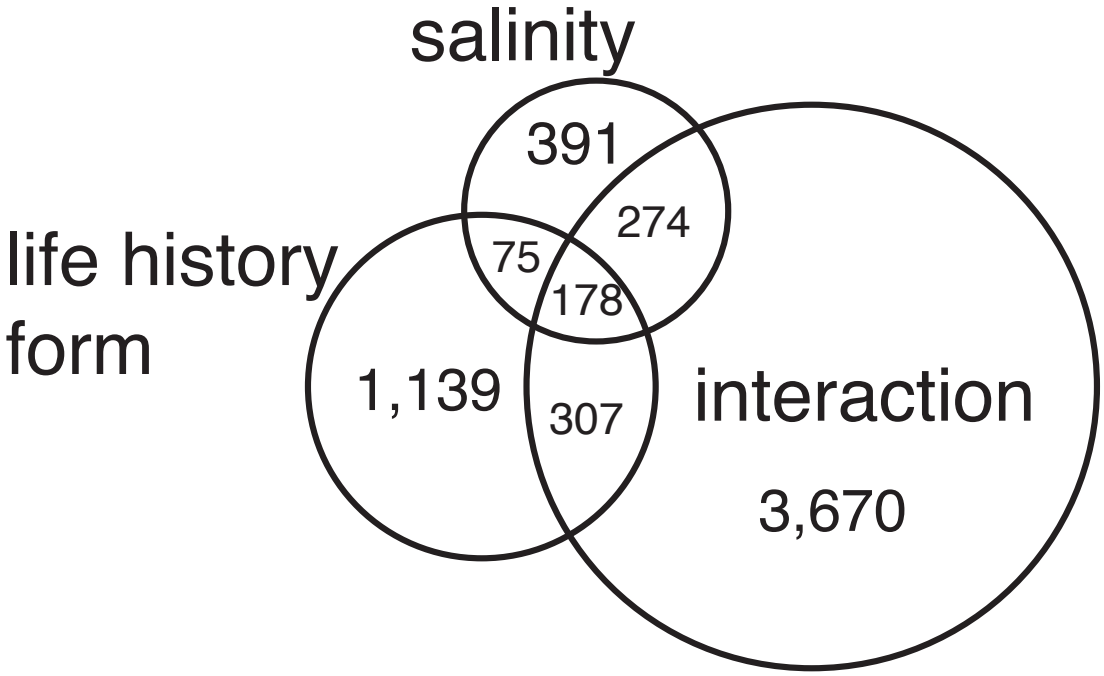


**Figure 4** Alewife gill transcripts exhibiting differential expression in each of three factors of a GLM. Significant transcripts were those with a corrected P-Value (FDR) < 0.05. Venn diagram bubble size is proportional to the number of differentially expressed transcripts.

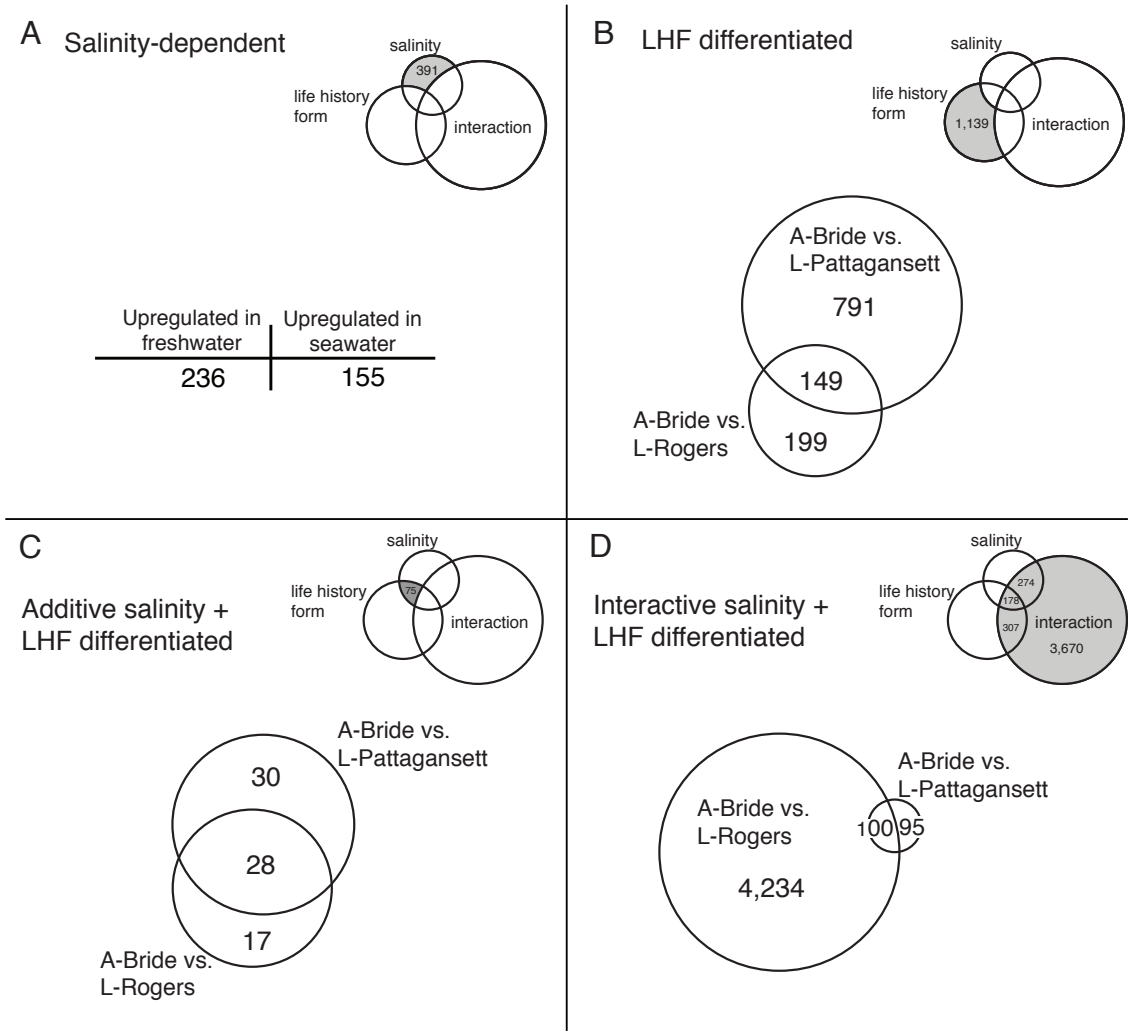
A
Salinity-dependent
salinity
391
life history form
interaction
Upregulated in freshwater
Upregulated in seawater
236
155
B
LHF differentiated
salinity
life history form
1,139
interaction
A-Bride vs. L-Pattagansett
791
149
A-Bride vs. L-Rogers
199
C
Additive salinity + LHF differentiated
salinity
life history form
75
interaction
A-Bride vs. L-Pattagansett
30
28
17
A-Bride vs. L-Rogers
D
Interactive salinity + LHF differentiated
salinity
life history form
274
178
307
interaction
3,670
A-Bride vs. L-Pattagansett
A-Bride vs. L-Rogers
100
95
4,234

**Figure 5** Transcripts differentiated either commonly (between A-Bride and both landlocked populations) or uniquely (between A-Bride and one landlocked population but not the other) in each of the four differential expression categories. A: salinity-dependent. Transcripts upregulated in freshwater (greater expression in freshwater than seawater) vs. those upregulated in seawater (greater expression in seawater than freshwater) are presented. B: Transcripts exhibiting a significant life history form (LHF) differentiated effect. C: Transcripts exhibiting a significant additive salinity and LHF effect (salinity + LHF effect in GLM). D: Transcripts exhibiting a significant interactive salinity and LHF effect (salinity x LHF effect in GLM). Significant transcripts were those with a corrected P-Value (FDR) < 0.05. Venn diagram bubble size is proportional to the number of differentially expressed transcripts.

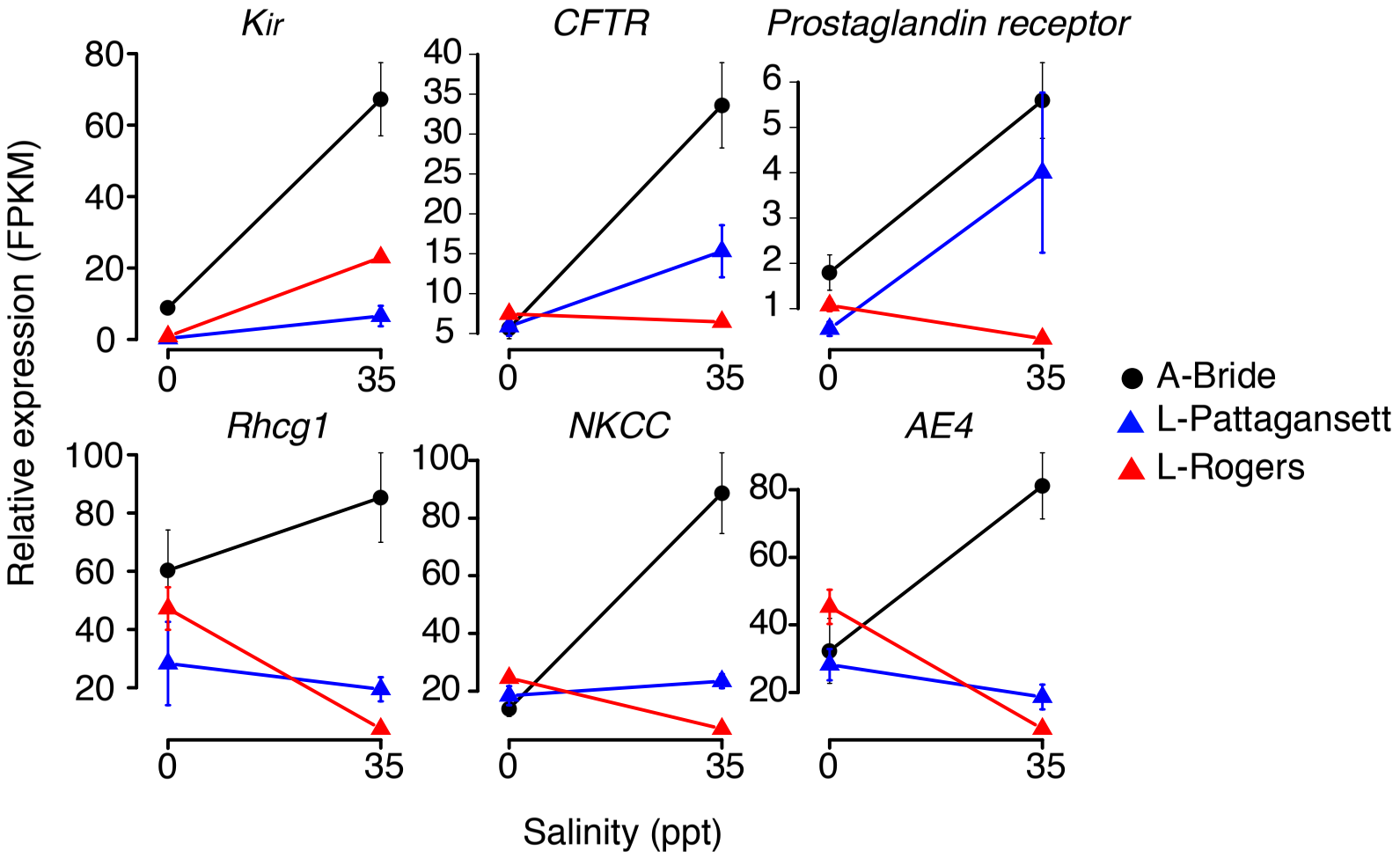
Kir
CFTR
Prostaglandin receptor
Rhcg1
NKCC
AE4
Relative expression (FPKM)
Salinity (ppt)
A-Bride
L-Pattagansett
L-Rogers

**Figure 6** Landlocked Alewives exhibit reduced SW expression of six genes involved in gill ion exchange and osmoregulation: $K^+$ inwardly-rectifying channel *($K_{ir}$)*, cystic fibrosis transmembrane conductance regulator (*CFTR*), *prostaglandin E receptor*, Rhesus blood group-associated A glycoprotein (*Rhcg1*), $Na^+/K^+/2Cl^-$ cotransporter (*NKCC*), and anion exchanger member 4 (*AE4*). Plots are reaction norms of landlocked (triangles) and anadromous (circles) Alewives challenged in 0 ppt freshwater and 35 ppt seawater. A significant salinity x LHF interaction was detected for all genes (see Tables 6-7). Values are mean TMM-normalized FPKM expression ± standard error of the mean. Note that y-axis differs in each case.

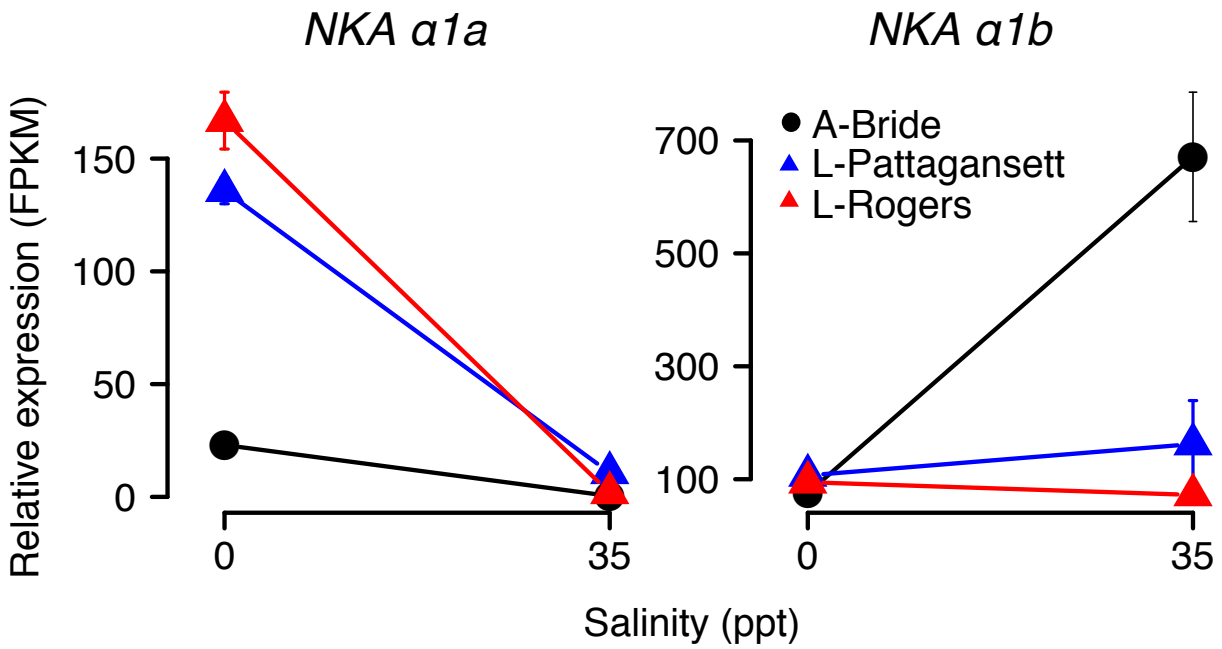


**Figure 7** Gene expression of $N^+$/ $K^+$-ATPase α1a (*NKA α1a*) is enhanced in 0 ppt freshwater among landlocked (triangles) compared to anadromous Alewives (circles), while expression of *NKA α1b* is reduced in 35 ppt seawater. Significant FDR corrected (*NKA α1a*) and nominal (*NKA α1b*) P-values for the interaction of salinity and life history form were detected (see text and Table 6). Values are mean TMM-normalized FPKM expression ± standard error of the mean. Note that y-axis differs in each case.

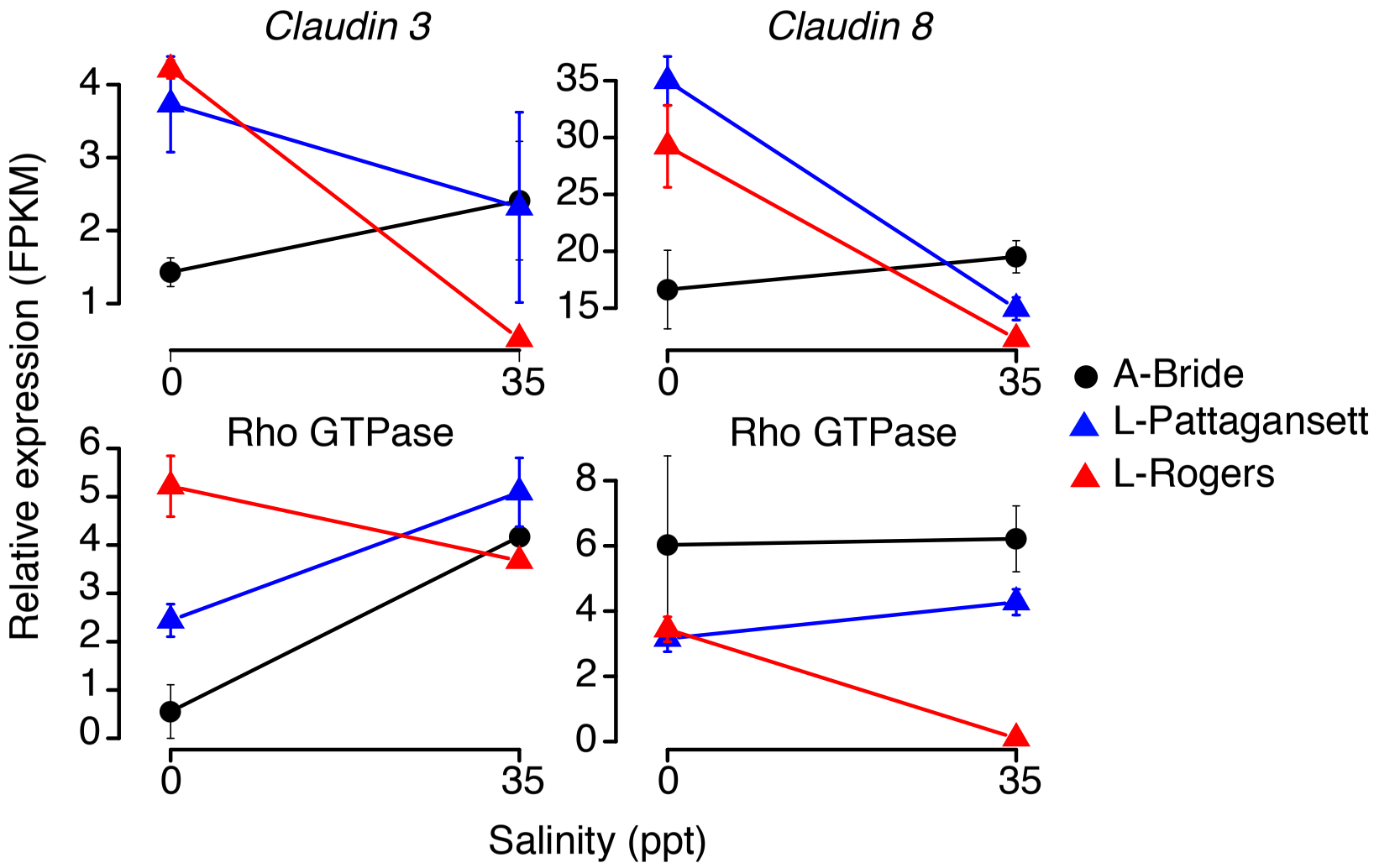
Claudin 3
Claudin 8
Rho GTPase
Rho GTPase
Relative expression (FPKM)
Salinity (ppt)
A-Bride
L-Pattagansett
L-Rogers

**Figure 8** Expression of genes involved in tight junction assembly is differentiated between landlocked and anadromous Alewives. Plots are reaction norms of landlocked (triangles) and anadromous (circles) Alewives challenged in 0 ppt freshwater and 35 ppt seawater. Reaction norms for *claudin 3*, *claudin 8*, and the leftmost transcript of *Rho GTPase 17* indicate enhanced FW function among landlocked Alewives. Significant interactions were detected for *claudin 8* and *Rho GTPase 17*, which fit the reciprocal expression model of differentiation (Table 7), while a significant life history form effect was detected for *claudin 3* (Table 5). The rightmost *Rho GTPase 17* transcript fits the reduced SW function model of differentiation (Table 7). Values are mean TMM-normalized FPKM expression ± standard error of the mean. Note that y-axis differs in each case.

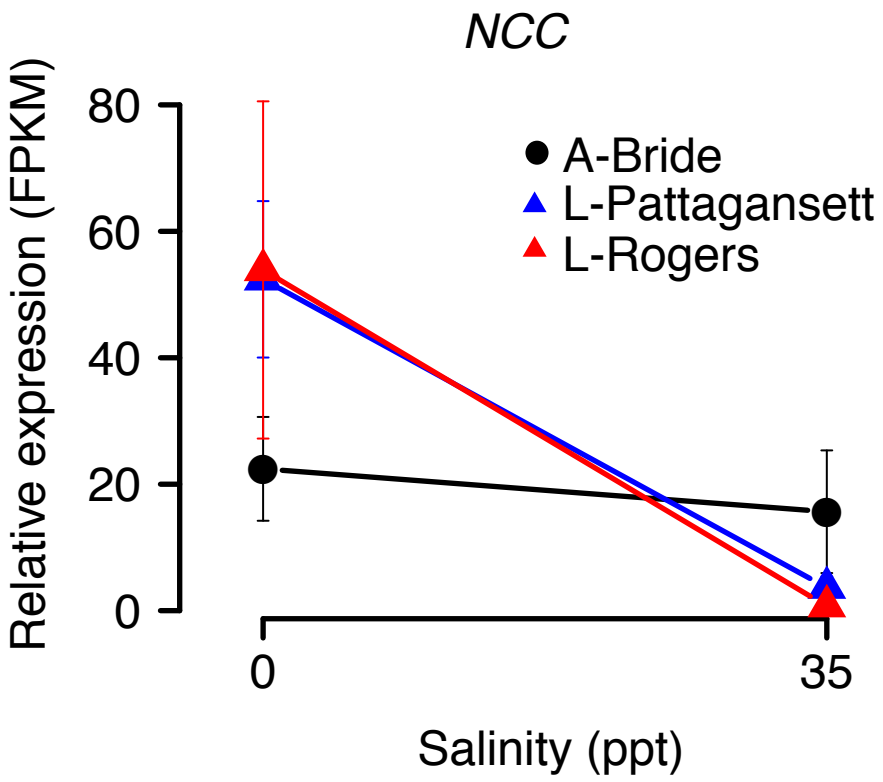


**Figure 9** $Na^+/Cl^-$ co-transporter regulates ion uptake in the freshwater gill and is more highly expressed among landlocked (triangle) than anadromous Alewives (circles) challenged in 0 ppt freshwater and 35 ppt SW. Values are mean TMM-normalized FPKM expression ± standard error of the mean.

**Supplementary Table S1** Table of enriched terms for each Gene Ontology (GO) domain (Biological Process, Molecular Function, Cellular Component) within each differential expression (DE) category (see Figure 2). The trimmed Trinity/Mira hybrid assembly was used as a background. Enrichment tests were implemented in GOrilla (Eden et al 2009). Nominal P-values and false discovery rate (FDR) corrected P-values are reported. Enrichment score was calculated as follows: (b/n) / (B/N), where N = the total number of genes in the background set, B = the number of genes associated with each GO term, n = the total number of genes in each DE category, b = the number of genes associated with each GO term within each DE category.

| GO domain | GO Term | Description | P-value | FDR | Enrichment | N | B | n | b | DE category |
|---|---|---|---|---|---|---|---|---|---|---|
| Biological Process | GO:0052697 | xenobiotic glucuronidation | 1.73E-06 | 2.01E-02 | 82.73 | 11168 | 3 | 135 | 3 | salinity-dependent |
| Biological Process | GO:0052696 | flavonoid glucuronidation | 9.25E-05 | 5.39E-01 | 31.02 | 11168 | 8 | 135 | 3 | salinity-dependent |
| Biological Process | GO:0009813 | flavonoid biosynthetic process | 9.25E-05 | 3.59E-01 | 31.02 | 11168 | 8 | 135 | 3 | salinity-dependent |
| Biological Process | GO:0071495 | cellular response to endogenous stimulus | 1.07E-04 | 3.11E-01 | 3.07 | 11168 | 404 | 135 | 15 | salinity-dependent |
| Biological Process | GO:0052695 | cellular glucuronidation | 1.38E-04 | 3.20E-01 | 27.58 | 11168 | 9 | 135 | 3 | salinity-dependent |
| Biological Process | GO:0006063 | uronic acid metabolic process | 1.38E-04 | 2.67E-01 | 27.58 | 11168 | 9 | 135 | 3 | salinity-dependent |
| Biological Process | GO:0019585 | glucuronate metabolic process | 1.38E-04 | 2.29E-01 | 27.58 | 11168 | 9 | 135 | 3 | salinity-dependent |
| Biological Process | GO:0009812 | flavonoid metabolic process | 1.38E-04 | 2.00E-01 | 27.58 | 11168 | 9 | 135 | 3 | salinity-dependent |
| Biological Process | GO:0006805 | xenobiotic metabolic process | 1.51E-04 | 1.96E-01 | 14.39 | 11168 | 23 | 135 | 4 | salinity-dependent |
| Biological Process | GO:0032870 | cellular response to hormone stimulus | 1.87E-04 | 2.18E-01 | 4.04 | 11168 | 205 | 135 | 10 | salinity-dependent |

Table S1 continued

| | | | | | | | | | | |
|---|---|---|---|---|---|---|---|---|---|---|
| Biological Process | GO:0071310 | cellular response to organic substance | 2.25E-04 | 2.39E-01 | 2.4 | 11168 | 690 | 135 | 20 | salinity-dependent |
| Biological Process | GO:0009725 | response to hormone | 3.49E-04 | 3.39E-01 | 3.22 | 11168 | 308 | 135 | 12 | salinity-dependent |
| Biological Process | GO:0010033 | response to organic substance | 3.82E-04 | 3.42E-01 | 2.06 | 11168 | 1006 | 135 | 25 | salinity-dependent |
| Biological Process | GO:0042221 | response to chemical | 4.79E-04 | 3.98E-01 | 1.87 | 11168 | 1329 | 135 | 30 | salinity-dependent |
| Biological Process | GO:0001580 | detection of chemical stimulus involved in sensory perception of bitter taste | 8.57E-04 | 6.65E-01 | 41.36 | 11168 | 4 | 135 | 2 | salinity-dependent |
| Biological Process | GO:0036376 | sodium ion export from cell | 8.57E-04 | 6.24E-01 | 41.36 | 11168 | 4 | 135 | 2 | salinity-dependent |
| Biological Process | GO:0043124 | negative regulation of I-kappaB kinase/NF-kappaB signaling | 9.90E-04 | 6.78E-01 | 8.94 | 11168 | 37 | 135 | 4 | salinity-dependent |
| Biological Process | GO:0051239 | regulation of multicellular organismal process | 2.23E-06 | 2.60E-02 | 1.59 | 11168 | 1423 | 458 | 93 | LHF differentiated |
| Biological Process | GO:0015718 | monocarboxylic acid transport | 4.56E-06 | 2.66E-02 | 4.88 | 11168 | 60 | 458 | 12 | LHF differentiated |
| Biological Process | GO:0006936 | muscle contraction | 2.09E-05 | 8.12E-02 | 3.71 | 11168 | 92 | 458 | 14 | LHF differentiated |
| Biological Process | GO:0003012 | muscle system process | 2.18E-05 | 6.34E-02 | 3.33 | 11168 | 117 | 458 | 16 | LHF differentiated |
| Biological Process | GO:0002684 | positive regulation of immune system process | 3.57E-05 | 8.33E-02 | 2.18 | 11168 | 346 | 458 | 31 | LHF differentiated |
| Biological Process | GO:0044057 | regulation of system process | 3.75E-05 | 7.29E-02 | 2.48 | 11168 | 236 | 458 | 24 | LHF differentiated |
| Biological Process | GO:0015849 | organic acid transport | 4.52E-05 | 7.52E-02 | 3.15 | 11168 | 124 | 458 | 16 | LHF differentiated |
| Biological Process | GO:0046942 | carboxylic acid transport | 4.52E-05 | 6.58E-02 | 3.15 | 11168 | 124 | 458 | 16 | LHF differentiated |
| Biological Process | GO:0055006 | cardiac cell development | 6.22E-05 | 8.04E-02 | 6.56 | 11168 | 26 | 458 | 7 | LHF differentiated |
| Biological Process | GO:0006941 | striated muscle contraction | 8.63E-05 | 1.01E-01 | 4.77 | 11168 | 46 | 458 | 9 | LHF differentiated |

Table S1 continued

| | | | | | | | | | | |
|---|---|---|---|---|---|---|---|---|---|---|
| Biological Process | GO:0002682 | regulation of immune system process | 9.83E-05 | 1.04E-01 | 1.85 | 11168 | 540 | 458 | 41 | LHF differentiated |
| Biological Process | GO:0022610 | biological adhesion | 1.28E-04 | 1.24E-01 | 1.96 | 11168 | 422 | 458 | 34 | LHF differentiated |
| Biological Process | GO:0036003 | positive regulation of transcription from RNA polymerase II promoter in response to stress | 1.71E-04 | 1.54E-01 | 12.19 | 11168 | 8 | 458 | 4 | LHF differentiated |
| Biological Process | GO:0001817 | regulation of cytokine production | 1.73E-04 | 1.44E-01 | 2.25 | 11168 | 260 | 458 | 24 | LHF differentiated |
| Biological Process | GO:0032088 | negative regulation of NF-kappaB transcription factor activity | 1.99E-04 | 1.54E-01 | 4.3 | 11168 | 51 | 458 | 9 | LHF differentiated |
| Biological Process | GO:0002687 | positive regulation of leukocyte migration | 1.99E-04 | 1.45E-01 | 4.3 | 11168 | 51 | 458 | 9 | LHF differentiated |
| Biological Process | GO:0001819 | positive regulation of cytokine production | 2.10E-04 | 1.44E-01 | 2.58 | 11168 | 170 | 458 | 18 | LHF differentiated |
| Biological Process | GO:0008285 | negative regulation of cell proliferation | 2.36E-04 | 1.53E-01 | 2 | 11168 | 366 | 458 | 30 | LHF differentiated |
| Biological Process | GO:0002381 | immunoglobulin production involved in immunoglobulin mediated immune response | 2.66E-04 | 1.63E-01 | 18.29 | 11168 | 4 | 458 | 3 | LHF differentiated |
| Biological Process | GO:0031581 | hemidesmosome assembly | 2.66E-04 | 1.55E-01 | 18.29 | 11168 | 4 | 458 | 3 | LHF differentiated |
| Biological Process | GO:0042345 | regulation of NF-kappaB import into nucleus | 3.30E-04 | 1.83E-01 | 6.1 | 11168 | 24 | 458 | 6 | LHF differentiated |
| Biological Process | GO:0032879 | regulation of localization | 3.37E-04 | 1.79E-01 | 1.47 | 11168 | 1242 | 458 | 75 | LHF differentiated |
| Biological Process | GO:0044699 | single-organism process | 3.41E-04 | 1.73E-01 | 1.14 | 11168 | 6378 | 458 | 297 | LHF differentiated |
| Biological Process | GO:0051050 | positive regulation of transport | 3.46E-04 | 1.68E-01 | 1.86 | 11168 | 445 | 458 | 34 | LHF differentiated |
| Biological Process | GO:0042742 | defense response to bacterium | 3.70E-04 | 1.73E-01 | 3.64 | 11168 | 67 | 458 | 10 | LHF differentiated |
| Biological Process | GO:0044712 | single-organism catabolic process | 3.71E-04 | 1.66E-01 | 1.69 | 11168 | 650 | 458 | 45 | LHF differentiated |

Table S1 continued

| | | | | | | | | | | |
|---|---|---|---|---|---|---|---|---|---|---|
| Biological Process | GO:0015711 | organic anion transport | 3.97E-04 | 1.71E-01 | 2.45 | 11168 | 179 | 458 | 18 | LHF differentiated |
| Biological Process | GO:0060048 | cardiac muscle contraction | 4.19E-04 | 1.74E-01 | 5.85 | 11168 | 25 | 458 | 6 | LHF differentiated |
| Biological Process | GO:0003008 | system process | 4.25E-04 | 1.71E-01 | 1.74 | 11168 | 560 | 458 | 40 | LHF differentiated |
| Biological Process | GO:0006629 | lipid metabolic process | 4.34E-04 | 1.68E-01 | 1.71 | 11168 | 598 | 458 | 42 | LHF differentiated |
| Biological Process | GO:0044236 | multicellular organismal metabolic process | 4.62E-04 | 1.73E-01 | 4.88 | 11168 | 35 | 458 | 7 | LHF differentiated |
| Biological Process | GO:0019886 | antigen processing and presentation of exogenous peptide antigen via MHC class II | 4.81E-04 | 1.75E-01 | 9.75 | 11168 | 10 | 458 | 4 | LHF differentiated |
| Biological Process | GO:0043433 | negative regulation of sequence-specific DNA binding transcription factor activity | 4.86E-04 | 1.72E-01 | 3.08 | 11168 | 95 | 458 | 12 | LHF differentiated |
| Biological Process | GO:0042990 | regulation of transcription factor import into nucleus | 4.97E-04 | 1.70E-01 | 4.24 | 11168 | 46 | 458 | 8 | LHF differentiated |
| Biological Process | GO:0001523 | retinoid metabolic process | 5.26E-04 | 1.75E-01 | 5.63 | 11168 | 26 | 458 | 6 | LHF differentiated |
| Biological Process | GO:0072091 | regulation of stem cell proliferation | 5.31E-04 | 1.72E-01 | 3.48 | 11168 | 70 | 458 | 10 | LHF differentiated |
| Biological Process | GO:0070887 | cellular response to chemical stimulus | 5.55E-04 | 1.75E-01 | 1.56 | 11168 | 877 | 458 | 56 | LHF differentiated |
| Biological Process | GO:2000147 | positive regulation of cell motility | 5.63E-04 | 1.73E-01 | 2.21 | 11168 | 232 | 458 | 21 | LHF differentiated |
| Biological Process | GO:0002685 | regulation of leukocyte migration | 5.96E-04 | 1.78E-01 | 3.43 | 11168 | 71 | 458 | 10 | LHF differentiated |
| Biological Process | GO:0050707 | regulation of cytokine secretion | 5.96E-04 | 1.74E-01 | 3.43 | 11168 | 71 | 458 | 10 | LHF differentiated |
| Biological Process | GO:0042221 | response to chemical | 6.03E-04 | 1.71E-01 | 1.43 | 11168 | 1329 | 458 | 78 | LHF differentiated |
| Biological Process | GO:0044255 | cellular lipid metabolic process | 6.06E-04 | 1.68E-01 | 1.81 | 11168 | 459 | 458 | 34 | LHF differentiated |
| Biological Process | GO:0002376 | immune system process | 6.09E-04 | 1.65E-01 | 1.68 | 11168 | 608 | 458 | 42 | LHF differentiated |

Table S1 continued

| | | | | | | | | | | |
|---|---|---|---|---|---|---|---|---|---|---|
| Biological Process | GO:0006820 | anion transport | 6.31E-04 | 1.67E-01 | 2.19 | 11168 | 234 | 458 | 21 | LHF differentiated |
| Biological Process | GO:1903522 | regulation of blood circulation | 6.42E-04 | 1.66E-01 | 2.71 | 11168 | 126 | 458 | 14 | LHF differentiated |
| Biological Process | GO:0016101 | diterpenoid metabolic process | 6.53E-04 | 1.65E-01 | 5.42 | 11168 | 27 | 458 | 6 | LHF differentiated |
| Biological Process | GO:0043124 | negative regulation of I-kappaB kinase/NF-kappaB signaling | 6.58E-04 | 1.63E-01 | 4.61 | 11168 | 37 | 458 | 7 | LHF differentiated |
| Biological Process | GO:0098542 | defense response to other organism | 6.95E-04 | 1.69E-01 | 2.69 | 11168 | 127 | 458 | 14 | LHF differentiated |
| Biological Process | GO:0050778 | positive regulation of immune response | 6.96E-04 | 1.65E-01 | 2.41 | 11168 | 172 | 458 | 17 | LHF differentiated |
| Biological Process | GO:0043616 | keratinocyte proliferation | 7.32E-04 | 1.70E-01 | 8.87 | 11168 | 11 | 458 | 4 | LHF differentiated |
| Biological Process | GO:0002577 | regulation of antigen processing and presentation | 7.32E-04 | 1.67E-01 | 8.87 | 11168 | 11 | 458 | 4 | LHF differentiated |
| Biological Process | GO:0002440 | production of molecular mediator of immune response | 7.32E-04 | 1.64E-01 | 8.87 | 11168 | 11 | 458 | 4 | LHF differentiated |
| Biological Process | GO:0002495 | antigen processing and presentation of peptide antigen via MHC class II | 7.32E-04 | 1.61E-01 | 8.87 | 11168 | 11 | 458 | 4 | LHF differentiated |
| Biological Process | GO:0050704 | regulation of interleukin-1 secretion | 7.32E-04 | 1.58E-01 | 8.87 | 11168 | 11 | 458 | 4 | LHF differentiated |
| Biological Process | GO:0042347 | negative regulation of NF-kappaB import into nucleus | 7.32E-04 | 1.55E-01 | 8.87 | 11168 | 11 | 458 | 4 | LHF differentiated |
| Biological Process | GO:0032787 | monocarboxylic acid metabolic process | 7.34E-04 | 1.53E-01 | 2.08 | 11168 | 270 | 458 | 23 | LHF differentiated |
| Biological Process | GO:0051047 | positive regulation of secretion | 7.61E-04 | 1.55E-01 | 2.32 | 11168 | 189 | 458 | 18 | LHF differentiated |
| Biological Process | GO:0051272 | positive regulation of cellular component movement | 8.30E-04 | 1.67E-01 | 2.14 | 11168 | 239 | 458 | 21 | LHF differentiated |

Table S1 continued

| | | | | | | | | | | |
|---|---|---|---|---|---|---|---|---|---|---|
| Biological Process | GO:0051270 | regulation of cellular component movement | 8.64E-04 | 1.71E-01 | 1.79 | 11168 | 450 | 458 | 33 | LHF differentiated |
| Biological Process | GO:0007155 | cell adhesion | 9.13E-04 | 1.77E-01 | 1.82 | 11168 | 415 | 458 | 31 | LHF differentiated |
| Biological Process | GO:0032963 | collagen metabolic process | 9.78E-04 | 1.87E-01 | 5.05 | 11168 | 29 | 458 | 6 | LHF differentiated |
| Biological Process | GO:0031943 | regulation of glucocorticoid metabolic process | 3.64E-04 | 1.00E+00 | 68.05 | 11160 | 8 | 41 | 2 | additive salinity + LHF |
| Biological Process | GO:0042402 | cellular biogenic amine catabolic process | 4.66E-04 | 1.00E+00 | 60.49 | 11160 | 9 | 41 | 2 | additive salinity + LHF |
| Biological Process | GO:0009310 | amine catabolic process | 4.66E-04 | 1.00E+00 | 60.49 | 11160 | 9 | 41 | 2 | additive salinity + LHF |
| Biological Process | GO:0008380 | RNA splicing | 8.50E-06 | 9.89E-02 | 1.73 | 11168 | 201 | 1899 | 59 | interactive salinity + LHF |
| Biological Process | GO:0032836 | glomerular basement membrane development | 2.77E-05 | 1.61E-01 | 5.15 | 11168 | 8 | 1899 | 7 | interactive salinity + LHF |
| Biological Process | GO:0048813 | dendrite morphogenesis | 1.10E-04 | 4.27E-01 | 2.94 | 11168 | 26 | 1899 | 13 | interactive salinity + LHF |
| Biological Process | GO:0003012 | muscle system process | 1.67E-04 | 4.85E-01 | 1.81 | 11168 | 117 | 1899 | 36 | interactive salinity + LHF |
| Biological Process | GO:0006412 | translation | 1.70E-04 | 3.96E-01 | 1.59 | 11168 | 207 | 1899 | 56 | interactive salinity + LHF |
| Biological Process | GO:0030198 | extracellular matrix organization | 1.77E-04 | 3.43E-01 | 1.77 | 11168 | 126 | 1899 | 38 | interactive salinity + LHF |
| Biological Process | GO:0043062 | extracellular structure organization | 1.77E-04 | 2.94E-01 | 1.77 | 11168 | 126 | 1899 | 38 | interactive salinity + LHF |
| Biological Process | GO:0016071 | mRNA metabolic process | 2.46E-04 | 3.57E-01 | 1.46 | 11168 | 310 | 1899 | 77 | interactive salinity + LHF |
| Biological Process | GO:0033275 | actin-myosin filament sliding | 4.91E-04 | 6.36E-01 | 4.41 | 11168 | 8 | 1899 | 6 | interactive salinity + LHF |
| Biological Process | GO:0006397 | mRNA processing | 6.02E-04 | 7.00E-01 | 1.47 | 11168 | 260 | 1899 | 65 | interactive salinity + LHF |
| Biological Process | GO:0006396 | RNA processing | 7.06E-04 | 7.47E-01 | 1.34 | 11168 | 451 | 1899 | 103 | interactive salinity + LHF |
| Molecular Function | GO:0001968 | fibronectin binding | 4.71E-05 | 1.95E-01 | 6.83 | 11168 | 25 | 458 | 7 | LHF differentiated |

Table S1 continued

| | | | | | | | | | | |
|---|---|---|---|---|---|---|---|---|---|---|
| Molecular Function | GO:0005515 | protein binding | 1.21E-04 | 2.50E-01 | 1.2 | 11168 | 4785 | 458 | 235 | LHF differentiated |
| Molecular Function | GO:0008092 | cytoskeletal protein binding | 1.52E-04 | 2.10E-01 | 1.81 | 11168 | 551 | 458 | 41 | LHF differentiated |
| Molecular Function | GO:0004497 | monooxygenase activity | 1.93E-04 | 1.99E-01 | 3.93 | 11168 | 62 | 458 | 10 | LHF differentiated |
| Molecular Function | GO:0043236 | laminin binding | 1.96E-04 | 1.62E-01 | 6.65 | 11168 | 22 | 458 | 6 | LHF differentiated |
| Molecular Function | GO:0005200 | structural constituent of cytoskeleton | 3.83E-04 | 2.64E-01 | 5.02 | 11168 | 34 | 458 | 7 | LHF differentiated |
| Molecular Function | GO:0000987 | core promoter proximal region sequence-specific DNA binding | 6.95E-04 | 4.11E-01 | 2.69 | 11168 | 127 | 458 | 14 | LHF differentiated |
| Molecular Function | GO:0045295 | gamma-catenin binding | 7.32E-04 | 3.78E-01 | 8.87 | 11168 | 11 | 458 | 4 | LHF differentiated |
| Molecular Function | GO:0001159 | core promoter proximal region DNA binding | 7.52E-04 | 3.46E-01 | 2.67 | 11168 | 128 | 458 | 14 | LHF differentiated |
| Molecular Function | GO:0032403 | protein complex binding | 8.08E-04 | 3.34E-01 | 1.64 | 11168 | 655 | 458 | 44 | LHF differentiated |
| Molecular Function | GO:0030955 | potassium ion binding | 3.64E-04 | 1.00E+00 | 68.05 | 11160 | 8 | 41 | 2 | additive salinity + LHF |
| Molecular Function | GO:0042800 | histone methyltransferase activity (H3-K4 specific) | 8.49E-04 | 1.00E+00 | 45.37 | 11160 | 12 | 41 | 2 | additive salinity + LHF |
| Molecular Function | GO:0005198 | structural molecule activity | 6.29E-12 | 2.60E-08 | 1.95 | 11168 | 292 | 1899 | 97 | interactive salinity + LHF |
| Molecular Function | GO:0003735 | structural constituent of ribosome | 8.96E-09 | 1.85E-05 | 2.4 | 11168 | 103 | 1899 | 42 | interactive salinity + LHF |
| Molecular Function | GO:0005201 | extracellular matrix structural constituent | 1.03E-05 | 1.42E-02 | 3.48 | 11168 | 22 | 1899 | 13 | interactive salinity + LHF |
| Molecular Function | GO:0016859 | cis-trans isomerase activity | 2.38E-04 | 2.46E-01 | 2.66 | 11168 | 31 | 1899 | 14 | interactive salinity + LHF |
| Molecular Function | GO:0003755 | peptidyl-prolyl cis-trans isomerase activity | 4.33E-04 | 3.58E-01 | 2.64 | 11168 | 29 | 1899 | 13 | interactive salinity + LHF |
| Molecular Function | GO:0001055 | RNA polymerase II activity | 4.91E-04 | 3.39E-01 | 4.41 | 11168 | 8 | 1899 | 6 | interactive salinity + LHF |
| Molecular Function | GO:0005200 | structural constituent of cytoskeleton | 7.52E-04 | 4.45E-01 | 2.42 | 11168 | 34 | 1899 | 14 | interactive salinity + LHF |

Table S1 continued

| | | | | | | | | | | |
|---|---|---|---|---|---|---|---|---|---|---|
| Cellular Component | GO:0044425 | membrane part | 2.05E-04 | 2.78E-01 | 1.5 | 11168 | 3253 | 135 | 59 | salinity-dependent |
| Cellular Component | GO:0098533 | ATPase dependent transmembrane transport complex | 8.57E-04 | 5.81E-01 | 41.36 | 11168 | 4 | 135 | 2 | salinity-dependent |
| Cellular Component | GO:0005890 | sodium:potassium-exchanging ATPase complex | 8.57E-04 | 3.87E-01 | 41.36 | 11168 | 4 | 135 | 2 | salinity-dependent |
| Cellular Component | GO:0090533 | cation-transporting ATPase complex | 8.57E-04 | 2.90E-01 | 41.36 | 11168 | 4 | 135 | 2 | salinity-dependent |
| Cellular Component | GO:0044421 | extracellular region part | 4.93E-08 | 6.69E-05 | 1.53 | 11168 | 2150 | 458 | 135 | LHF differentiated |
| Cellular Component | GO:0030054 | cell junction | 1.25E-07 | 8.49E-05 | 2 | 11168 | 744 | 458 | 61 | LHF differentiated |
| Cellular Component | GO:1903561 | extracellular vesicle | 5.42E-07 | 2.45E-04 | 1.56 | 11168 | 1718 | 458 | 110 | LHF differentiated |
| Cellular Component | GO:0070062 | extracellular vesicular exosome | 5.42E-07 | 1.84E-04 | 1.56 | 11168 | 1718 | 458 | 110 | LHF differentiated |
| Cellular Component | GO:0043230 | extracellular organelle | 5.59E-07 | 1.51E-04 | 1.56 | 11168 | 1719 | 458 | 110 | LHF differentiated |
| Cellular Component | GO:0065010 | extracellular membrane-bounded organelle | 5.59E-07 | 1.26E-04 | 1.56 | 11168 | 1719 | 458 | 110 | LHF differentiated |
| Cellular Component | GO:0044459 | plasma membrane part | 6.09E-07 | 1.18E-04 | 1.78 | 11168 | 998 | 458 | 73 | LHF differentiated |
| Cellular Component | GO:0005886 | plasma membrane | 8.54E-07 | 1.45E-04 | 1.52 | 11168 | 1898 | 458 | 118 | LHF differentiated |
| Cellular Component | GO:0031982 | vesicle | 8.85E-07 | 1.33E-04 | 1.47 | 11168 | 2150 | 458 | 130 | LHF differentiated |
| Cellular Component | GO:0031988 | membrane-bounded vesicle | 1.37E-06 | 1.86E-04 | 1.5 | 11168 | 1957 | 458 | 120 | LHF differentiated |
| Cellular Component | GO:0044449 | contractile fiber part | 1.75E-06 | 2.16E-04 | 3.66 | 11168 | 120 | 458 | 18 | LHF differentiated |
| Cellular Component | GO:0005615 | extracellular space | 1.90E-06 | 2.14E-04 | 2.09 | 11168 | 524 | 458 | 45 | LHF differentiated |
| Cellular Component | GO:0098589 | membrane region | 3.31E-06 | 3.45E-04 | 2.05 | 11168 | 535 | 458 | 45 | LHF differentiated |
| Cellular Component | GO:0070161 | anchoring junction | 3.95E-06 | 3.82E-04 | 2.36 | 11168 | 341 | 458 | 33 | LHF differentiated |

Table S1 continued

| | | | | | | | | | | |
|---|---|---|---|---|---|---|---|---|---|---|
| Cellular Component | GO:0044444 | cytoplasmic part | 5.36E-06 | 4.85E-04 | 1.25 | 11168 | 4436 | 458 | 228 | LHF differentiated |
| Cellular Component | GO:0016020 | membrane | 1.11E-05 | 9.44E-04 | 1.23 | 11168 | 4810 | 458 | 242 | LHF differentiated |
| Cellular Component | GO:0005912 | adherens junction | 1.33E-05 | 1.06E-03 | 2.3 | 11168 | 329 | 458 | 31 | LHF differentiated |
| Cellular Component | GO:0030055 | cell-substrate junction | 2.39E-05 | 1.80E-03 | 2.35 | 11168 | 291 | 458 | 28 | LHF differentiated |
| Cellular Component | GO:0005911 | cell-cell junction | 5.55E-05 | 3.96E-03 | 2.32 | 11168 | 273 | 458 | 26 | LHF differentiated |
| Cellular Component | GO:0005925 | focal adhesion | 9.53E-05 | 6.46E-03 | 2.25 | 11168 | 282 | 458 | 26 | LHF differentiated |
| Cellular Component | GO:0005924 | cell-substrate adherens junction | 1.20E-04 | 7.75E-03 | 2.22 | 11168 | 286 | 458 | 26 | LHF differentiated |
| Cellular Component | GO:0043292 | contractile fiber | 1.51E-04 | 9.29E-03 | 5 | 11168 | 39 | 458 | 8 | LHF differentiated |
| Cellular Component | GO:0044430 | cytoskeletal part | 2.21E-04 | 1.30E-02 | 1.59 | 11168 | 904 | 458 | 59 | LHF differentiated |
| Cellular Component | GO:0005856 | cytoskeleton | 2.48E-04 | 1.40E-02 | 1.58 | 11168 | 908 | 458 | 59 | LHF differentiated |
| Cellular Component | GO:0030056 | hemidesmosome | 2.98E-04 | 1.62E-02 | 10.84 | 11168 | 9 | 458 | 4 | LHF differentiated |
| Cellular Component | GO:0009986 | cell surface | 5.22E-04 | 2.72E-02 | 2.02 | 11168 | 314 | 458 | 26 | LHF differentiated |
| Cellular Component | GO:0009925 | basal plasma membrane | 5.26E-04 | 2.64E-02 | 5.63 | 11168 | 26 | 458 | 6 | LHF differentiated |
| Cellular Component | GO:0043228 | non-membrane-bounded organelle | 5.61E-04 | 2.72E-02 | 1.36 | 11168 | 1814 | 458 | 101 | LHF differentiated |
| Cellular Component | GO:0043232 | intracellular non-membrane-bounded organelle | 5.61E-04 | 2.62E-02 | 1.36 | 11168 | 1814 | 458 | 101 | LHF differentiated |
| Cellular Component | GO:0030016 | myofibril | 6.53E-04 | 2.95E-02 | 5.42 | 11168 | 27 | 458 | 6 | LHF differentiated |
| Cellular Component | GO:0016459 | myosin complex | 6.69E-04 | 2.93E-02 | 4.06 | 11168 | 48 | 458 | 8 | LHF differentiated |
| Cellular Component | GO:0005737 | cytoplasm | 7.16E-04 | 3.03E-02 | 1.2 | 11168 | 4096 | 458 | 201 | LHF differentiated |
| Cellular Component | GO:0005739 | mitochondrion | 1.67E-16 | 2.26E-13 | 1.51 | 11168 | 1254 | 1899 | 321 | interactive salinity + LHF |

Table S1 continued

| | | | | | | | | | | |
|---|---|---|---|---|---|---|---|---|---|---|
| Cellular Component | GO:0044429 | mitochondrial part | 1.99E-11 | 1.35E-08 | 1.67 | 11168 | 525 | 1899 | 149 | interactive salinity + LHF |
| Cellular Component | GO:0030529 | ribonucleoprotein complex | 2.70E-10 | 1.22E-07 | 1.67 | 11168 | 469 | 1899 | 133 | interactive salinity + LHF |
| Cellular Component | GO:0005840 | ribosome | 4.71E-10 | 1.60E-07 | 2.28 | 11168 | 142 | 1899 | 55 | interactive salinity + LHF |
| Cellular Component | GO:0031966 | mitochondrial membrane | 2.22E-08 | 6.02E-06 | 1.65 | 11168 | 384 | 1899 | 108 | interactive salinity + LHF |
| Cellular Component | GO:0044444 | cytoplasmic part | 6.25E-08 | 1.41E-05 | 1.14 | 11168 | 4436 | 1899 | 858 | interactive salinity + LHF |
| Cellular Component | GO:0005743 | mitochondrial inner membrane | 2.70E-07 | 5.22E-05 | 1.69 | 11168 | 296 | 1899 | 85 | interactive salinity + LHF |
| Cellular Component | GO:0019866 | organelle inner membrane | 5.00E-07 | 8.47E-05 | 1.66 | 11168 | 309 | 1899 | 87 | interactive salinity + LHF |
| Cellular Component | GO:0043230 | extracellular organelle | 5.94E-07 | 8.95E-05 | 1.25 | 11168 | 1719 | 1899 | 364 | interactive salinity + LHF |
| Cellular Component | GO:0065010 | extracellular membrane-bounded organelle | 5.94E-07 | 8.06E-05 | 1.25 | 11168 | 1719 | 1899 | 364 | interactive salinity + LHF |
| Cellular Component | GO:0044421 | extracellular region part | 7.05E-07 | 8.69E-05 | 1.21 | 11168 | 2150 | 1899 | 443 | interactive salinity + LHF |
| Cellular Component | GO:1903561 | extracellular vesicle | 7.81E-07 | 8.82E-05 | 1.24 | 11168 | 1718 | 1899 | 363 | interactive salinity + LHF |
| Cellular Component | GO:0070062 | extracellular vesicular exosome | 7.81E-07 | 8.14E-05 | 1.24 | 11168 | 1718 | 1899 | 363 | interactive salinity + LHF |
| Cellular Component | GO:0005578 | proteinaceous extracellular matrix | 3.37E-06 | 3.27E-04 | 1.79 | 11168 | 187 | 1899 | 57 | interactive salinity + LHF |
| Cellular Component | GO:0031988 | membrane-bounded vesicle | 7.06E-06 | 6.38E-04 | 1.2 | 11168 | 1957 | 1899 | 400 | interactive salinity + LHF |
| Cellular Component | GO:0031982 | vesicle | 7.44E-06 | 6.31E-04 | 1.19 | 11168 | 2150 | 1899 | 435 | interactive salinity + LHF |
| Cellular Component | GO:0070469 | respiratory chain | 1.24E-05 | 9.89E-04 | 2.46 | 11168 | 55 | 1899 | 23 | interactive salinity + LHF |
| Cellular Component | GO:0000314 | organellar small ribosomal subunit | 1.52E-05 | 1.14E-03 | 3.81 | 11168 | 17 | 1899 | 11 | interactive salinity + LHF |
| Cellular Component | GO:0005763 | mitochondrial small ribosomal subunit | 1.52E-05 | 1.08E-03 | 3.81 | 11168 | 17 | 1899 | 11 | interactive salinity + LHF |
| Cellular Component | GO:0043227 | membrane-bounded organelle | 1.94E-05 | 1.31E-03 | 1.06 | 11168 | 7137 | 1899 | 1292 | interactive salinity + LHF |

Table S1 continued

| | | | | | | | | | | |
|---|---|---|---|---|---|---|---|---|---|---|
| Cellular Component | GO:0044391 | ribosomal subunit | 3.38E-05 | 2.18E-03 | 1.98 | 11168 | 101 | 1899 | 34 | interactive salinity + LHF |
| Cellular Component | GO:0005581 | collagen trimer | 4.22E-05 | 2.60E-03 | 2.18 | 11168 | 70 | 1899 | 26 | interactive salinity + LHF |
| Cellular Component | GO:0005665 | DNA-directed RNA polymerase II, core complex | 4.32E-05 | 2.55E-03 | 4.07 | 11168 | 13 | 1899 | 9 | interactive salinity + LHF |
| Cellular Component | GO:0031012 | extracellular matrix | 5.37E-05 | 3.03E-03 | 1.58 | 11168 | 245 | 1899 | 66 | interactive salinity + LHF |
| Cellular Component | GO:0044420 | extracellular matrix part | 5.61E-05 | 3.04E-03 | 1.98 | 11168 | 95 | 1899 | 32 | interactive salinity + LHF |
| Cellular Component | GO:0032991 | macromolecular complex | 6.06E-05 | 3.16E-03 | 1.13 | 11168 | 3125 | 1899 | 601 | interactive salinity + LHF |
| Cellular Component | GO:0030964 | NADH dehydrogenase complex | 7.17E-05 | 3.60E-03 | 2.69 | 11168 | 35 | 1899 | 16 | interactive salinity + LHF |
| Cellular Component | GO:0045271 | respiratory chain complex I | 7.17E-05 | 3.47E-03 | 2.69 | 11168 | 35 | 1899 | 16 | interactive salinity + LHF |
| Cellular Component | GO:0005747 | mitochondrial respiratory chain complex I | 7.17E-05 | 3.35E-03 | 2.69 | 11168 | 35 | 1899 | 16 | interactive salinity + LHF |
| Cellular Component | GO:0031090 | organelle membrane | 8.43E-05 | 3.81E-03 | 1.26 | 11168 | 1009 | 1899 | 216 | interactive salinity + LHF |
| Cellular Component | GO:0016459 | myosin complex | 1.69E-04 | 7.38E-03 | 2.33 | 11168 | 48 | 1899 | 19 | interactive salinity + LHF |
| Cellular Component | GO:0033268 | node of Ranvier | 1.78E-04 | 7.55E-03 | 3.92 | 11168 | 12 | 1899 | 8 | interactive salinity + LHF |
| Cellular Component | GO:0032982 | myosin filament | 2.18E-04 | 8.96E-03 | 3.53 | 11168 | 15 | 1899 | 9 | interactive salinity + LHF |
| Cellular Component | GO:0005689 | U12-type spliceosomal complex | 2.22E-04 | 8.84E-03 | 3.08 | 11168 | 21 | 1899 | 11 | interactive salinity + LHF |
| Cellular Component | GO:0005576 | extracellular region | 2.25E-04 | 8.73E-03 | 1.29 | 11168 | 714 | 1899 | 157 | interactive salinity + LHF |
| Cellular Component | GO:0005685 | U1 snRNP | 3.02E-04 | 1.14E-02 | 4.12 | 11168 | 10 | 1899 | 7 | interactive salinity + LHF |
| Cellular Component | GO:0044446 | intracellular organelle part | 3.05E-04 | 1.12E-02 | 1.11 | 11168 | 3499 | 1899 | 659 | interactive salinity + LHF |
| Cellular Component | GO:0005604 | basement membrane | 3.44E-04 | 1.23E-02 | 2.05 | 11168 | 66 | 1899 | 23 | interactive salinity + LHF |
| Cellular Component | GO:0034719 | SMN-Sm protein complex | 3.94E-04 | 1.37E-02 | 3.62 | 11168 | 13 | 1899 | 8 | interactive salinity + LHF |

Table S1 continued

| | | | | | | | | | | |
|---|---|---|---|---|---|---|---|---|---|---|
| Cellular Component | GO:0000315 | organellar large ribosomal subunit | 4.11E-04 | 1.39E-02 | 3.1 | 11168 | 19 | 1899 | 10 | interactive salinity + LHF |
| Cellular Component | GO:0005762 | mitochondrial large ribosomal subunit | 4.11E-04 | 1.36E-02 | 3.1 | 11168 | 19 | 1899 | 10 | interactive salinity + LHF |
| Cellular Component | GO:0005859 | muscle myosin complex | 4.91E-04 | 1.59E-02 | 4.41 | 11168 | 8 | 1899 | 6 | interactive salinity + LHF |
| Cellular Component | GO:0044422 | organelle part | 5.23E-04 | 1.65E-02 | 1.1 | 11168 | 3624 | 1899 | 678 | interactive salinity + LHF |
| Cellular Component | GO:0005681 | spliceosomal complex | 5.27E-04 | 1.62E-02 | 1.73 | 11168 | 119 | 1899 | 35 | interactive salinity + LHF |
| Cellular Component | GO:0044455 | mitochondrial membrane part | 6.73E-04 | 2.03E-02 | 1.72 | 11168 | 116 | 1899 | 34 | interactive salinity + LHF |
| Cellular Component | GO:0005605 | basal lamina | 7.83E-04 | 2.31E-02 | 3.36 | 11168 | 14 | 1899 | 8 | interactive salinity + LHF |
| Cellular Component | GO:0030008 | TRAPP complex | 8.34E-04 | 2.41E-02 | 5.88 | 11168 | 4 | 1899 | 4 | interactive salinity + LHF |

# Chapter 5

## Reductions in swimming performance follow freshwater-colonization in two populations of landlocked Alewife


### Abstract

Whole-organism performance can be broken into two integrated components: regulatory performance, which measures homeostatic capabilities, and dynamic performance, which measures physically challenging movements of the body. I used populations of Alewife (*Alosa pseudoharengus*) to examine whether evolutionary changes to regulatory performance can influence the evolution of dynamic performance. Ancestrally anadromous Alewives have recently formed multiple, independently derived, exclusively freshwater (landlocked) populations, which exhibit greater tolerance of freshwater and reduced tolerance of seawater relative to the anadromous ancestor. I tested whether differences in osmoregulatory performance are associated with changes in an ecologically relevant measure of dynamic performance, critical swimming speed ($U_{crit}$), by challenging anadromous and landlocked Alewives with freshwater and seawater prior to $U_{crit}$ measurement. I found that landlocked Alewives exhibit substantially reduced swimming performance across all salinities despite differences in osmotic balance. This indicates that evolved differences in regulatory performance do not influence dynamic performance in Alewives. I then described patterns of body shape variation between Alewife life history forms in order to determine whether differentiation in shape is linked to differences in $U_{crit}$. I found that landlocked Alewives are more fusiform than their robust anadromous ancestor. Although fusiform shapes should in theory provide a swimming advantage over robust shapes, the opposite is true in Alewives. Reductions in swimming performance among landlocked Alewives are likely to be a function of relaxed selection on the capacity to migrate to and from breeding grounds, a trait that landlocked Alewives no longer possess.

## Introduction

Investigations into the evolution of whole-organism performance are central to our understanding of the patterns and processes of natural selection in the wild (Irschick et al. 2008). Performance is classically viewed as a measure of how well an organism accomplishes an ecologically relevant task (e.g., Arnold 1983; Irschick 2003), and is generally thought of as a holistic manifestation of the entire organism (Husak et al 2009). Recently, two types of performance have been recognized (Husak et al 2009): regulatory performance, which measures how organisms regulate physiological processes essential to homeostasis (e.g., regulation of water and ions; McCormick 2009), and dynamic performance, which measures physically challenging movements of the body (e.g., swimming performance; Langerhans 2009). Regulatory and dynamic performance measures are linked to organismal fitness, since they represent an integrated measure of how well an organism can accomplish a vital task (Husak et al 2009). Understanding the integration of regulatory and dynamic performance is essential to our understanding of how whole-organism performance evolves. Whether evolutionary changes in regulatory performance can influence the evolution of dynamic aspects of performance has received little attention. I examined whether adaptations of the osmoregulatory system (i.e., the regulation of water and ions) mediate changes in swimming performance in populations of an ancestrally anadromous fish that have recently colonized freshwater.

Impairments to regulatory performance may negatively impact dynamic aspects of performance by limiting an animal's homeostatic capability. For example, in several euryhaline fishes, transfer to a different salinity reduces maximal swimming performance (Kolok and Sharkey 1997; Swanson 1998). In Coho Salmon parr (*Oncorhynchus kisutch*), reduced hypoosmoregulatory ability is linked to reductions in swimming performance via an increase in blood ion concentration, which affects oxygen delivery and contractility of muscles involved in

swimming (Brauner et al 1999). For aquatic organisms, transition to novel salinity environments leads to evolutionary shifts in osmoregulatory performance optima and tolerance limits at different salinities (Scott et al 2004; Fuller 2009; McCairns and Bernatchez 2010; Lee et al 2011; Whitehead et al 2011, 2012; DeFaveri and Merila 2013; Velotta et al 2014; chapter 3). Whether evolutionary shifts in osmoregulatory performance at different salinities can influence dynamic aspects of performance has not been explored, yet should yield insights into the evolutionary linkages between regulatory and dynamic performance.

Populations of Alewife (*Alosa pseudoharengus*) represent a unique opportunity to explore whether the evolution of regulatory performance has dynamic performance consequences. Alewives are ancestrally anadromous and of a distinctly marine family (Clupeidae; Li and Orti 2007). Multiple exclusively freshwater (landlocked) populations have formed independently from an anadromous ancestor, most likely as a result of dams built during the American colonial-period (circa 300-400 years ago; Palkovacs et al 2008). I have shown previously that landlocked Alewife populations are locally adapted to freshwater, and that this adaptation results in a trade-off in osmoregulatory performance; landlocking is associated with greater tolerance of freshwater, as well as reduced tolerance of, and osmotic balance in, seawater (Velotta et al 2014; chapter 3). This system is ideal to test whether evolutionary changes to osmoregulatory function correspond to changes in dynamic performance. The existence of independently derived landlocked populations allows us to test whether changes in whole-organism performance have occurred in parallel, a pattern that points to natural selection as the driver of change (Schluter 2000).

I tested whether evolutionary changes in osmoregulatory performance have influenced an ecologically relevant measure of dynamic performance – sustained swimming – by comparing

two independently evolved populations of landlocked Alewife to the ancestral anadromous form. To do so, I subjected laboratory-acclimated Alewives from one anadromous and two landlocked populations to 24 hour freshwater and seawater treatments, after which I measured sustained swimming performance (critical swimming speed or $U_{crit}$; Brett 1964). I chose to measure critical swimming speed since it is ecologically relevant in species that migrate and/or live in the open ocean (Plaut 2001). If evolutionary changes in osmoregulatory performance affect dynamic aspects of performance in Alewives, then I expect to see 1) enhanced swimming performance capacity in freshwater, and 2) reduced swimming performance capacity in seawater for landlocked Alewives compared to anadromous forms. This result would indicate that variation in swimming performance between life history forms is correlated with evolutionary changes in salinity tolerance.

I tested whether differences in osmoregulatory capacity influence differences in swimming performance at the individual level by measuring plasma osmolality (plasma solute concentration) of fish after each swim trial. Teleost fishes actively maintain internal osmolality to ensure proper cellular function. Plasma ion concentration can serve as an indicator of osmoregulatory capacity or osmotic balance (e.g., Zydlewski and McCormick 1997, Whitehead et al 2011, 2012; Velotta et al 2014; chapter 3), and excursions beyond acclimation osmolality indicate a reduction in capacity. If differences in dynamic performance are the result of differences in osmoregulatory function, then I expect that plasma osmolality will be correlated with $U_{crit}$. The direction of this correlation depends on the exposure salinity: in freshwater, lower values of plasma osmolality imply reduced hyperosmoregulatory capacity, while in seawater, higher plasma osmolality implies reduced hypoosmoregulatory function. Therefore, I expected

that osmolality and critical swimming speed would be positively correlated in freshwater and negatively correlated in seawater.

I explored whether morphological divergence has an overriding influence on swimming performance in Alewives by describing patterns of shape variation between anadromous and landlocked forms. Morphology and body shape have well-documented influences on dynamic performance, including fish locomotion (Langerhans and Reznick 2009). A recent analysis demonstrated that landlocked Alewives are more fusiform in shape, have smaller heads, and narrower caudal peduncles compared to more robustly shaped anadromous forms (Jones et al 2013). Fusiform shapes should improve swimming efficiency over robust body shapes, which are generally thought to facilitate acceleration and maneuverability (Walker 1997; Langerhans 2009). This leads to the prediction that landlocked Alewife forms will exhibit greater swimming performance than anadromous forms. I tested this prediction by relating patterns of shape divergence to variation in swimming performance using a geometric morphometrics approach. This analysis will help to shed light on the extent to which body shape and regulatory performance evolution interact to influence dynamic performance. If body shape variation has a disproportionately strong effect on dynamic performance, then it should be a significant predictor of swimming performance in any salinity. By contrast, if osmoregulatory performance has a stronger influence on dynamic performance, then osmoregulatory capacity should be a significant predictor of swimming performance regardless of body shape. Overall, this study will yield important insights into how evolution has shaped several integrated aspects of whole-organism performance.

## Methods

*Animals and experimental procedures*

Juvenile (young-of-the-year) anadromous and landlocked Alewives were captured by purse seine from their natal lakes in Connecticut in August 2013, and immediately transported to the Conte Anadromous Fish Research Center in Turners Falls, Massachusetts. All animals were handled in accordance with the University of Connecticut Institute for Animal Care and Use Committee (protocol #A12-042). I captured Alewives from three locations: an anadromous population from Bride Lake (A-Bride; East Lyme, Connecticut; 41.33N, 72.24W), and landlocked populations from Pattagansett Lake (L-Pattagansett; East Lyme, Connecticut; 43.47N, 72.23W) and Rogers Lake (L-Rogers; Old Lyme, Connecticut; 41.37N, 72.30W). Fish were transported in aerated 190-liter cylindrical containers at 1 ppt containing lake water mixed with artificial sea salt (Instant Ocean, Spectrum Brands, Madison, WI, USA). Once in the laboratory, Alewives were held at 1 ppt for 1 day, after which salinity was decreased to 0.5 ppt (final rearing salinity). I segregated Alewives by site and held them in separate 1,200-liter re-circulating oval tanks fitted with charcoal filtration systems for one month prior to experimentation. Fish were maintained at ambient water temperature and kept on an ambient photoperiod.

To test whether evolved differences in osmoregulatory performance can influence dynamic performance, I measured critical swimming speed of anadromous and landlocked Alewives subjected to acute (24 hour) treatments of freshwater and seawater. Prior to each swimming trial, Alewives from each site were transferred from rearing tanks (0.5 ppt) directly to aerated 250-liter oval tanks containing either 0 ppt freshwater, 35 ppt or 40 ppt seawater, or a 0.5 ppt control for 24 hours. Control and seawater treatments were achieved by mixing de-

chlorinated tap water with artificial sea salt (Crystal Sea Marine Mix, Marine Enterprises International, Baltimore, MD, USA), while the freshwater treatment (0 ppt) consisted of de-chlorinated tap water only. Tank temperature was maintained between 17-18 °C with electric tank heaters. Due to time constraints, I conducted a maximum of three swimming performance trials per day (fish were swum one at a time; see below), which limited me to the following trial schedule: 24 hours prior to each trial day, approximately 6-8 Alewives from one of the three sites was transferred to one of the four salinity treatments, after which three individual fish from this site and salinity treatment group were measured for $U_{crit}$. I repeated this procedure until a total of 5-6 individuals per site per salinity treatment were measured. Trials lasted from October – November 2013. For each swimming performance trial, I matched the temperature and salinity of the swim tunnel apparatus to that of the 24-hour exposure tank.

*Measurement of critical swimming speed ($U_{crit}$)*

To measure $U_{crit}$, I swam one fish per trial in a 5-L Brett style swim tunnel (Loligo Systems Inc., Hobro, Denmark), in which water velocity was increased incrementally until the fish failed to maintain position in the water column. My protocol was modified from those published previously (Fangue et al 2008; Dalziel et al 2012). Before each trial, I placed one fish in the tunnel and allowed it acclimate at 0.5 body lengths per second (BL/s) for one hour. After the acclimation period, I increased the velocity in the chamber by 0.5 BL/s every 2 minutes until the fish reached 5 BL/s, which is 50% of a pre-determined average $U_{crit}$ (10 BL/s). I calculated this average $U_{crit}$ value based on the results of a pilot study conducted in May 2012 on anadromous fish reared in the laboratory. After the initial increase to 5 BL/s, velocity was increased by 0.5 BL/s every 10 minutes until the fish remained pinned against the downstream barrier of the tunnel for > 10 seconds. This measure of failure was determined during the pilot

study, in which I observed that fish pinned for longer than 10 seconds tended not to return to swimming. Since the size of each fish was less than 25% of the cross-sectional area of the tunnel, correction for solid blocking effects was not needed.

Critical swimming speed was determined using the following formula:

$$U_{crit} = U_i + \left( \frac{t_i}{t_{ii}} \, x \, U_{ii} \right) \quad (1)$$

where $U_i$ is the highest speed the fish is able to swim for a full 10 minute interval (BL/s), $U_{ii}$ is increment at which speed is increased (0.5 BL/s), $t_i$ is the time the fish swam at the final velocity (minutes), and $t_{ii}$ is the amount of time fish swam at each interval (10 minutes).

Differences in $U_{crit}$ between Alewife life history forms and salinity treatments were tested using linear mixed effects models (LMMs) generated using the *lmer* function in R (*lme4* package; R version 3.1.0). Full models included site (A-Bride, L-Pattagansett, or L-Rogers) and salinity (0 ppt, 0.5 ppt, 35 ppt, and 40 ppt) as fixed effects, and length ($L_t$) as a covariate. I included trial date as a random effect in the models. P-values were calculated with the *anova* function in the *LmerTest* package (R version 3.1.0) using restricted maximum likelihood and Satterthwaite estimation for denominator degrees of freedom. I implemented a model reduction approach, whereby non-significant ($P > 0.05$) interactions terms were eliminated sequentially. Tukey HSD post-hoc tests (*multcomp* package in R) were used to determine pairwise differences among sites and salinity treatments.

Because velocity in the swim tunnel was increased by a fixed proportion of fish length (0.5 BL/s), I estimated the total length of each fish photographically before each trial. Images were used to measure length, since the removal of Alewives from water results in significant stress and injury (*personal observation*). After a fish was removed from the salinity treatment tank, it was placed immediately in a 10-liter bucket filled with 2 liters of water and a ruler. I then

photographed each fish (Pentax Optio WG camera, Ricoh Imaging Americas Corp., Denver, CO, USA) and estimated $L_t$ in ImageJ (Schneider et al 2012). In some cases, the estimated length differed from the actual length observed after the trial (length deviations were 3 mm on average). In these cases, I calculated an adjusted $U_i$ by dividing the velocity at failure (cm/s) by the actual $L_t$, which led to an adjusted value of $U_{crit}$ (see equation 1).

*Plasma osmolality and morphometric analysis*

After each trial, I euthanized fish in 250 mg $l^{-1}$ tricaine methanesulfonate (MS-222; Argent, Redmond, WA, USA) and measured them for fork length ($L_f$), total length ($L_t$), and weight. I then placed fish on a white background, straightened them with acupuncture pins, and photographed them from a standard distance. Next, I severed the caudal fin and removed blood from the caudal vessel with a 1 mL heparinized hematocrit tube. Blood was centrifuged at 3200g for 5 minutes, after which plasma was removed and transferred to 0.5 mL tubes and stored at -80°C. I measured plasma osmolality, the total plasma solute concentration, using a vapor pressure osmometer (Wescor Inc., Logan, Utah, USA) with approximately 8 μL of plasma following the manufacturer's instructions. Depending on the amount of available plasma, I ran samples in duplicate or triplicate and took the average reading as the final value of osmolality. Differences in plasma osmolality between life history forms were determined using LMMs, as above. Pearson's product moment correlations (implemented in R) were used to test for a relationship between plasma osmolality and $U_{crit}$. Values were log transformed to meet the assumptions of normality.

To quantify body shape variation, I used a landmark-based geometric morphometrics approach (Bookstein 1997; Adams et al 2004) following the procedure of Jones et al (2013). Briefly, I placed 11 landmarks using tpsDig2 v2.16 (Rohlf 2010) on approximately 20

individuals from each of the three sites. I then used the Procrustes fit function in MorphoJ v 1.02 (Klingenberg 2011) to generate the consensus shape and remove variation due to scaling, rotation, and translation (Rohlf and Slice 1990; Adams et al 2004; Zelditch 2004). To distinguish the axes of variation in body shape, I conducted principal components analysis (PCA) on the covariance matrix produced from the shape data in MorphoJ. In addition, I performed a discriminant function analysis (DFA) to describe the axis of body shape variation that best distinguishes landlocked from anadromous forms. I tested for statistical differences in PCA and DFA scores between sites using LMMs, where site was a main effect, trial a random effect, and $L_t$ a covariate. To determine whether body shape variation influences critical swimming speed, I correlated PCA scores from the first three principal components (PCs) with $U_{crit}$ using Pearson's product moment correlation. Body shape variations in the PCA and DFA were visualized using wireframe graphs generated in MorpoJ at a scale factor of ± 0.1.

**Results**

I found that critical swimming speed ($U_{crit}$) was significantly lower among landlocked Alewives from both sites across all salinities (Table 1; Figure 1). Anadromous Alewives exhibited an average $U_{crit}$ of 9.7 BL/s, 1.8 and 2.8 BL/s higher than landlocked Alewives from L-Pattagansett and L-Rogers, respectively (Figure 1). Full LMMs revealed no significant three-way or two-way interactions ($P > 0.05$), and so a reduced model included only main effects (site and salinity) and length as a covariate. This model revealed a significant main effect of site on $U_{crit}$ (Table 1). Post hoc tests revealed significant reductions in $U_{crit}$ in L-Pattagansett compared to A-Bride ($z = -3.05$; $P = 0.006$) and L-Rogers compared to A-Bride ($z = -4.422$, $P < 0.001$). I detected no statistically significant differences in $U_{crit}$ between the two landlocked sites ($P > 0.05$). No significant effect of length on $U_{crit}$ was observed (Table 1). Using absolute critical

swimming speed (in cm/s) in place of body-size normalized $U_{crit}$ (in BL/s) produced identical results with respect to the main effects of site and salinity.

Challenge in a hyper-saline (40 ppt) environment had a significant effect on swimming performance in both anadromous and landlocked Alewives; a reduced LMM revealed a significant main effect of salinity on $U_{crit}$ (Table 1; Figure 1). Post-hoc tests revealed that critical swimming speed was reduced at 40 ppt compared to control salinity (0.5 ppt; $z = -2.26$; $P = 0.02$), 0 ppt freshwater ($z = -2.86$; $P = 0.02$), and 35 ppt seawater ($z = -3.15$; $P = 0.009$). I was unable to measure $U_{crit}$ in L-Rogers Alewives at 40 ppt since no individuals from this population survived hyper-saline challenge. This is consistent with previously reported survival data (chapter 3).

I found that plasma osmolality differed between salinity treatments and Alewife life history forms, though it was not a significant predictor of critical swimming speed at any salinity (Figure 2). After full models revealed no significant three-way or two-way interactions ($P > 0.05$), I ran a reduced LMM on plasma osmolality with salinity and site as main effects, and length as a covariate. This model detected a significant effect of salinity ($F_{3,13.5} = 138.9$; $P < 0.001$) and site on plasma osmolality ($F_{2,10.5,} = 4.6$; $P = 0.037$). Post-hoc analyses revealed that Alewives from freshwater and control (0.5 ppt) salinities had significantly lower plasma osmolality ($P < 0.001$ in each case) than Alewives from 35 ppt (0 ppt vs. 35 ppt: $z = 16.7$; 0.5 ppt vs. 35 ppt: $z = 11.7$) and 40 ppt (0 ppt vs. 40 ppt: $z = 13.1$; 0.5 ppt vs. 40 ppt: $z = 11.8$). Plasma osmolality was significantly higher among Alewives from L-Rogers compared to Alewives from A-Bride (Tukey's HSD post-hoc test; $z = 2.46$; $P = 0.037$). Pearson's product-moment correlations revealed non-significant relationships between $U_{crit}$ and plasma osmolality at 0 ppt ($r = - 0.15$; $P = 0.58$), 0.5 ppt control ($r = - 0.46$; $P = 0.08$, 35 ppt ($r = -0.39$; $P = 0.11$), and 40 ppt

($r$ = -0.54; P = 0.27). The overall correlation between osmolality and $U_{crit}$ was also non-significant (Figure 2). Within-population correlations revealed a significant negative relationship between plasma osmolality and $U_{crit}$ for L-Pattagansett Alewives ($r$ = 0.49; P = 0.03), though not for L-Rogers or A-Bride (P > 0.05).

Geometric morphometric analysis revealed that landlocked Alewives are generally more fusiform in shape than anadromous Alewives, and tend to have smaller heads and narrower caudal peduncles. In the PCA, the first three PC's described 68% of the variance in the data (34.9%, 18.5%, and 14.7%, respectively). I observed significant differences between sites along PC2 ($F_{2,13.7}$ = 4.5; P = 0.03; non-significant effect of $L_t$, P > 0.05), which describes general body shape, head size, and caudal peduncle size. Post-hoc analyses revealed that both landlocked populations were significantly different compared to A-Bride (L-Pattagansett: z = 2.7; P = 0.020; L-Rogers: z = 2.5; P = 0.037) along the PC2 axis. No significant differences at PC1 or PC3 were found (P > 0.05). Discriminant function analysis (DFA) confirmed that landlocked Alewives are more fusiform than anadromous Alewives and tended to have smaller heads and narrower caudal peduncles (Figure 3). A linear mixed effects model of DFA scores revealed a significant effect of site on body shape ($F_{2, 45}$ = 89.1; P < 0.001).

I found that body shape is correlated with swimming performance in Alewives (Figure 4). I correlated $U_{crit}$ with PC2 scores because Alewife life history forms have significantly differentiated along this shape axis, and because PC2 describes body shape variation that is most likely to influence critical swimming speed. Across all sites, $U_{crit}$ was significantly and negatively correlated with PC2 scores, indicating that fish with more fusiform body shapes have lower critical swimming speeds than those with robust shapes. Within population correlations

revealed a significant negative relationship between $U_{crit}$ and PC2 for L-Rogers Alewives ($r$ = 0.52; P = 0.04), and not for L-Pattagansett or A-Bride (P > 0.05).

**Discussion**

I explored the extent to which evolved shifts in osmoregulatory performance (Velotta et al 2014; chapter 3) can influence dynamic aspects of whole-organism performance in independently derived landlocked populations of Alewife. My results suggest that divergence in sustained swimming performance do not reflect changes in osmoregulatory performance. Instead, independently derived populations of landlocked Alewife have substantially reduced swimming performance regardless of salinity or homeostatic state. Putative body shape advantages do not provide more fusiform landlocked Alewives with swimming advantages over their more robust anadromous counterparts. I conclude that reductions in swimming performance among landlocked Alewives may be a function of the relaxation of selection on the capacity to migrate to and from breeding grounds.

Critical swimming speed was lower among landlocked Alewives from both sites by approximately 2-3 BL/s, and this result was consistent across all salinities (Figure 1). Landlocked forms are exclusively freshwater and exhibit improved tolerance of low-ion freshwater compared to anadromous Alewives (chapter 3). My results indicate that Alewives from both anadromous and landlocked sites maintain osmotic balance in response to freshwater equally well; life history forms do not differ significantly in plasma osmolality at 0 ppt, and freshwater osmolality is equivalent to that of the control (LMM; P > 0.05). It is not surprising that I find no relationship between hyperosmotic capacity and swimming performance in freshwater (Figure 2). It is possible that freshwater treatment used in this study (0 ppt; conductivity ~ 150 uS) was not sufficiently challenging to enable discrimination of life history

form differentiation in hyperosmoregulatory capacity. In previous studies, low-ion freshwater (0 ppt, conductivity ~ 20 uS) has been shown to resolve difference in freshwater tolerance between Alewife life history forms (chapter 3), whereas no tolerance differences were detected in freshwater at 1 ppt (Velotta et al 2014; chapter 3).

At 35 ppt seawater, landlocked Alewives exhibited reduced critical swimming speed (Figure 1), however, this reduction is not correlated with plasma ion concentration (Figure 2). I expected that reductions in swimming performance in seawater among landlocked Alewives would be related to a reduced hypoosmoregulatory capacity relative to anadromous Alewives. Although anadromous Alewives appear to have lower osmolality than landlocked forms (suggesting better homeostatic regulation; Figure 2), I detected no statistically significant differences (LMM; $P > 0.05$). I therefore find no evidence that known life history form level differentiation in hypoosmoregulatory capacity (Velotta et al 2014; chapter 3) can explain reductions in critical swimming speed among landlocked Alewives in seawater. These results suggest that changes in regulatory performance in Alewives do not influence dynamic whole-organism performance measures.

Osmotic perturbations negatively influence swimming performance in Alewives, though both landlocked and anadromous forms are affected equivalently. Challenge at 40 ppt seawater resulted in reduced critical swimming speed in landlocked and anadromous Alewives. This result is consistent with observations in other species of fish in which transfer to a different salinity reduces overall swimming performance (Kolok and Sharkey 1997; Swanson 1998; Brauner et al 1992). One possible mechanism for this reduction is that high plasma ion concentrations – the result of reduced hypoosmoregulatory capacity - may reduce moisture content in the muscles, lowering the efficiency of contractions and thereby negatively affecting swimming performance

(Brauner et al 1992). In this study, I found that the magnitude of the reduction in swimming performance at 40 ppt was the same (i.e., I found no site x salinity interaction; see Results section) in both A-Bride and L-Pattagansett (no fish from L-Rogers survived 24 challenge at 40 ppt).

Since swimming performance was lower among landlocked Alewives at all salinities, and since osmoregulatory capacity is unrelated to critical swimming speed, I suggest that relaxed selection on migratory ability has led to changes in morphological or physiological characteristics that maintain sustained aerobic swimming performance in anadromous Alewives. Along their native range, anadromous Alewives make long distance breeding migrations from the sea to rivers and coastal lakes (Fay et al 1983). This migration likely exerts strong selection pressure on sustained aerobic swimming performance capabilities. By contrast, landlocked Alewives, which are restricted to their natal lakes and ponds, do not migrate. Several studies have shown that populations of freshwater-resident, non-migratory fish exhibit reduced sustained swimming performance compared to ancestrally anadromous or highly migratory populations (Threespine Stickleback (*Gasterosteus aculeatus*; Taylor and McPhail 1986; Tudorache et al 2007; Dalziel et al 2012) and Sockeye salmon (*Oncorhynchus nerka*; Taylor and Foote 1991)). My results provide strong support for the prediction that loss of anadromous migration results in reduced swimming performance capacities.

Theory predicts that the removal of a selection pressure on a trait will lead to its reduction or loss by either neutral or selective processes. Mutations in alleles for traits under relaxed selection may lead to a slow decline in function, while natural selection may eliminate trait function rapidly as the result of direct (e.g., a high maintenance cost) or indirect (e.g., trade-offs) processes (Lahti et al 2009). Previous work has demonstrated that performance trade-offs can

substantially influence swimming ability, suggesting that indirect fitness costs play an important role in sustained swimming performance reductions. For example, high juvenile growth rate is correlated with low critical swimming speed in several species of fish (Kolok and Oris 1995; Farrel et al 1997; Billerbeck et al 2001; Alvarez and Metcalfe 2001; Lee et al 2010). The underlying mechanisms that contribute to a growth rate/swimming performance trade-off are not well understood, but may be influenced by differences in aerobic scope (Arnott et al 2006). Landlocked populations of Alewife exhibit slower growth rates than their anadromous ancestor in the wild (Scott and Crossman 1973) and when reared in full-strength seawater in the laboratory (J. Velotta, unpublished data). Thus, the available data suggest that trade-offs with growth rate and swimming performance do not occur in the predicted direction, and therefore are not likely to account for the reductions in swimming performance among landlocked Alewives.

Sustained swimming performance has also been shown to trade-off with burst swimming performance in several species (Threespine Stickleback: Taylor and McPhail 1986; Trinidadian guppy: Langerhans 2009; Oufiero et al 2011). Performance trade-offs in swimming ability appear to be mediated by morphological traits that act antagonistically, such that traits that maximize one type of performance limit the other (Langerhans and Reznick 2009). Morphological features that facilitate high sustained swimming performance abilities are those that reduce drag, including a shallow, streamlined body form, small head, and thin caudal peduncle (Langerhans and Reznick 2009). Consistent with Jones et al (2013), I found that landlocked Alewives possess traits that should theoretically reduce drag and lead to improved swimming performance capabilities over anadromous Alewives, while landlocked forms are more streamlined, have smaller heads, and thinner caudal peduncles (Figure 3 and 4). Swimming performance results suggest the opposite; that a streamlined body form is associated with lower

critical swimming abilities, whereas more robust features are associated with higher sustained performance (Figure 4). Thus, morphological differentiation between landlocked and anadromous Alewives is inconsistent with the hypothesis that trade-offs between burst and sustained performance mediate the divergence in swimming ability. I do not know, however, whether Alewife life history forms exhibit differentiation in burst swimming performance. Future work should be aimed at assessing whether swimming performance trade-offs mediate reductions in critical swimming speed in Alewives.

A potential cause of swimming performance differences among landlocked Alewives may be differentiation in metabolic rate, which has been shown to mediate swimming performance differences in several species. In non-migratory Threespine Stickleback, reduced maximum metabolic rate is a likely driver of reduced swimming performance compared to migratory marine/anadromous populations (Dalziel et al 2012). In the Atlantic silverside, fast-growing northern populations, which have a reduced scope for aerobic activity, exhibit lower critical swimming speeds than do slower-growing southern populations (Arnott et al 2006). Future studies should address whether landlocked and anadromous populations differ in metabolic rate, and the extent to which any differences influence sustained swimming performance.

*Conclusions*

In summary, I find that landlocked Alewives exhibit reduced critical swimming speeds compared to anadromous Alewives at any salinity. My results are inconsistent with the hypothesis that differentiation in osmoregulatory performance results in differentiation in a dynamic measure of performance. Furthermore, reduced sustained swimming performance was

observed among landlocked Alewives despite possessing body forms that are expected to facilitate high swimming speeds. Though landlocked Alewives are more tolerant of freshwater and possess putatively adaptive body forms, they exhibit reduced sustained swimming performance, which is likely to be the result of relaxed selection on traits that facilitate migration ability.

This work adds to the growing body of literature suggesting that relaxed selection has a substantial influence on dynamic whole-organism performance traits. I demonstrate for the first time that swimming performance reductions can occur relatively rapidly in nature, since landlocked Alewife populations diverged from the anadromous ancestor recently (circa 300-400 years; Palkovacs et al 2008). This is a considerably shorter time period than has been shown previously (e.g., in non-migratory Threespine stickleback which diverged from a marine ancestor circa 10,000 years ago; Bell and Foster 1994). Since independently derived populations of landlocked Alewife exhibit lower critical swimming speeds in parallel, my results support the role of natural selection in driving swimming performance reductions. The extent to which direct or indirect costs mediate this reduction is not known, but my results suggest that trade-offs with growth rate or bust swimming performance are unlikely. Differentiation in metabolic rate represents a strong possibility by which differences in sustained swimming performance may be mediated in Alewives, and should be the focus of future work. Other functional traits that influence migration ability will also need to be explored, for example: differences in the uptake, transport and utilization of oxygen, and differences in muscle performance that may limit swimming performance in Alewives.

**References**

Adams, D.C., Rohlf, F.J., and Slice, D.E. (2004). Geometric morphometrics: Ten years of progress following the “revolution.” Ital. J. Zool. *71*, 5–16.

Álvarez, D., and Metcalfe, N.B. (2005). Catch-up growth and swimming performance in threespine sticklebacks (*Gasterosteus aculeatus*): seasonal changes in the cost of compensation. Can. J. Fish. Aquat. Sci. *62*, 2169–2176.

Arnold, S.J. (1983). Morphology, performance and fitness. Amer. Zool. *23*, 347–361.

Bookstein, F.L. (1997). Morphometric Tools for Landmark Data: Geometry and Biology (Cambridge University Press).

Brauner, C.J., Iwama, G.K., and Randall, D.J. (1994). The effect of short-duration seawater exposure on the swimming performance of wild and hatchery-reared juvenile coho salmon (*Oncorhynchus kisutch*) during smoltification. Can. J. Fish. Aquat. Sci. *51*, 2188–2194.

Brett, J.R. (1964). The respiratory metabolism and swimming performance of young sockeye salmon. J. Fish. Res. Bd. Can. *21*, 1183–1226.

Dalziel, A.C., Vines, T.H., and Schulte, P.M. (2012). Reductions in prolonged swimming capacity following freshwater colonization in multiple Threespine Stickleback populations. Evolution *66*, 1226–1239.

DeFaveri, J., and Merilä, J. (2014). Local adaptation to salinity in the three-spined stickleback? J. Evol. Biol. *27*, 290–302.

Fangue, N.A., Mandic, M., Richards, J.G., and Schulte, P.M. (2008). Swimming performance and energetics as a function of temperature in killifish *Fundulus heteroclitus*. Physiol. Biochem. Zool. *81*, 389–401.

Farrell, A.P., Bennett, W., and Devlin, R.H. (1997). Growth-enhanced transgenic salmon can be inferior swimmers. Can. J. Zool. *75*, 335–337.

Fay, C.W., Neves, R.J., and Pardue, G.B. (1982). Species profiles: life histories and environmental requirements of coastal fishes and invertebrates (Mid-Atlantic). Alewife/Blueback Herring. Biological Report - United States Fish and Wildlife Service *82*.

Fuller, R.C. (2009). A test for a trade-off in salinity tolerance in early life-history stages in *Lucania goodei* and *L. parva.* Copeia *2008*, 154–157.

Husak, J.F., Irschick, D.J., McCormick, S.D., and Moore, I.T. (2009). Hormonal regulation of whole-animal performance: implications for selection. Integr. Comp. Biol. *49*, 349–353.

Irschick, D.J., Meyers, J.J., Husak, J.F., and Galliard, J.-F.L. (2008). How does selection operate on whole-organism functional performance capacities? A review and synthesis. Evol. Ecol. Res. *10*, 177–197.

Jones, A.W., Palkovacs, E.P., and Post, D.M. (2013). Recent parallel divergence in body shape and diet source of alewife life history forms. Evol. Ecol. *27*, 1175–1187.

Klingenberg, C.P. (2011). MorphoJ: an integrated software package for geometric morphometrics. Mol. Ecol. Resour. *11*, 353–357.

Kolok, A.S., and Oris, J.T. (1995). The relationship between specific growth rate and swimming performance in male fathead minnows (*Pimephales promelas*). Can. J. Zool. *73*, 2165–2167.

Kolok, A.S., and Sharkey, D. (1997). Effect of freshwater acclimation on the swimming performance and plasma osmolarity of the euryhaline gulf killifish. Trans. Am. Fish. Soc. *126*, 866–870.

Lahti, D.C., Johnson, N.A., Ajie, B.C., Otto, S.P., Hendry, A.P., Blumstein, D.T., Coss, R.G., Donohue, K., and Foster, S.A. (2009). Relaxed selection in the wild. Trends Ecol. Evol. *24*, 487–496.

Langerhans, R.B. (2009). Trade-off between steady and unsteady swimming underlies predator-driven divergence in *Gambusia affinis*. J. Evol. Biol. *22*, 1057–1075.

Langerhans, R.B., and Reznick, D.N. (2009). Ecology and evolution of swimming performance in fishes: predicting evolution with biomechanics. In Fish Locomotion: An Etho-Ecological Perspective, (Science Publishers).

Lee, C.E., Bell, M.A., Lee, C.E., and Bell, M.A. (1999). Causes and consequences of recent freshwater invasions by saltwater animals. Trends Ecol. Evol. *14*, 284–288.

Lee, C.G., Farrell, A.P., Lotto, A., MacNutt, M.J., Hinch, S.G., and Healey, M.C. (2003). The effect of temperature on swimming performance and oxygen consumption in adult sockeye (*Oncorhynchus nerka*) and coho (*O. kisutch*) salmon stocks. J. Exp. Biol. *206*, 3239–3251.

Li, C., and Ortí, G. (2007). Molecular phylogeny of Clupeiformes (Actinopterygii) inferred from nuclear and mitochondrial DNA sequences. Mol. Phylogenet. Evol. *44*, 386–398.

McCairns, R.J.S., and Bernatchez, L. (2010). Adaptive divergence between freshwater and marine sticklebacks: insights into the role of phenotypic plasticity from an integrated analysis of candidate gene expression. Evolution *64*, 1029–1047.

McCormick, S.D. (2009). Evolution of the hormonal control of animal performance: insights from the seaward migration of salmon. Integr. Comp. Biol. *49*, 408–422.

Oufiero, C.E., Walsh, M.R., Reznick, D.N., and Jr., T.G. (2011). Swimming performance trade-offs across a gradient in community composition in Trinidadian killifish (*Rivulus hartii*). Ecology *92*, 170–179.

Palkovacs, E.P., Dion, K.B., Post, D.M., and Caccone, A. (2008). Independent evolutionary origins of landlocked alewife populations and rapid parallel evolution of phenotypic traits. Mol. Ecol. *17*, 582–597.

Plaut, I. (2001). Critical swimming speed: its ecological relevance. Comp. Biochem. Phys. A *131*, 41–50.

Rohlf, F.J. (2010). TPSDig2. 2.16.

Rohlf, F.J., and Slice, D. (1990). Extensions of the procrustes method for the optimal superimposition of landmarks. Syst. Biol. *39*, 40–59.

Schluter, D. (2000). The Ecology of Adaptive Radiation (Oxford University Press).

Scott, W., and Crossman, E. (1973). Freshwater fishes of Canada. Fisheries Research Board of Canada Bulletin *184*.

Scott, G.R., Rogers, J.T., Richards, J.G., Wood, C.M., and Schulte, P.M. (2004). Intraspecific divergence of ionoregulatory physiology in the euryhaline teleost *Fundulus heteroclitus*: possible mechanisms of freshwater adaptation. J. Exp. Biol. *207*, 3399–3410.

Swanson, C. (1998). Interactive effects of salinity on metabolic rate, activity, growth and osmoregulation in the euryhaline milkfish (*Chanos chanos*). J. Exp. Biol. *201*, 3355–3366.

Taylor, E.B., and Foote, C.J. (1991). Critical swimming velocities of juvenile sockeye salmon and kokanee, the anadromous and non-anadromous forms of *Oncorhynchus nerka* (Walbaum). J. Fish Biol. *38*, 407–419.

Taylor, E.B., and McPhail, J.D. (1986). Prolonged and burst swimming in anadromous and freshwater threespine stickleback, *Gasterosteus aculeatus*. Can. J. Zool. *64*, 416–420.

Tudorache, C., Blust, R., and De Boeck, G. (2007). Swimming capacity and energetics of migrating and non-migrating morphs of three-spined stickleback *Gasterosteus aculeatus* L. and their ecological implications. J. Fish Biol. *71*, 1448–1456.

Velotta, J.P., McCormick, S.D., O'Neill, R.J., and Schultz, E.T. (2014). Relaxed selection causes microevolution of seawater osmoregulation and gene expression in landlocked Alewives. Oecologia *175*, 1081–1092.

Walker, J.A. (1997). Ecological morphology of lacustrine threespine stickleback *Gasterosteus aculeatus* L. (Gasterosteidae) body shape. Biol. J. Linn. Soc. *61*, 3–50.

Whitehead, A., Roach, J.L., Zhang, S., and Galvez, F. (2011). Genomic mechanisms of evolved physiological plasticity in killifish distributed along an environmental salinity gradient. PNAS *108*, 6193–6198.

Whitehead, A., Roach, J.L., Zhang, S., and Galvez, F. (2012). Salinity- and population-dependent genome regulatory response during osmotic acclimation in the killifish (*Fundulus heteroclitus*) gill. J. Exp. Biol. *215*, 1293–1305.

Zelditch, M.L., Swiderski, D.L., and Sheets, H.D. (2004). Geometric Morphometrics for Biologists: A Primer (Academic Press).

Zydlewski, J., and McCormick, S.D. (1997). The loss of hyperosmoregulatory ability in migrating juvenile American shad, *Alosa sapidissima*. Can. J. Fish. Aquat. Sci. *54*, 2377–2387.

**Table 1** Analysis of covariance table of reduced linear mixed effects model exploring the effect of site, salinity, and fish length on $U_{crit}$. The main effect of site has three levels: A-Bride, L-Pattagansett, and L-Rogers. The main effect of salinity has four levels: 0 ppt, 0.5 ppt, 35 ppt, and 40 ppt. $L_t$ is total length (cm). NumDF = numerator degrees of freedom. DenDF = denominator degrees of freedom, which was generated by the Satterthwaite approximation method. Bold P-values denote statistical significance at the $P < 0.05$ level.

| | NumDF | DenDF | F-value | P-value |
|---|---|---|---|---|
| Site | 2 | 13.4 | 17.7 | **< 0.001** |
| Salinity | 3 | 14.7 | 3.7 | **0.037** |
| $L_t$ | 1 | 43.3 | 0.5 | 0.466 |

**Figures**

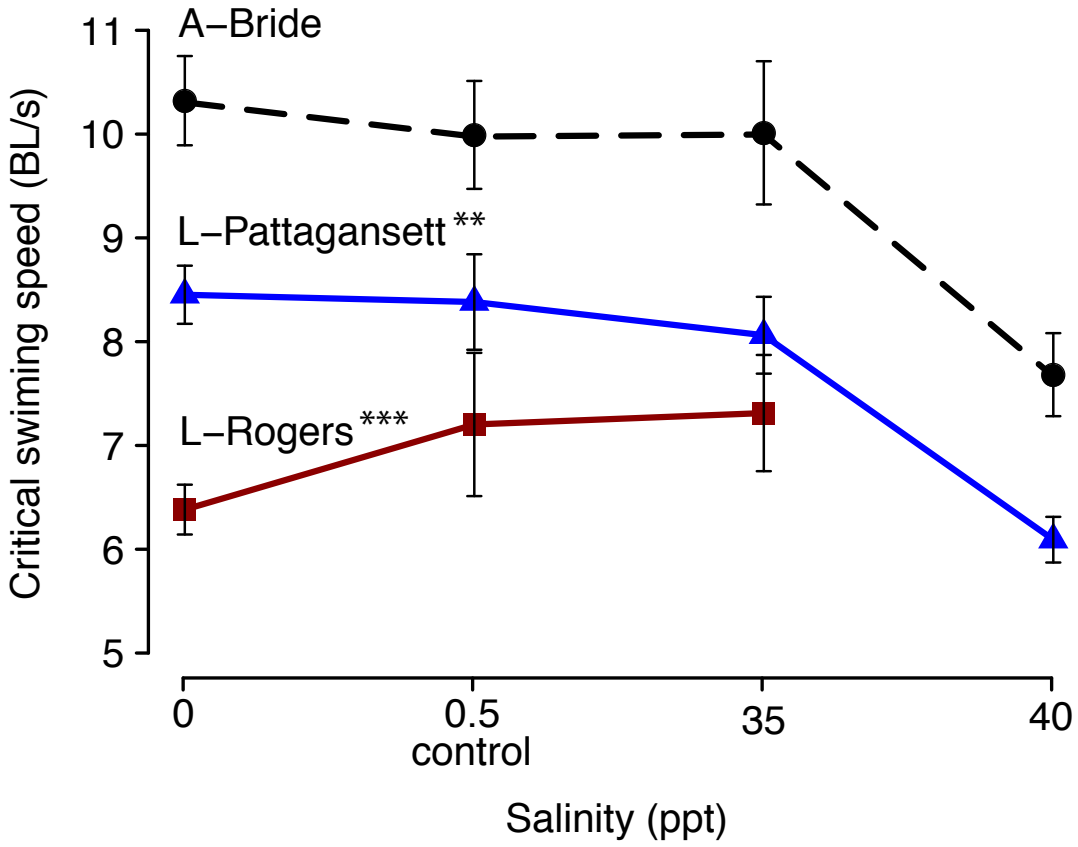


**Figure 1** Critical swimming speed ($U_{crit}$; BL/s) of landlocked (solid lines; L-Pattagansett (blue) and L-Rogers (red)) and anadromous (dashed line; A-Bride (black)) Alewives subjected to 24 hour challenge at 0 ppt, 0.5 ppt (control; rearing salinity), 35 ppt, or 40 ppt prior to assessment of swimming performance. n = 4-6 per salinity per site. Data are presented as mean $U_{crit}$ ± standard error of the mean. ** $P < 0.01$, *** $P < 0.001$ for main effect of site relative to A-Bride.

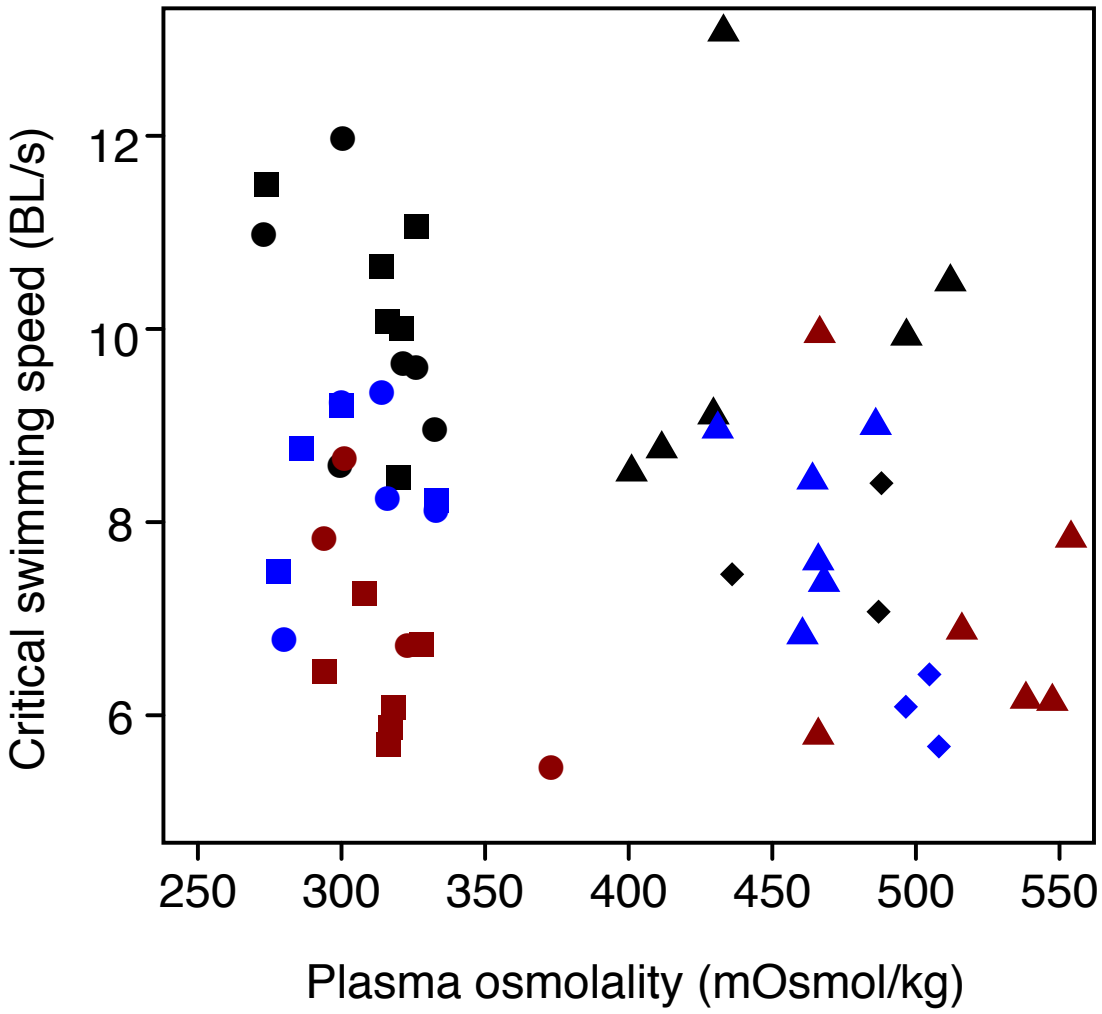


**Figure 2** Plot of the relationship between plasma osmolality (mosmol/kg) and critical swimming speed (BL/s). Colors denote sites (black, A-Bride; blue, L-Pattagansett; red, L-Rogers); symbols denote treatment salinities (squares, 0 ppt; circles, 0.5 ppt control; triangles, 35 ppt; diamonds, 40 ppt). No statistically significant correlation was detected.

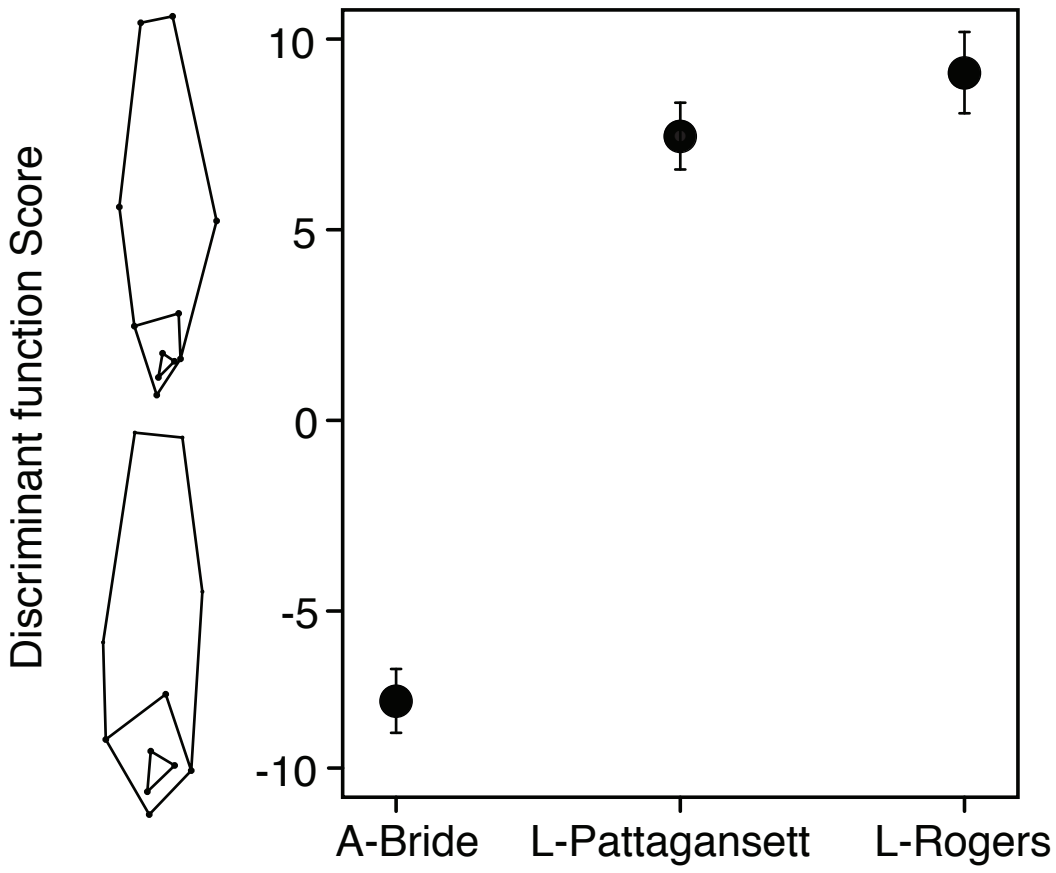


**Figure 3** Patterns of body shape divergence between anadromous (A-Bride) and landlocked (L-Pattagansett and L-Rogers) Alewives. Values are mean discriminant function analysis (DFA) scores for each site, which describe the axis of variation that best distinguished anadromous and landlocked body forms. Error bars represent 95% confidence intervals. Figures along the y-axis represent extreme cases of shape variation according the DFA.

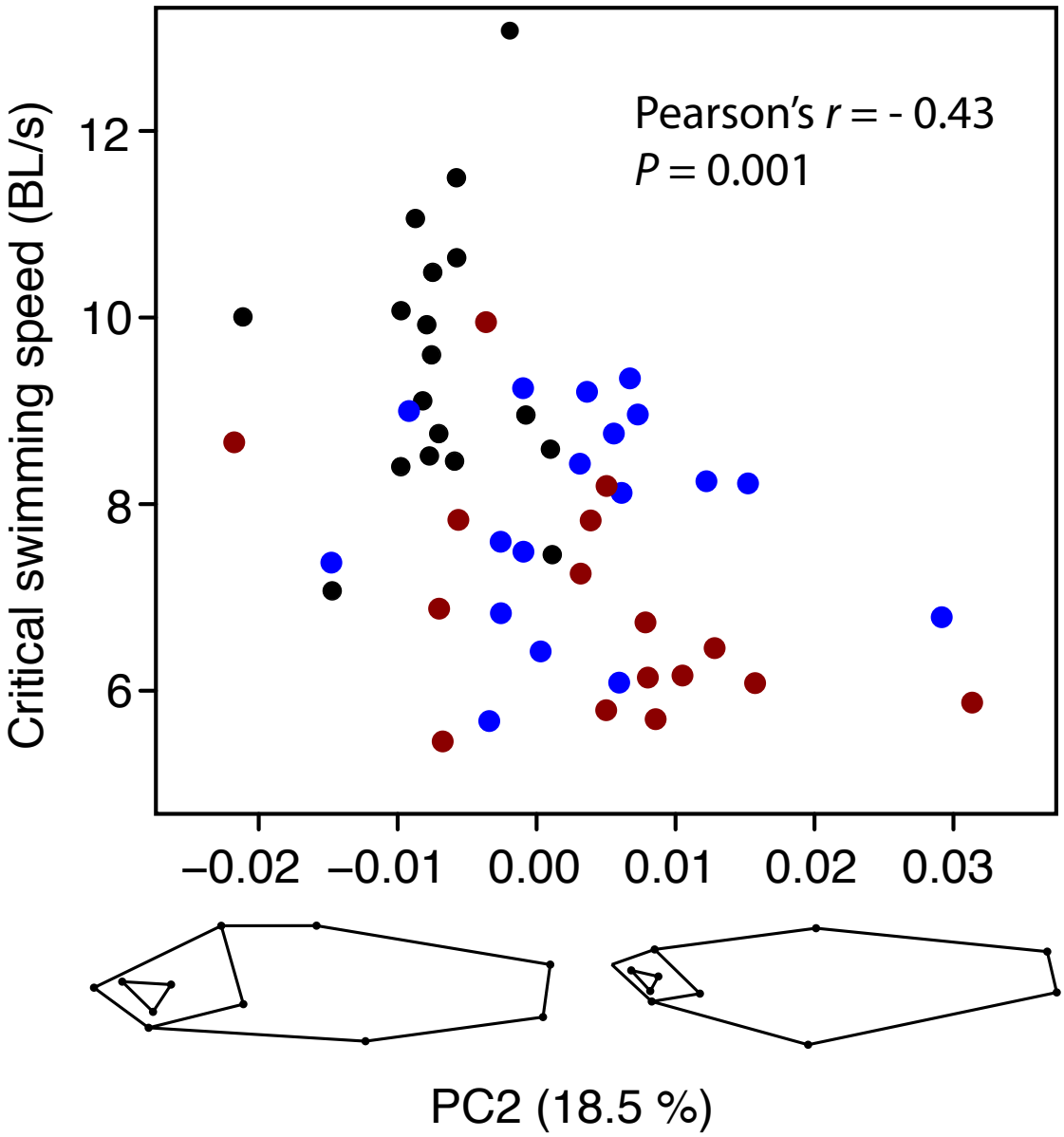


**Figure 4** Plot of the relationship between critical swimming speed (BL/s) and body shape as described by PC2. PC2 scores described the general body shape, head size and caudal peduncle size. Figures underneath the plot represent extreme cases of shape variation along PC2. Colors denote sites (black, A-Bride; blue, L-Pattagansett; red, L-Rogers).